

การวัดค่าความหนืดและสมการความสัมพันธ์สำหรับน้ำมัน และ อิมัลชัน จากแหล่งน้ำมันฝาง



บทคัดย่อและแฟ้มข้อมูลฉบับเต็มของวิทยานิพนธ์ตั้งแต่ปีการศึกษา 2554 ที่ให้บริการในคลังปัญญาจุฬาฯ (CUIR)
เป็นแฟ้มข้อมูลของนิสิตเจ้าของวิทยานิพนธ์ ที่ส่งผ่านทางบัณฑิตวิทยาลัย

The abstract and full text of theses from the academic year 2011 in Chulalongkorn University Intellectual Repository (CUIR)
are the thesis authors' files submitted through the University Graduate School.

วิทยานิพนธ์นี้เป็นส่วนหนึ่งของการศึกษาตามหลักสูตรปริญญาวิศวกรรมศาสตรมหาบัณฑิต
สาขาวิชาวิศวกรรมทรัพยากรธรณี ภาควิชาวิศวกรรมเหมืองแร่และปิโตรเลียม
คณะวิศวกรรมศาสตร์ จุฬาลงกรณ์มหาวิทยาลัย
ปีการศึกษา 2558
ลิขสิทธิ์ของจุฬาลงกรณ์มหาวิทยาลัย

Viscosity measurement and correlation for oil and its emulsion from Fang oilfield.

Miss Onchanok Juntarasakul



A Thesis Submitted in Partial Fulfillment of the Requirements
for the Degree of Master of Engineering Program in Georesources Engineering
Department of Mining and Petroleum Engineering
Faculty of Engineering
Chulalongkorn University
Academic Year 2015
Copyright of Chulalongkorn University

Thesis Title	Viscosity measurement and correlation for oil and its emulsion from Fang oilfield.
By	Miss Onchanok Juntarasakul
Field of Study	Georesources Engineering
Thesis Advisor	Assistant Professor Kreangkrai Maneeintr, Ph.D.

Accepted by the Faculty of Engineering, Chulalongkorn University in
Partial Fulfillment of the Requirements for the Master's Degree

..... Dean of the Faculty of Engineering
(Associate Professor Supot Teachavorasinskun, Ph.D.)

THESIS COMMITTEE

..... Chairman
(Assistant Professor Sunthorn Pumjan, Ph.D.)

..... Thesis Advisor
(Assistant Professor Kreangkrai Maneeintr, Ph.D.)

..... External Examiner
(Associate Professor Pinyo Meechumna, Ph.D.)

จุฬาลงกรณ์มหาวิทยาลัย
CHULALONGKORN UNIVERSITY

อรชนก จันทรสกุล : การวัดค่าความหนืดและสมการความสัมพันธ์สำหรับน้ำมัน และ อิมัลชัน จากแหล่งน้ำมันฝาง (Viscosity measurement and correlation for oil and its emulsion from Fang oilfield.) อ.ที่ปริกษาวิทยานิพนธ์หลัก: ศศ. ดร. เกรียงไกร มณีอินทร์, หน้า.

ในอุตสาหกรรมปิโตรเลียม อิมัลชันเกิดจากน้ำมันและน้ำจากหลุมผลิตผสมกันซึ่งจะพบเจอ เป็นปกติในกระบวนการผลิตน้ำมัน โดยอิมัลชันจะเกิดได้ในหลายกระบวนการตั้งแต่กระบวนการ ภาศสนามไปจนถึง กระบวนการในอุตสาหกรรม เช่น กระบวนการขนส่ง กระบวนการแยกเพื่อ ผลิตเป็นต้น และอิมัลชันนี้จะเป็นปัญหา และรบกวนการผลิตน้ำมันเป็นอย่างมาก ซึ่งความหนืด และเสถียรภาพของ จะเป็นคุณสมบัติที่สำคัญของอิมัลชันที่มีผลโดยตรงต่อการไหล ใน กระบวนการขนส่งและ การผลิต ดังนั้นจุดประสงค์ของงานวิจัยนี้คือ การวัดความหนืดของ อิมัลชันโดยอาศัยตัวแปรต้นสามตัวที่มีผลกระทบต่อความหนืด คือ อุณหภูมิ ปริมาณน้ำในน้ำมัน และ แรงเฉือน โดยค่าที่ใช้ในการศึกษาคือ 50 ถึง 60 องศาเซลเซียส, ร้อยละ 0 ถึง 60 และ 3.75 ถึง 60 หนึ่งส่วนวินาที นอกจากนี้ยังศึกษาการกระจายตัวของเม็ดน้ำในอิมัลชันที่ส่งผลต่อ เสถียรภาพของอิมัลชันอีกด้วย จากการศึกษาได้พบว่า ความหนืดจะมีค่าน้อยลง เมื่ออุณหภูมิ และ ปริมาณน้ำในน้ำมันมีค่าเพิ่มขึ้น ส่วนแรงเฉือนกลับให้ผลที่ตรงข้ามคือ การเพิ่มแรงเฉือน ทำให้ อิมัลชันมีความหนืดเพิ่มขึ้นด้วย ในส่วนของการศึกษาการกระจายตัวของเม็ดน้ำสภาวะที่ แรงเฉือน ต่างกันนั้นเห็นได้ว่า เมื่อเพิ่มแรงเฉือนมากขึ้นทำให้ เม็ดน้ำแตกตัวเป็นเม็ดที่เล็กลง ทำให้อิมัลชัน เสถียรมากขึ้น นอกจากนี้ยังศึกษาเกี่ยวกับการสร้าง สมการความสัมพันธ์ระหว่างตัวแปรที่เกี่ยวข้อง และความหนืด เพื่อใช้ในการพัฒนา และ คาดการณ์ ความหนืดของแหล่งน้ำมันฝางในประเทศไทย อีกด้วย

ภาควิชา วิศวกรรมเหมืองแร่และปิโตรเลียม ลายมือชื่อนิติติ

สาขาวิชา วิศวกรรมทรัพยากรธรณี ลายมือชื่อ อ.ที่ปริกษาหลัก

ปีการศึกษา 2558

5670459921 : MAJOR GEORESOURCES ENGINEERING

KEYWORDS: VISCOSITY, EMULSION, SHEAR RATE, WATER CONTENT

ONCHANOK JUNTARASAKUL: Viscosity measurement and correlation for oil and its emulsion from Fang oilfield.. ADVISOR: ASST. PROF. KREANGKRAI MANEEINTR, Ph.D., pp.

In petroleum industry, emulsion, a mixture of oil and produced water can be formed from oil recovery. It is found in many processes such as production, pipeline transportation and separation. This emulsion can result in several problems in handling facilities and separation. Viscosity and stability of emulsion are the key parameters to transport and separate oil and water to meet sales specification. Therefore, the objectives of this work are to measure the viscosity of emulsion and to evaluate the stability of emulsion of light oil from Fang oilfield in Thailand. The parameters of this study are temperature, shear rate and water cut ranging from 50 to 80 °C, 3.75 to 60 s⁻¹ and 0 to 60 percent, respectively. Also, the droplets of oil and water are investigated to evaluate the stability of emulsion. These effects of parameters on viscosity and stability of emulsion are required to design the process and to increase oil production. The results shows that viscosity decreases as temperature and shear rate increase and water cut becomes lower. Droplet sizes at different shear rates are also investigated. Droplet sizes become smaller when high shear rate applies and emulsion becomes more stable. Furthermore, correlations are developed to predict the viscosity and stability of the oil and emulsion from Thailand.

Department: Mining and Petroleum Student's Signature

Engineering Advisor's Signature

Field of Study: Georesources

Engineering

Academic Year: 2015

ACKNOWLEDGEMENTS

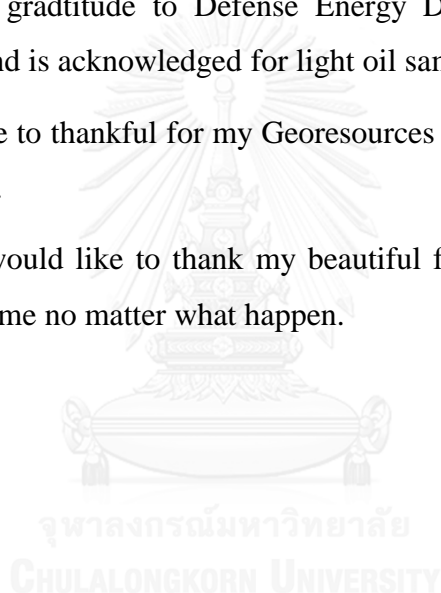
First of all, I would like to express my sincere gratitude to Assistant professor Dr. Kreangkrai Maneeintr, my thesis advisor for support and knowledge for my experiment.

I appreciate to The 90th Anniversary of Chulalongkorn University, Rachadapisak Sompote Fund and Graduate School Thesis Grant, Chulalongkorn University for financial support.

I am very grateful to Defense Energy Department at Fang district, Chiang Mai, Thailand is acknowledged for light oil sample.

I would like to thank for my Georesources Engineering friends for help and good friendship.

Finally, I would like to thank my beautiful family for great support and always stay besides me no matter what happen.



CONTENTS

	Page
THAI ABSTRACT	iv
ENGLISH ABSTRACT.....	v
ACKNOWLEDGEMENTS	vi
CONTENTS.....	vii
List of Figures	ix
List of Tables	xi
Chapter 1 Introduction	1
1.1 Petroleum emulsion formation	1
1.2 Problems of petroleum emulsion.....	4
1.3 Objectives of this research.....	5
Chapter 2 Theory and Literature review	7
2.1 Stability of Emulsions	7
2.2 Viscosity of Emulsions.....	10
2.3 Literature Review	14
2.4 Correlations	15
Chapter 3 Experiment	19
3.1 Chemicals and Equipment.....	19
3.2 Experiment Procedure	23
3.3 Correlation development	24
Chapter 4 Results and Discussions	27
4.1 Verification of the equipment.....	27
4.2 Effect of temperature on viscosity.....	27
4.3 Effect of water content on viscosity	31
4.4 Effect of shear rate on viscosity	34
4.5 Droplets size distribution.....	36
Chapter 5 Conclusions	61
.....	63
REFERENCES	63

VITA.....	Page 118
-----------	-------------



List of Figures

Figure 1.1 Emulsion's formation	1
Figure 1.2 Photomicrograph of a water-in-oil emulsion.....	2
Figure 1.3 Photomicrograph of an oil-in-water emulsion.....	3
Figure 1.4 Photomicrograph of an water-in-oil-in-water emulsion	3
Figure 2.1 Stability of emulsion.....	8
Figure 2.2 Droplet size and size distribution of emulsion	8
Figure 2.3 Corrosion Inhibitors in the Oilfield	9
Figure 2.4 Mechanisms leading of an oil-in-water emulsion	10
Figure 2.5 Viscosity of fluid	11
Figure 2.6 Shear stress and Shear rate for a Newtonian fluid.....	12
Figure 2.7 Shear stress/shear rate relationships in liquids	12
Figure 3.1 Brookfield viscometer model LVDV2T.....	22
Figure 3.2 Methodology flowchart	26
Figure 4.1 Effect of temperature on viscosity with 0percent water content	29
Figure 4.2 Effect of temperature on viscosity with 20percent water content	29
Figure 4.3 Effect of temperature on viscosity with 40percent water content	30
Figure 4.4 Effect of temperature on viscosity with 60percent water content	30
Figure 4.5 Effect of water content on viscosity at 3.75 s Shear rate.....	31
Figure 4.6 Effect of water content on viscosity at 7.5 s Shear rate.....	32
Figure 4.7 Effect of water content on viscosity at 15 s Shear rate.....	32
Figure 4.8 Effect of water content on viscosity at 30 s Shear rate.....	33
Figure 4.9 Effect of water content on viscosity at 60 s Shear rate.....	33
Figure 4.10 Effect of shear rate on viscosity at 50°C temperature.....	34
Figure 4.11 Effect of shear rate on viscosity at 60°C temperature.....	35
Figure 4.12 Effect of shear rate on viscosity at 70°C temperature.....	35
Figure 4.13 Effect of shear rate on viscosity at 80°C temperature.....	36
Figure 4.14 Microscopic observation of water droplet at 15 s ⁻¹ shear rate.....	37

Figure 4.15 Microscopic observation of water droplet in 20percent	37
Figure 4.16 Microscopic observation of water droplet in 20percent	38
Figure 4.17 Droplets size distribution at 3.75 s^{-1} shear rate.....	38
Figure 4.18 Droplets size distribution at 7.5 s^{-1} shear rate.....	39
Figure 4.19 Droplets size distribution at 15 s^{-1} shear rate.....	39
Figure 4.20 Droplets size distribution at 30 s^{-1} shear rate.....	40
Figure 4.21 Droplets size distribution at 60 s^{-1} shear rate.....	40
Figure 4.22 Experiment data and calculated data at 3.75 s^{-1} shear rate.	44
Figure 4.23 Experiment data and calculated data at 7.5 s^{-1} shear rate	45
Figure 4.24 Experiment data and calculated data at 15 s^{-1} shear rate.	45
Figure 4.25 Experiment data and calculated data at 30 s^{-1} shear rate	46
Figure 4.26 Experiment data and calculated data at 60 s^{-1} shear rate	46
Figure 4.27 Experiment data and calculated data at 3.7 s^{-1} shear rate	50
Figure 4.28 Experiment data and calculated data at 7.5s^{-1} shear rate	51
Figure 4.29 Experiment data and calculated data at 15 s^{-1} shear rate	51
Figure 4.30 Experiment data and calculated data at 30 s^{-1} shear rate	52
Figure 4.31 Experiment data and calculated data at 60 s^{-1} shear rate	52
Figure 4.32 Experiment data and calculated data at 50°C temperature.....	57
Figure 4.33Experiment data and calculated data at 60°C temperature.....	57
Figure 4.34 Experiment data and calculated data at 70°C temperature.....	58
Figure 4.35 Experiment data and calculated data at 80°C temperature.....	58
Figure 4.36 Experiment data and calculated data with Ronningsen's correlation.....	59
Figure 4.37 Experiment data and calculated data with Farah's correlation.....	59
Figure 4.38 Experiment data and calculated data with Al-Roomi's correlation.....	60

List of Tables

Table 3.1 Composition of oil sample	19
Table 3.2 Density of oil sample	20
Table 3.3 Composition of the produced water	21
Table 4.1 Viscosities of oil and its emulsion.	28
Table 4.2 The constants of Ronningsen's correlation from mathematical method.	41
Table 4.3 experiment data and calculated data at 3.75 s^{-1} shear rate equation.	42
Table 4.4 experiment data and calculated data at 7.5 s^{-1} shear rate equation.	42
Table 4.5 experiment data and calculated data at 15 s^{-1} shear rate equation	43
Table 4.6 experiment data and calculated data at 30 s^{-1} shear rate equation	43
Table 4.7 experiment data and calculated data at 60 s^{-1} shear rate equation.	44
Table 4.8 The constants of Farah's correlation from mathematical method.	47
Table 4.9 Experiment data and calculated data at 3.75 s^{-1} shear rate equation.....	48
Table 4.10 Experiment data and calculated data at 7.5 s^{-1} shear rate equation.....	48
Table 4.11 Experiment data and calculated data at 15 s^{-1} shear rate equation.....	49
Table 4.12 Experiment data and calculated data at 30 s^{-1} shear rate equation.....	49
Table 4.13 Experiment data and calculated data at 60 s^{-1} shear rate equation.....	50
Table 4.14 Constants for Al-Roomi's correlation.....	53
Table 4.15 Experiment data and calculated data of Al-Roomi's correlation.....	54
Table 4.16 percentAAD of correlation	60

Chapter 1

Introduction

Recently, the demand of energy resources varies with increasing population. The energy resources can be divided into renewable resources like solar energy, wind power and fossil fuels such as coal and petroleum products.

1.1 Petroleum emulsion formation

Petroleum products, crude oil and natural gases, are a naturally occurring, found in underground geological formations. Crude oil is important as an energy resource. However, while oil is recovered with produced water, it generally is mixed with water to form emulsion at many stages from underground to the surface as shown in Figure 1.1.

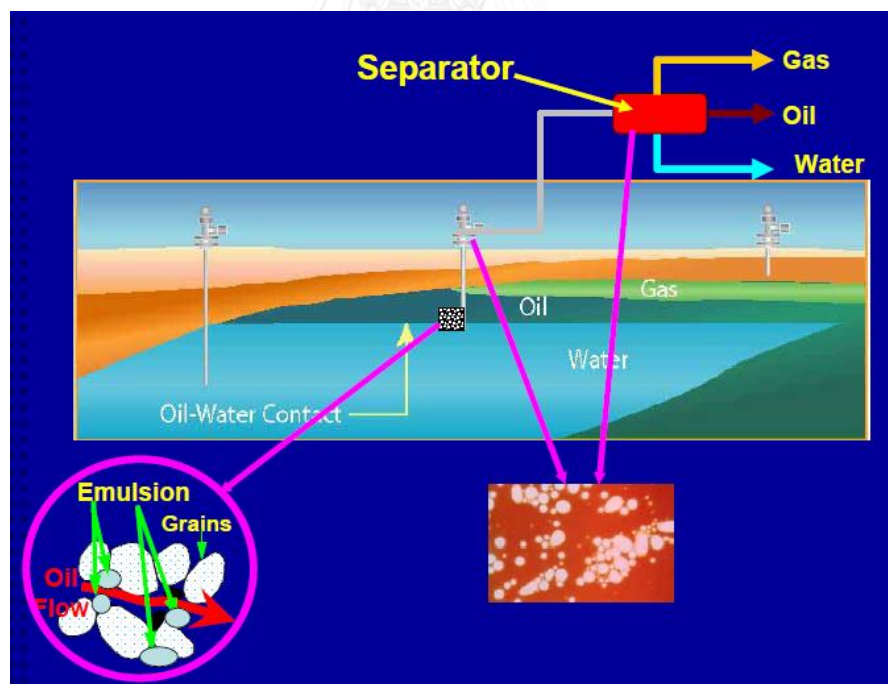


Figure 1.1 Emulsion's formation
(Kokal & Aramco, 2006)

Emulsion is a dispersion of one liquid in another immiscible liquid. Crude oil emulsion can be classified into three groups such as water-in-oil emulsions consisting of water droplets in a continuous oil phase as presented in Figure 1.2

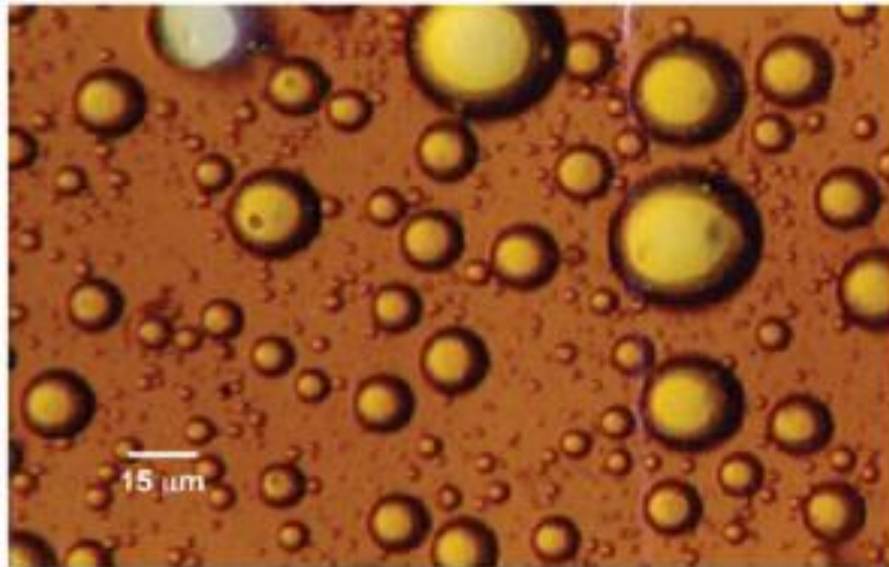


Figure 1.2 Photomicrograph of a water-in-oil emulsion
(Kokal & Aramco, 2006)

Figure 1.3 shows oil droplets in water as a continuous phase called oil-in-water emulsions. The last one is multiple or complex emulsions consisting of tiny droplets suspended in bigger droplets that are suspended in a continuous phase as shown in Figure 1.4. However, the types of emulsion formed depend on various factors (Ronningsen, 1995). Moreover, emulsion can be classified by the size of the droplets in the continuous phase. Macroemulsion is the dispersed droplets are larger than 10 μm . When the droplets smaller than 10 nm. called microemulsion (Kokal & Aramco, 2006).

Most of petroleum emulsions found in oil industry are water-in-oil type. Emulsion may contain not just oil and water but also solid particles and even gas (Kokal & Aramco, 2006).

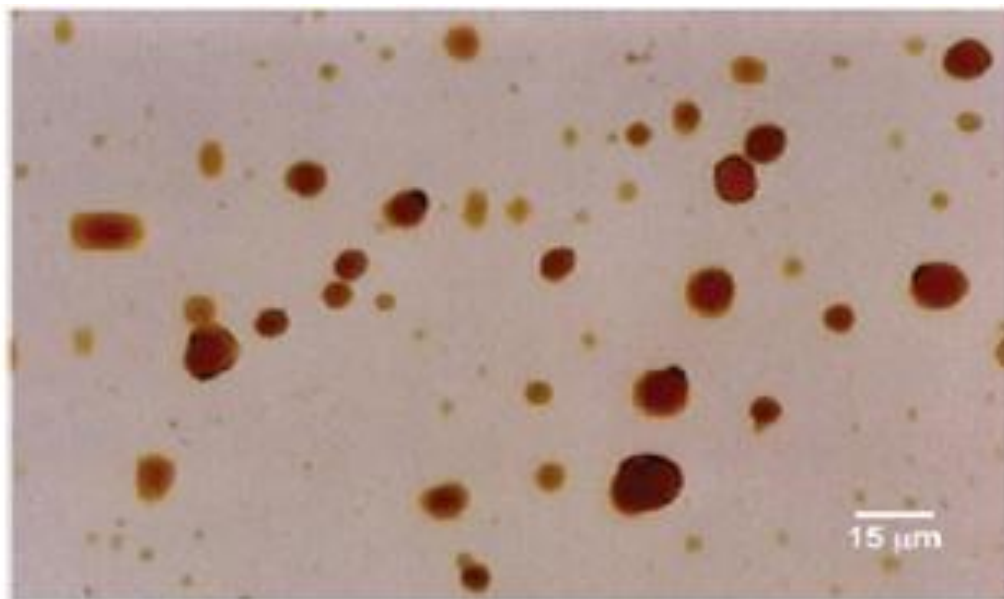


Figure 1.3 Photomicrograph of an oil-in-water emulsion
(Kokal & Aramco, 2006)

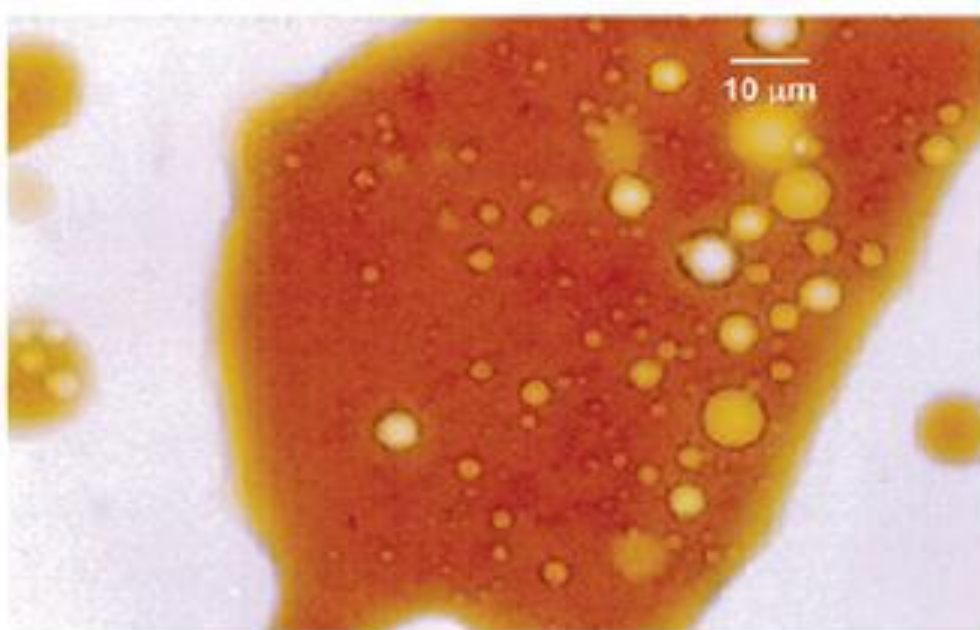


Figure 1.4 Photomicrograph of an water-in-oil-in-water emulsion
(Kokal & Aramco, 2006)

Crude oil emulsion is formed when oil and water come into contact with each other. There are two important factors in petroleum emulsion forming: emulsifying agent and a degree of mixing (Kokal & Aramco, 2006).

The first one is emulsifying agent. Emulsions contain oil, water and emulsifying agent. The emulsifying agent may lower interfacial tension. The natural emulsifiers in a crude oil are resident in the heavy fraction. Crude with a small amount of emulsifier forms a less stable emulsion and separates easily conversely crude oil with many emulsifier which is very stable or tight emulsions (Kokal & Aramco, 2006).

The second one is a degree of mixing. The large amount of degree of mixing can form very stable emulsion or tight emulsion. During crude oil production, there are several sources of mixing, the amount of shear, flow through reservoir rock (bottom hole perforations), flow through tubing, flow lines, and production headers (valves, fittings, chokes), surface equipment (Kokal & Aramco, 2006).

1.2 Problems of petroleum emulsion

General, crude oil in industry formed in emulsion. It is well known that the crude oil emulsion is in the center of several economic and technical problems because the water in emulsion increases the unit cost of oil production and water treatment. Normally, oilfield emulsion is a dispersion of water droplets in oil, water-in-oil emulsion.

It is evident from the previous discussion that emulsion is formed by a degree of mixing. Therefore, emulsion is found in many processes such as production drilling fluid, process plant, pipeline transportation and separation (Kokal & Aramco, 2006). This emulsion can result in several problems in handling facilities and separation, effects to oil production cost and most important, treatment cost (Schramm, 1992). Viscosity and stability of emulsion are the key parameters to transport and separate oil and water to meet sales specification (Kokal & Aramco, 2006).

Stability of emulsion is attributed to surface-active films consisting of several components (Neumann & Paczynska-Lahme, 1996) implicated with viscosity because stable emulsions might be classified by their viscoelastic, elastic and viscosity, properties (Fingas & Fieldhouse, 2012), so viscosity relates with stability of emulsion. Temperature, shear rate and water content are parameters that affects with viscosity because the viscosity of an emulsion, in general depends upon several factors like shear rate, temperature, volume fraction of dispersed phase (Ronningsen, 1995). In addition, the viscosity of water in oil emulsions is strongly augmented by increasing its water volume ratio and by decreasing the temperature (Krieger & Dougherty, 1959).

The viscosity of emulsion effects on oil production process such as the flow rate in pipeline, pressure in wells and pumping. Therefore, the prediction of viscosity is needed in process to develop oil industry.

1.3 Objectives of this research

The objectives of this work are to measure and investigate the viscosity and stability of emulsion. Furthermore, the results of viscosity and stability of the oil and emulsion from Fang oilfield in Thailand will be correlated by using the equations from the previous work and applied to predict the viscosities of oil and its emulsion. It is evident from the previous discussion that about problems of emulsion so the objectives of research are to investigate the effects of parameters (temperature, water content, shear rate) on viscosities of petroleum emulsion and set up the correlation of parameter with viscosity.

The Contribution of research is to understand more on oil and emulsion production in Thailand and provide the fundamental data to improve develop technology for petroleum.

The scope of the research is to investigate the crude oil emulsions from Fang oilfield, Thailand. The parameters of research are temperature, water content, shear rate. Correlation between parameters and viscosities will be developed.

The outline of this thesis is as follows Chapter 2 the relevant theory in the research and introduces the interesting literatures related with the topic of research.

The condition of research and methodology is presented in Chapter 3. And then the result and discussion of viscosity with various conditions, correlation for predicting viscosity, droplets size distribution as shown in Chapter 4. Finally, Chapter 5 presents the conclusion and commendation of this research.



Chapter 2

Theory and Literature review

This chapter presents the basic knowledge of emulsion and stability of emulsion. The literature review relates to this work will be presented here.

Normally, emulsions are stable over a period of time. The first reason leading to emulsion formation is the increase in mixing energy or turbulence so it is classified in three groups. Emulsions separate in a few minutes is loose emulsions. Medium emulsions separate in tens of minutes and tight emulsions separate hardly in days (Kokal & Aramco, 2006).

2.1 Stability of Emulsions

Stability of emulsions is a consequence of the small droplet size and interfacial film on the droplet in emulsion. Oil field emulsions are stabilized by films formed around the water droplets at the oil/water interface as shown in Figure 2.1.

As mentioned earlier, various factors effect on interfacial film such as temperature, droplets size and droplets size distribution and brine composition can affect the emulsion stability (Kokal & Aramco, 2006).

Temperature is the normal factor effecting on stability because it affects with physical properties of oil, water, interfacial film directly. When the emulsions become waxes, the temperature is below its cold point, and emulsion can't flow easily. Moreover, temperature effects on the buildup of interfacial films because it changes the absorption rate and characteristic interface.

Droplets size and Droplets size distributions for emulsion can range from less than micron to more than 50 microns. For emulsion stability, emulsion with smaller droplets size and droplets size distribution effects on viscosity of emulsion because when the droplets are smaller and viscosity become higher. Figure 2.2 shows droplet size and size distribution for classify type of emulsion.

It is evident that emulsion is the mixing of oil and water. Demulsification is the breaking of a crude oil emulsion into water and oil phase by destroyed the interfacial film of emulsion. Therefore, demulsification or breaking emulsion is linked directly to remove of the interfacial film. Temperature and shear rate are the factors that affect with breaking emulsion.

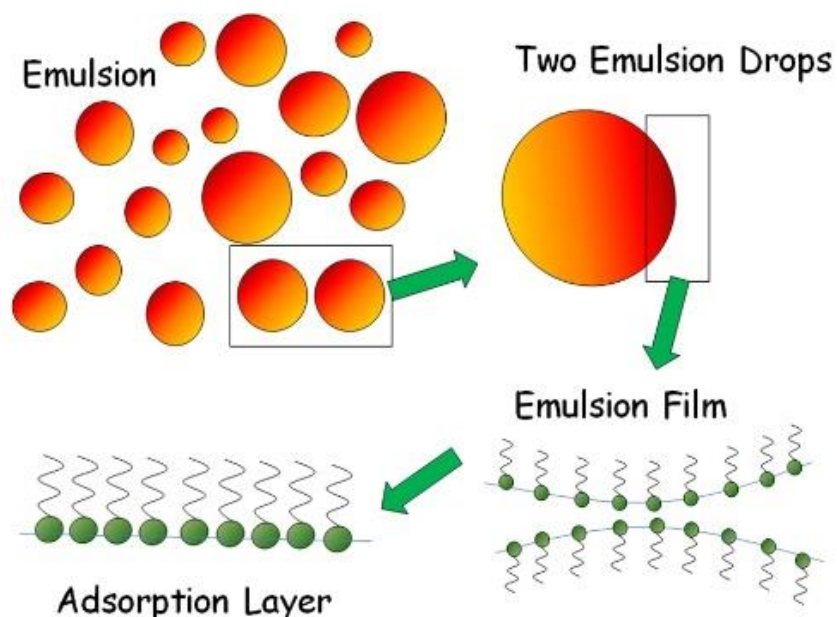


Figure 2.1 Stability of emulsion

(Sinterface, 2016)

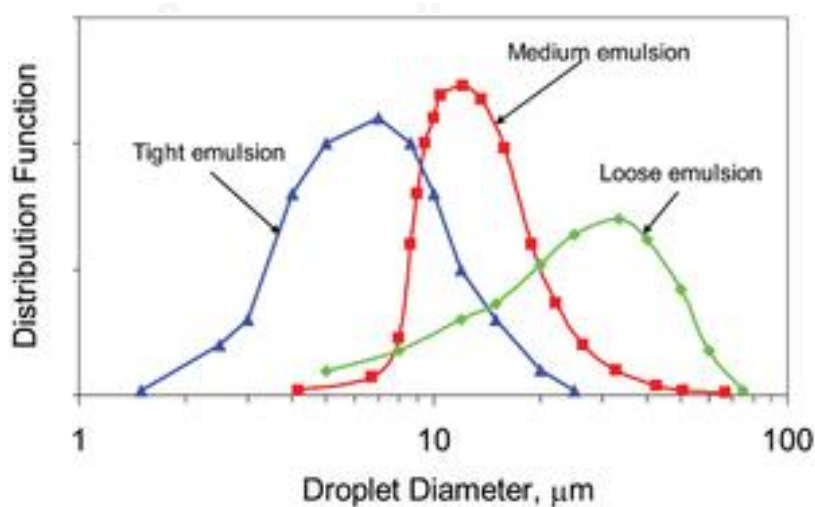


Figure 2.2 Droplet size and size distribution of emulsion

(Kokal & Aramco, 2006)

Temperature or heat can separate emulsion into oil/water phase. Increasing temperature has the various effects such as reducing the viscosity of the oil, increasing the mobility of the water droplets and increasing droplet collisions.

Shear or agitation, normally, reducing shear lowers the stability of emulsion. High shear makes droplet size become smaller. Smaller droplet is more stable than larger droplet.

The mechanisms involved in demulsification are sedimentation, aggregation or flocculation, coalescence, phase separation as shown in Figures 2.3 and 2.4.

Aggregation or flocculation is the first step for separation, grouping together of water droplets in an emulsion without a change in surface area. The rate of flocculation depends in various factors such as water content in the emulsion. It is higher when water content is higher. Also, temperature of the emulsion is high and viscosity of oil is low.

Coalescence is the second step of demulsification. The fusion of droplets to form larger drops will be achieved with reduction of total surface area. This is an irreversible process that leads to decrease in the number of water droplets and complete demulsification. Coalescence is enhanced by many factors such as high rate of flocculation, high interfacial tension, and high temperature and high the water content increases the frequency of collisions between droplets.

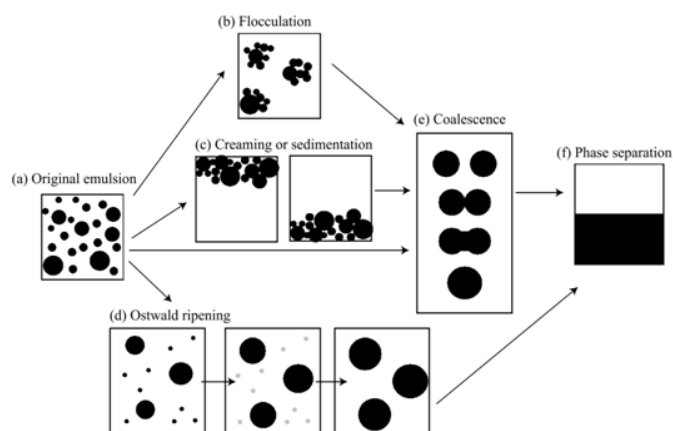


Figure 2.3 Corrosion Inhibitors in the Oilfield

(Ibrahim, 2011)

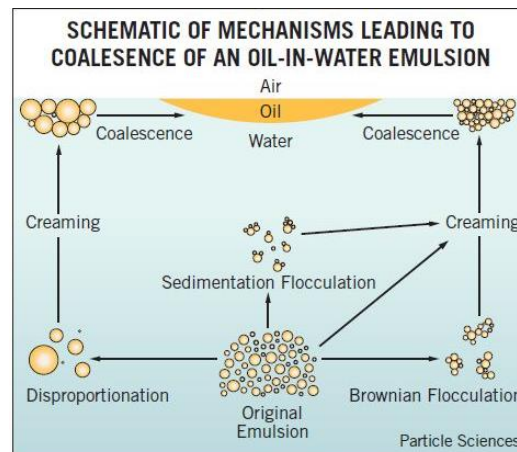


Figure 2.4 Mechanisms leading of an oil-in-water emulsion
(Sciences, 2011)

Sedimentation is the falling of water droplets from an emulsion. Creaming is the rising of oil droplets and water phase. Sedimentation and creaming are driven by the density difference between oil and water and may not result in the breaking of an emulsion.

2.2 Viscosity of Emulsions

Viscosity is the internal friction of emulsion and this friction becomes noticeable when a layer of fluid is made to move in relation to another layer as shown in Figure 2.5. Newton wrote the equation about viscosity:

$$\frac{F}{A} = \eta \frac{dv}{dx} \quad (2.1)$$

Where η is viscosity, $\frac{dv}{dx}$ is velocity gradient or called “shear rate(γ)”, $\frac{F(\text{Force})}{A(\text{Area})}$ is the force per unit area or called “shear stress(τ)”. So the equation can develop in this formula:

$$\eta = \frac{\tau}{\gamma} \quad (2.2)$$

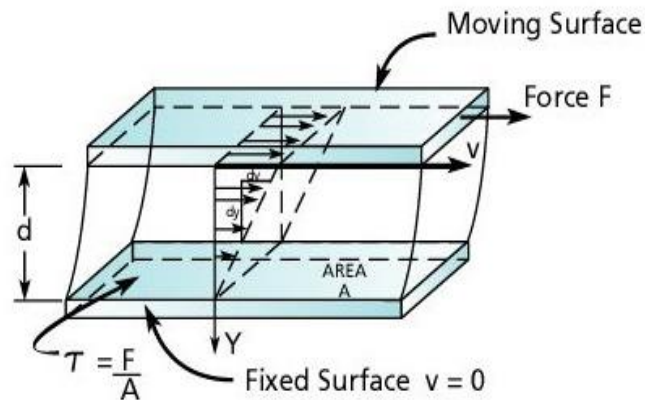


Figure 2.5 Viscosity of fluid
(Pumpfundamentals, 2010)

The fundamental unit of viscosity measurement is poise(P) or centipoise (cPs). Pascal-seconds (Pa·s) for International System of units (SI). The comparison between fundamental unit:

$$1 \text{ Pa} \cdot \text{s} = 10 \text{ P} \quad (2.3)$$

The flow behavior of fluids is classified in two types Newtonian fluid is the relationship between shear rate and shear stress as shown a straight line in Figure 2.6. The slope of this graph is viscosity. The stable viscosity of Newtonian fluid is not dependent on shear rate.

For Non-Newtonian fluid the viscosity of fluids will therefore change as the shear rate is varied. Non-Newtonian fluids are classified in two groups. There is pseudoplastic fluid or shear thinning fluid, viscosity decrease when shear rate increase, and dilatant fluid or shear thickening fluid, viscosity increase with shear rate.

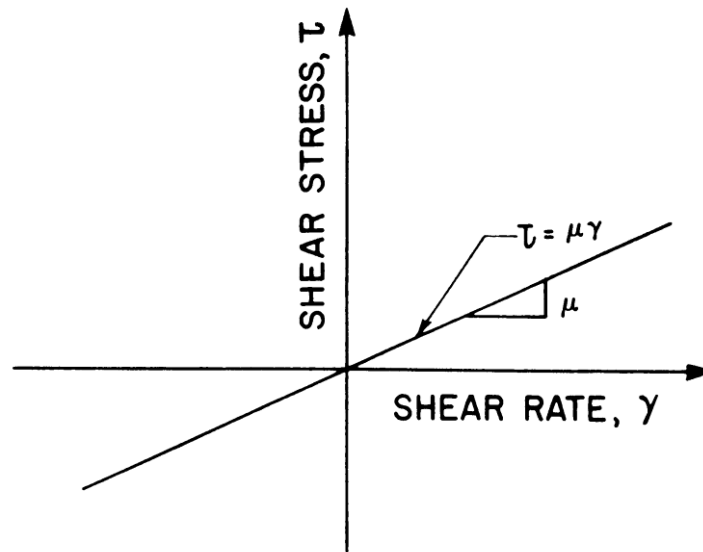


Figure 2.6 Shear stress and Shear rate for a Newtonian fluid
(Pumpfundamentals, 2010)

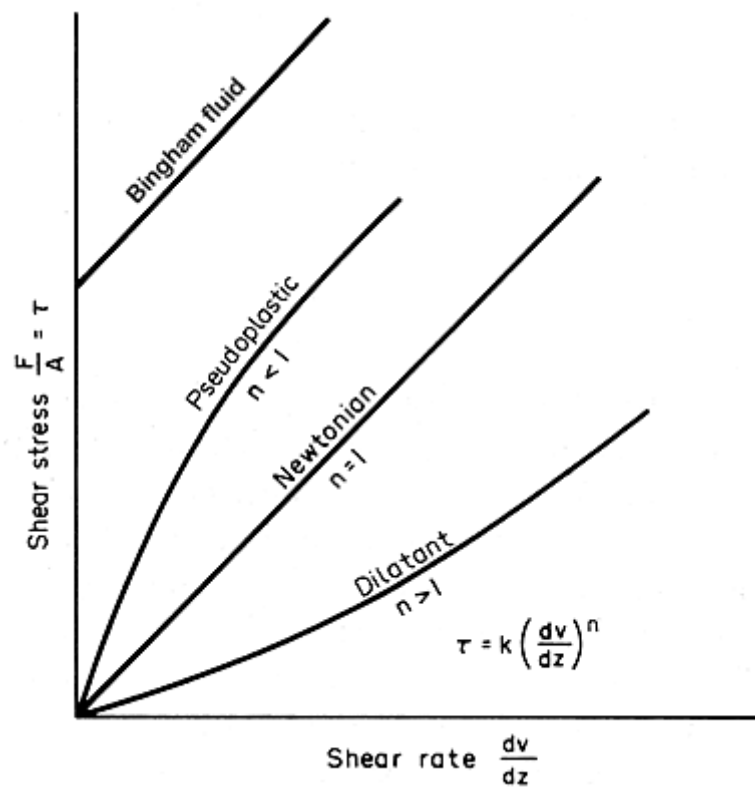


Figure 2.7 Shear stress/shear rate relationships in liquids
(Pumpfundamentals, 2010)

Figure 2.7 shows the relationship between shear rate and shear stress of fluid. Power-law equation is used for explanation:

$$\tau = k\left(\frac{dv}{dz}\right)^n \quad (2.4)$$

Where τ is shear stress, dv/dz is shear rate, k is a constant of proportionality. Where $n = 1$ the fluids are called Newtonian and $n > 1$ or $n < 1$, the fluids are called non-Newtonian.

Emulsions are non-Newtonian fluid. It means viscosity changes depending on shear rate, and is classified in two groups. The first group is a dilatant fluid or shear thickening which viscosity is increased with increasing shear rate such as starch thickener. The other group is a pseudoplastic fluid or shear thinning fluid which is increased viscosity with decreasing shear rate such as hydrocolloid or emulsion.

Generally, viscosity is easier to measure than other properties. Viscosity of emulsion depends on many factors such as temperature, volume fraction of dispersed phase, viscosity of dispersed phase, viscosity of continuous phase, nature and concentration of emulsifying agents, average droplet size and size distribution, solids phase (Ronningsen, 1995).

Volume fraction of dispersed phase is one of the most influential factor with viscosity of emulsion because increasing concentration of dispersed phase becomes more non-Newtonian (shear rate). Temperature is common factor influence with viscosity directly. Normally, viscosity of emulsion is shown in term of relative viscosity (μ_r);

$$\mu_r = \frac{\mu}{\mu_0} \quad (2.5)$$

Where μ and μ_0 are the viscosity of emulsion and viscosity of oil phase respectively.

2.3 Literature Review

Ronningsen (1995) studied about measurement of viscosity and correlations for predicting relative viscosity of water-in-oil emulsions from North Sea crude oils at temperature between 5 and 40°C, water cut from 10-60 percent and shear rate ranging from 30-500 s⁻¹ because they are general factors which are influential with viscosity. In addition droplet size distribution and relationship between viscosity and droplets size that normally increases when the mean droplet size decreases are presented here. The results of the three parameters with viscosity are that viscosities of water-in-oil emulsions decrease with increasing temperature, shear rate and decrease with water content.

Farah et. al (2005) investigated the viscosity of water-in-oil emulsion with temperature and water volume fraction as parameters. The objective of this study is the variation of kinematic viscosity of W/O emulsions. Six different crude oil with density ranging from 15° to 40° API in varying shear rate, temperature and volume fraction of dispersed phase. Water-in-oil emulsions were prepared with 10, 20, 30, 40 and 60 percent of saline water. Finally, correlations for predict viscosity of emulsion with 2 parameters (temperature and water content).

Maneeintr et al. (Maneeintr, Sasaki, & Sugai, 2013) studied the effects of parameters on viscosities and correlation of heavy oil from Oman and Japan and stability of its emulsion. Process is the normal method for heavy oil production. Heavy oil and steam from injection mixed in emulsion form. Droplets water in oil was investigated by Microscopy. The parameters for this study are temperature; 25, 40 and 60°C, water content (water oil ratio from 0 to 25 percent) and shear rate; 19.25, 38.4 and 76.85 s⁻¹. The relationship between Droplets size and stability showed a larger shear rate, the droplets sizes become smaller. Eventually, correlating of viscosity of Omani and Japanese oil for prediction has been developed. This correlation is in the form as show in equation:

$$\mu = AT^{-B} \quad (2.6)$$

Where μ is viscosity(cP), T is temperature, A and B are coefficients.

Fingas (1997) studied the stability of water-in-oil emulsions. Stability is common characteristic because it shows a stability or instability of a water-in-oil emulsion. Green Canyon, a Louisiana offshore oil (unstable and mesostable emulsions), Arabian Light (mesostable emulsions), Sockeye, a California oil (stable emulsion) are three oils were used in this study. The studies show that there are some variations in the formation of emulsions relating to the energy of formation.

Nour and Yunus (2006) investigated the water-in-oil emulsion. The sample from Iran and Malaysia oilfields mixing speed from 800 to 1800 rpm with temperature 28-30°C to become emulsion. Emulsion was investigated with four parameters; temperature, volume fractions of dispersed phase, phase ratio water-oil and surfactant concentration.

2.4 Correlations

Viscosity correlations have been proposed from many equations as shown below.

Ronningsen's Correlation

For Ronningsen's correlation, the equation is presented in term of temperature and water content. So when develop correlation there are many equations for difference shear rate.

This research correlated viscosity in terms of relative viscosity, η_r

$$\eta_r = \frac{\eta_e}{\eta_o} \quad (2.7)$$

η_e and η_o are the emulsion and oil phase viscosities.

Broughton and Squires (Broughton,1938) developed equation of relative viscosity from Richardson(1933) and add own constant of factor in the equation.

$$\eta_r = Ae^{K\phi} \quad (2.8)$$

Where A is correlation factor, K is Richardson constant and ϕ is water cut. It is easily linearized:

$$\ln \eta_r = a + K\phi \quad (2.9)$$

Ronningsen applied from Richardson equation under the conditions used in this study:

$$a = k_1 + k_2t \quad (2.10)$$

And

$$K = k_3 + k_4t \quad (2.11)$$

Inserting the expressions into Richardson's equation showed of the relative emulsion viscosity:

$$\ln \eta_r = k_1 + k_2t + k_3 + k_4t\phi \quad (2.12)$$

Where η_r is relative viscosity, t is temperature, ϕ is water content and k_1, k_2, k_3, k_4 are constant of correlation.

Farah's Correlation

For Farah's correlation, The equation is shown in term of temperature and water content like Ronningsen's correlation.

Equation's Farah was explicated from Richardson and Ronningsen showed in Eq.:

$$\ln(\ln(v + 0.7)) = k_1 + k_2V + k_3 \ln T + k_4V \ln T \quad (2.13)$$

Where v is relative viscosity, V is water content, T is temperature and k_1, k_2, k_3, k_4 are constant of correlation.

Al-Roomi's correlation

Al-roomi (2004) studied rheological model and correlated the parameters, water content temperature and shear rate. The correlation developed from equations is showed below;

$$\mu_r = e^{k\phi} \quad (2.14)$$

The equation showed relationship between relative viscosity (μ_r) and water content (ϕ). Where k is constant and depends on the type of emulsion.

The Arrhenius-type equation showed relationship between viscosity (μ) and temperature (T);

$$\mu = Ae^{B/T} \quad (2.15)$$

Where A and B are constant depends on shear rate and system.

The power-law's equation and apparent viscosity that showed relationship between viscosity and shear rate;

$$\mu = k\gamma^{n-1} \quad (2.16)$$

Where γ is shear rate, k and n are constants. The combination of equations to the Al-Roomi's correlation;

$$\mu = a\gamma^b \exp\left(c\phi + \frac{d}{T}\right) \quad (2.17)$$

Where a, b, c and d are constant, μ is viscosity, γ is shear rate, ϕ is water content.

Finally, the percent error (PE) and absolute average deviations (ADDs) are showed in;

$$PE = \left[\frac{\mu_{exp} - \mu_{calc}}{\mu_{exp}} \right] \times 100 \quad (2.18)$$

$$(2.19) \quad \text{percentADDs} = \frac{100}{n} \sum_{i=1}^n \left| \frac{P_{exp} - P_{cal}}{P_{exp}} \right|$$

Where n is the amount of data points.



Chapter 3

Experiment

3.1 Chemicals and Equipment

3.1.1 Oil Properties

The oil sample is obtained from Fang oilfield maesoon area, the Northern oilfield in Thailand. The viscosity of oil is 34 cP at 70°C, light oil with 0.85 g/cm³ density and the acid number of 0.89 mg KOH/g.

The composition of oil ranges from C7 to C35+ alkane and the distribution are as shown in Table 3.1.

Table 3.1 Composition of oil sample
(Saengnil, 2015)

Component	Percent by weight (percent)
C7	0.05
C8	0.68
C9	0.93
C10	1.00
C11	1.45
C12	1.84
C13	3.06
C14	3.52
C15	4.86
C16	3.87
C17	4.71
Pristane (C19H40)	2.44
C18	3.49

Phytane (C ₂₀ H ₄₂)	0.82
C19	3.89
C20	4.41
C21	4.81
C22	4.48
C23	4.97
C24	4.26
C25	4.42
C26	4.33
C27	4.56
C28	3.58
C29	3.97
C30	3.72
C31	3.27
C32	2.87
C33	3.64
C34	1.70
C35+	4.40

The Density of oil sample as shown in Table 3.2.

Table 3.2 Density of oil sample

Temperature (°C)	Oil density (g/cm ³)
70	0.850
80	0.849
90	0.848

3.1.2 Produced water Composition

Produced water composition at Fang oilfield as shown in Table 3.3

Table 3.3 Composition of the produced water
(Saengnil, 2015)

Chemical ions	Concentration (ppm)
Sodium, Na	256
Calcium, Ca	6.58
Magnesium, Mg	2.13
Barium, Ba	0.74
Chloride, Cl	21
Sulfate, SO ₄	18.7
Carbonate, CO ₃	54.0
Bicarbonate, HCO ₃	598
Hydroxide, OH	0

3.1.3 Equipment

Based on the objectives of this study, the viscosity measurements are preceded by Brookfield viscometer model LVDV2T with spindle number 40Z, 0.3 to 3000 cP, and 52Z, 4 to 92,000 cP as shown in Figure 3.1. Temperature is controlled by using a controlled temperature bath model Julabo F26 with $\pm 1.0^\circ\text{C}$ accuracy and glycol is used as a heating/cooling media.

The droplet size distribution is investigated by light microscope with trinocular head model Nikon japan 66788 1.5x with 200 times and eyepiece for droplet size measurement.

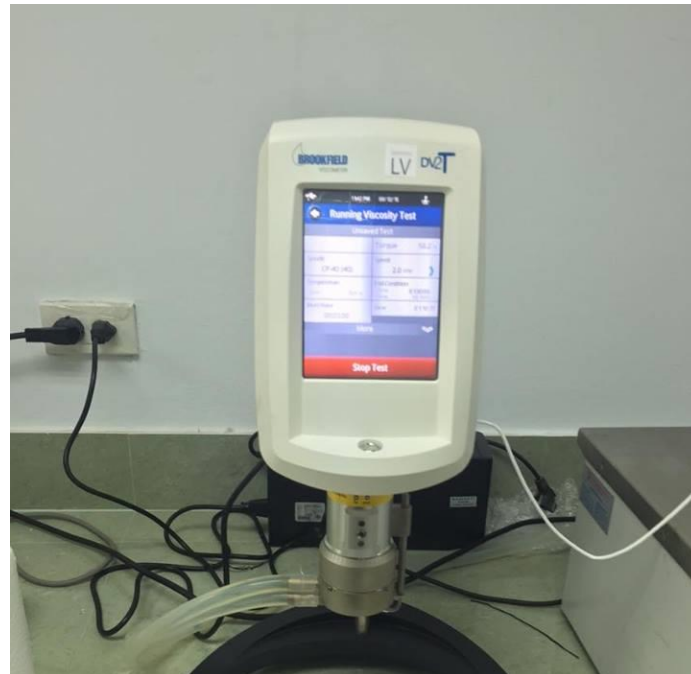


Figure 3.1 Brookfield viscometer model LVDV2T



Figure 3.2 Glycol solution bath

3.2 Experiment Procedure

3.2.1 Viscosity measurement

Verification of equipment is the first step of experiment to verify the equipment with standard solutions. Which are prepared and procedure by Brookfield Viscometer with spindle number 40Z and 52Z is used. Viscosity measurement of standard solutions is 498 cP and 989 cP at 25°C .They are tasted for 90 minutes and recorded for every 3 minutes with temperature of 25°C.

Emulsion preparation

The emulsion is prepared from mixing oil and water in volume percent to estimate percent water content at speed of 600 rpm for 15 minutes and used 0.5 ml sample for measurement. The temperature of emulsions is controlled at 50°C, the lowest temperature of condition in this study, by circulating glycol solution bath.

Data Collection

The measurement is performed for 90 minutes and recorded for every 3 minutes. Therefore, the viscosity of each sample is shown for 30 data and plotted them in graph.

3.2.2 Experiment conditions

The experiment conditions are operated by various at temperature of 50°C, 60°C, the spindle number 52Z is selected for high viscosity emulsion and at 70°C and 80°C spindle number 40Z is used.

The experiment operated at shear rate of $3.75s^{-1}$, $7.5s^{-1}$, $15s^{-1}$, $30s^{-1}$ and $60s^{-1}$. The emulsion is prepared at water content of 0percent 20percent 40percent and 60percent. All conditions are shown in Table 3.4

Table 3.4 Experimental operating conditions for this study

Parameter	Value
Temperature (°C)	50,60,70, and 80
Water content (percent)	0, 20, 40 and 60
Shear rate (s)	3.75, 7.5, 15, 30, and 60

3.2.3 Droplets size measurement

From the viscosity measurement, the sample is taken to measure the droplet size by using microscope with 200 times magnification and photograph of emulsion is taken. Finally, droplet size distribution is plotted in graph for discussion.

3.3 Correlation development

The correlations used in this study are adapted from the literature (Ronningsen 1995, Farah et. al 2005, Al-Roomi 2004) and applied to fit with these experimental data.

3.3.1 Ronningsen's correlation:

$$\ln \eta_r = k_1 + k_2 t + k_3 + k_4 t \phi \quad (3.1)$$

Where η_r is relative viscosity, t is temperature, ϕ is water content and k_1, k_2, k_3, k_4 are constant of correlation.

3.3.2 Farah's correlation :

Equation's Farah was explicated from Richardson and Ronningsen.

$$\ln(\ln(v + 0.7)) = k_1 + k_2 V + k_3 \ln T + k_4 V \ln T \quad (3.2)$$

Where v is relative viscosity, V is water content, T is temperature and k_1, k_2, k_3, k_4 are constant of correlation.

3.3.3 Al-Roomi's correlation:

Al-roomi (2004) studied rheological model and correlated the parameters, water content temperature and shear rate.

$$\mu = a\gamma^b \exp(c\phi + \frac{d}{T}) \quad (3.3)$$

Where a, b, c and d are constant, μ is viscosity, γ is shear rate, ϕ is water content.



Methodology flowchart of the study can be shown in Figure 3.4

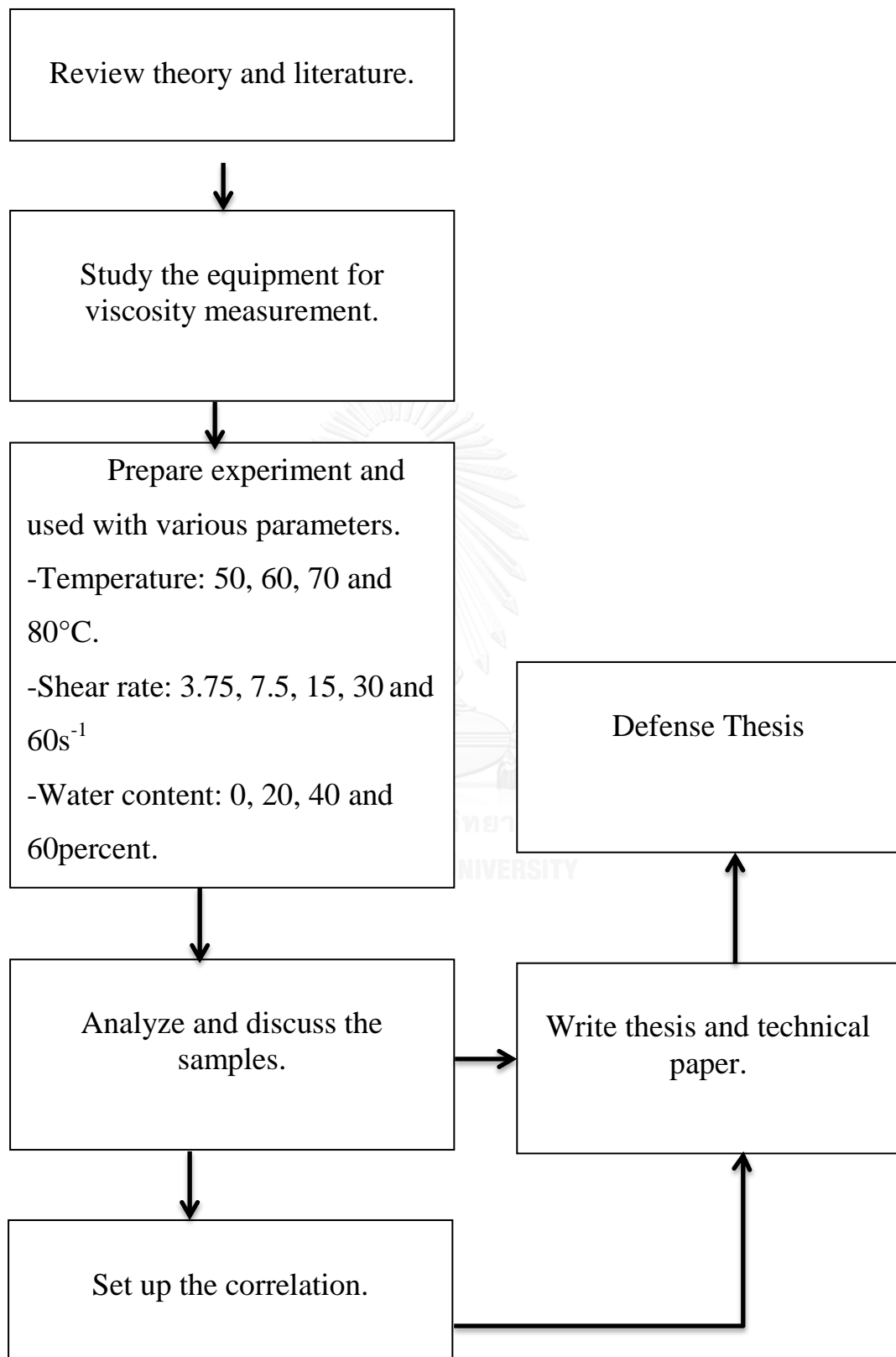


Figure 3.2 Methodology flowcha

Chapter 4

Results and Discussions

The effect of temperature, water content and shear rate on viscosity of oil and its emulsion and droplets size distribution are discussed in this chapter. Moreover the prediction of emulsion with correlations compared with experimental results is also presented in this chapter.

4.1 Verification of the equipment

The viscosity of standard solution supplied by Brookfield is 498 cP and 985 cP at temperature of 25°C. The viscosity of standard solution from experimental is at 499.5 cP and 984.2 cP at 25 °C measuring for 90 minutes. Percent of different is 0.38 percent so if low percent of deviation that mean equipment is well and can use for measuring.

4.2 Effect of temperature on viscosity

The results of the effect of temperature from 50°C to 80°C are shown in Table 4.1 with the several of water content and shear rate. The results shows that viscosities of the light oil and its emulsions decrease as temperature increase because higher temperature makes oil and emulsion molecules obtain higher energy from heat thus making them less viscous and oil can flow easily (Schramm, 1992).

From Figure 4.1, the viscosity of emulsion with 0 percent water content which is original oil from oilfield is decreased with increasing temperature. The viscosity of original oil extremely decrease from 70°C to 80°C, that show the high temperature is good in viscosity reduction.

The viscosity of emulsion at 20, 40 and 60 percent water content is shown Figure 4.2 to 4.4 respectively, the graph of viscosity at temperature 50°C and 60°C in each shear rate are difference more than original oil but temperature of 70°C and 80°C total similar with original oil. At low temperature, the temperature effect much on viscosity of emulsion.

Table 4.1 Viscosities of oil and its emulsion.

Temperature (°c)	Shear rate (s)	Viscosity (cP) with water content (percent)			
		0	20	40	60
50	3.75	90.02	220.70	401.20	1072.00
	7.5	87.83	166.80	313.50	397.20
	15	85.53	157.20	294.80	324.90
	30	82.32	146.20	229.75	257.64
	60	80.31	125.60	189.92	193.27
60	3.75	62.01	131.20	311.50	433.90
	7.5	55.18	111.90	213.70	343.30
	15	56.41	103.20	153.00	215.23
	30	52.02	93.02	143.90	169.23
	60	42.50	75.66	119.20	122.53
70	3.75	51.40	106.01	178.80	328.30
	7.5	45.37	72.04	142.80	206.10
	15	38.32	65.00	73.50	169.90
	30	27.29	56.43	94.20	143.90
	60	20.23	40.31	52.09	74.900
80	3.75	37.40	78.48	128.00	224.30
	7.5	35.80	70.20	129.10	154.20
	15	34.34	47.36	61.40	121.50
	30	21.52	35.97	56.97	66.97
	60	16.43	28.22	42.17	53.25

The ranges of percent different of viscosity at various temperatures compare with viscosity at 50°C in each water content 0.03-0.75percent. The percent at low different with increase temperature.

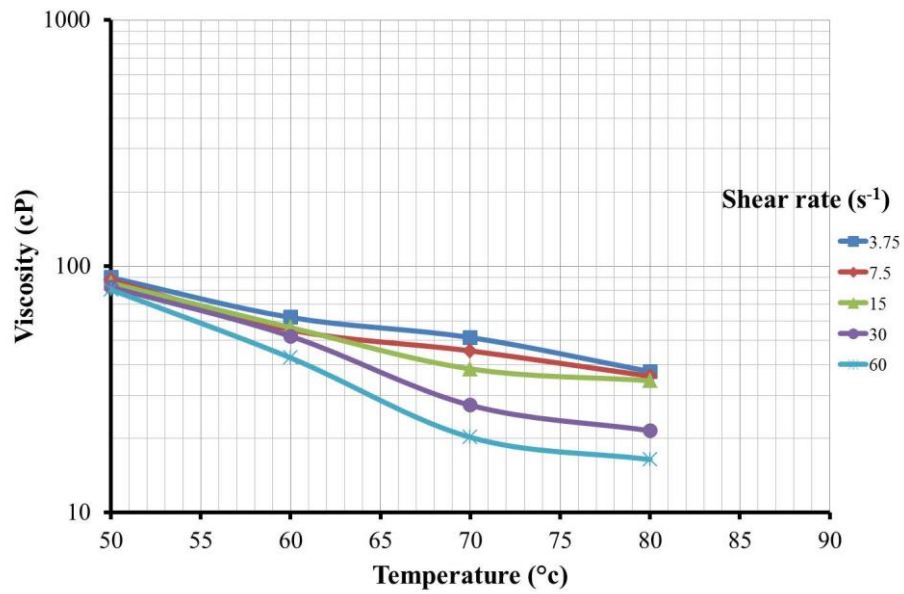


Figure 4.1 Effect of temperature on viscosity with 0 percent water content

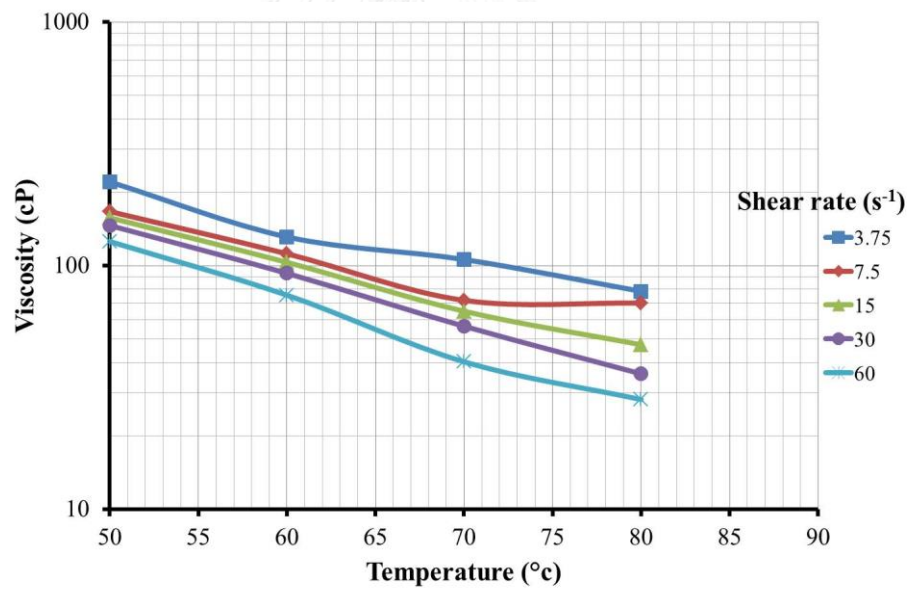


Figure 4.2 Effect of temperature on viscosity with 20 percent water content

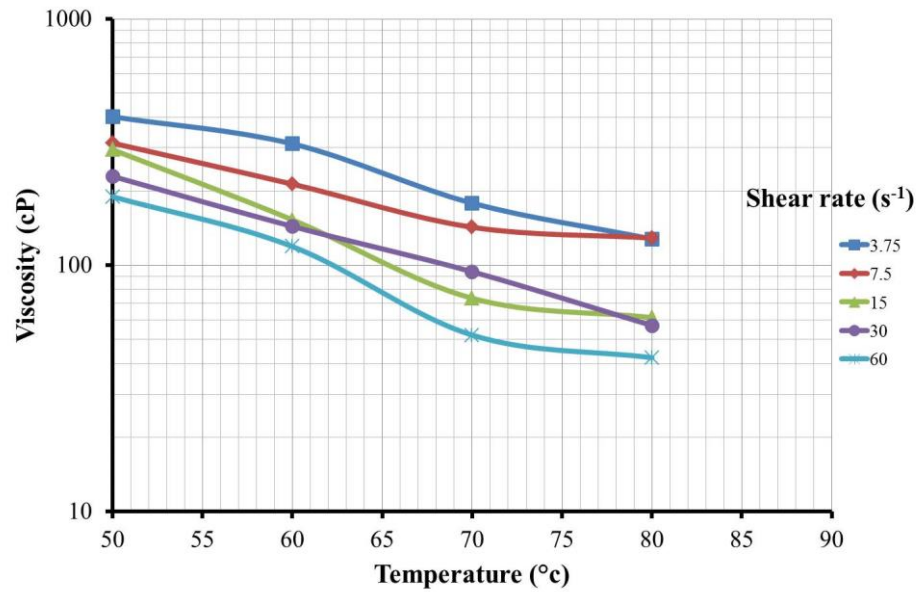


Figure 4.3 Effect of temperature on viscosity with 40 percent water content

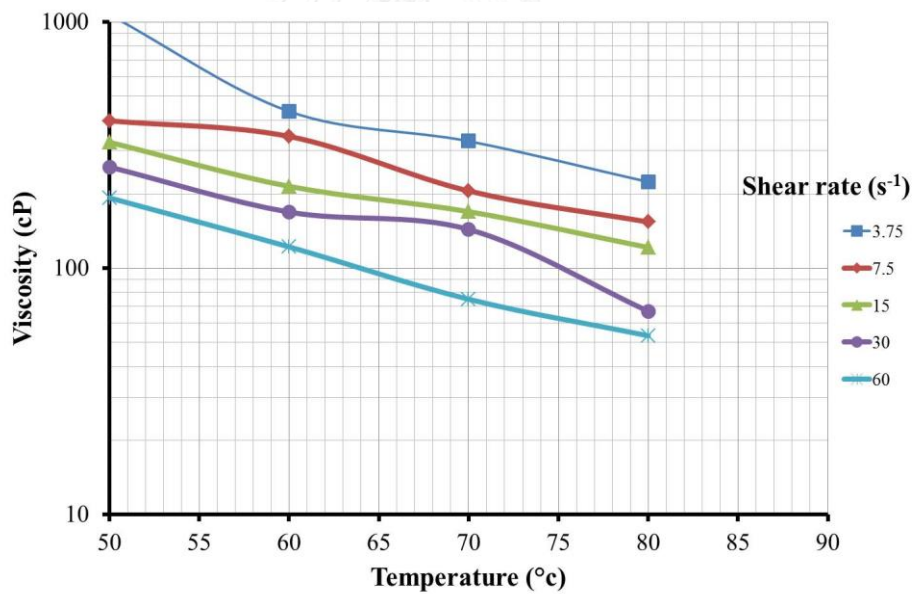


Figure 4.4 Effect of temperature on viscosity with 60 percent water content

4.3 Effect of water content on viscosity

Water contents for this experiment are at 0, 20, 40 and 60 percent. The results of the viscosity of emulsion are shown in the Table 4.1 by comparing at the same conditions. The viscosity becomes higher when water content is increased because when volume of water increase, the droplet-droplet interaction and water-oil interfacial area are greater. The percent of water content has influence on emulsion's viscosity at high temperature because the viscosity of oil less and close to water's viscosity, 1 cP at 20°C.

Figures 4.5 to 4.9, for this experiment, 0 percent water content are original oil. The results of viscosity at all percent of water content are decrease when the water content increase but at 40-60 percent are wavy graph that happen because of the effect of average droplet size and droplet size distribution will be discuss in the next section.

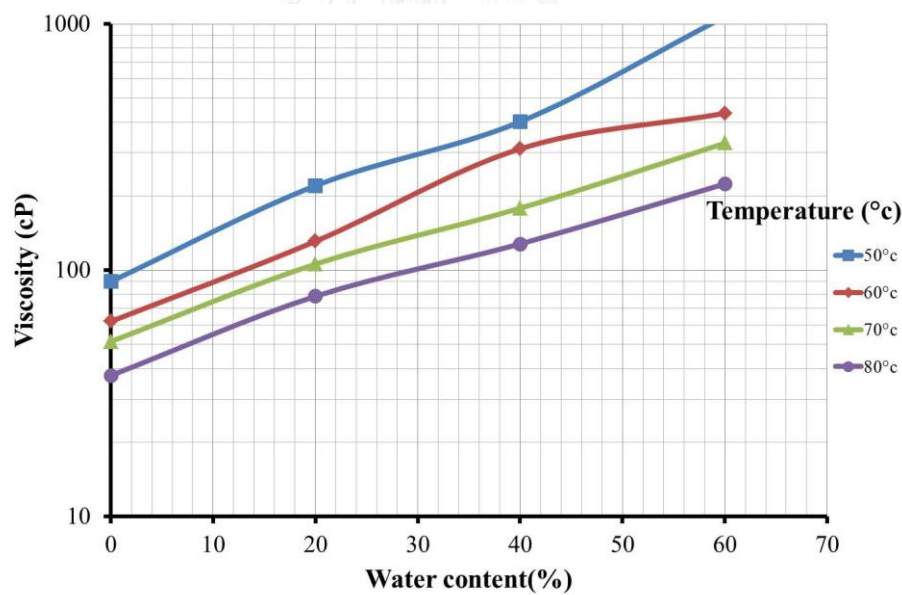


Figure 4.5 Effect of water content on viscosity at 3.75s^{-1} Shear rate

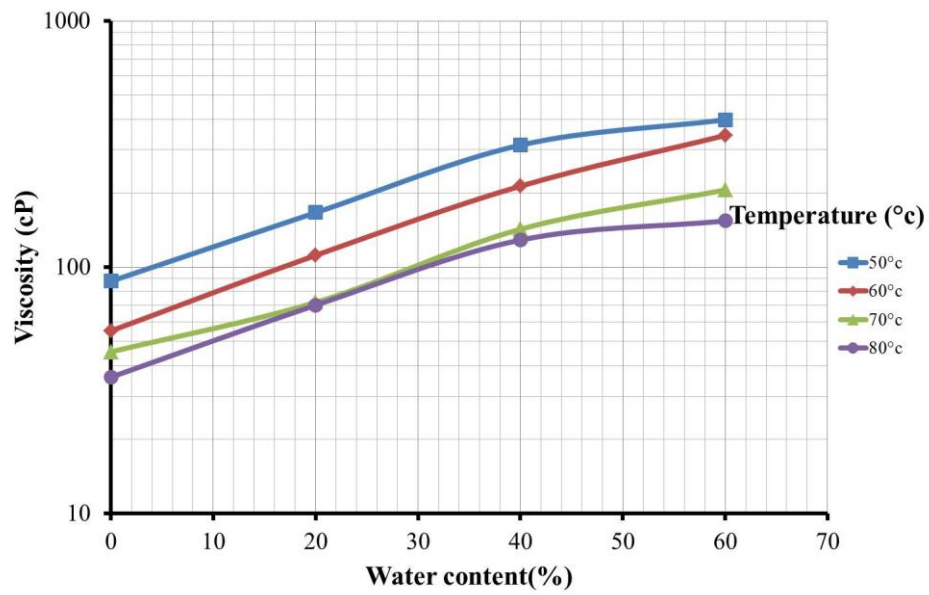


Figure 4.6 Effect of water content on viscosity at 7.5 s^{-1} Shear rate

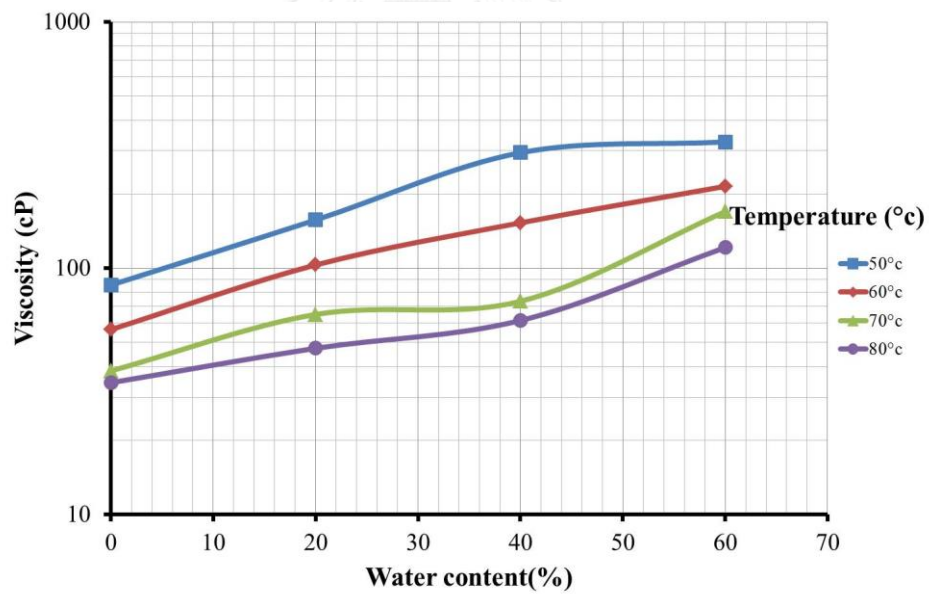


Figure 4.7 Effect of water content on viscosity at 15 s^{-1} Shear rate

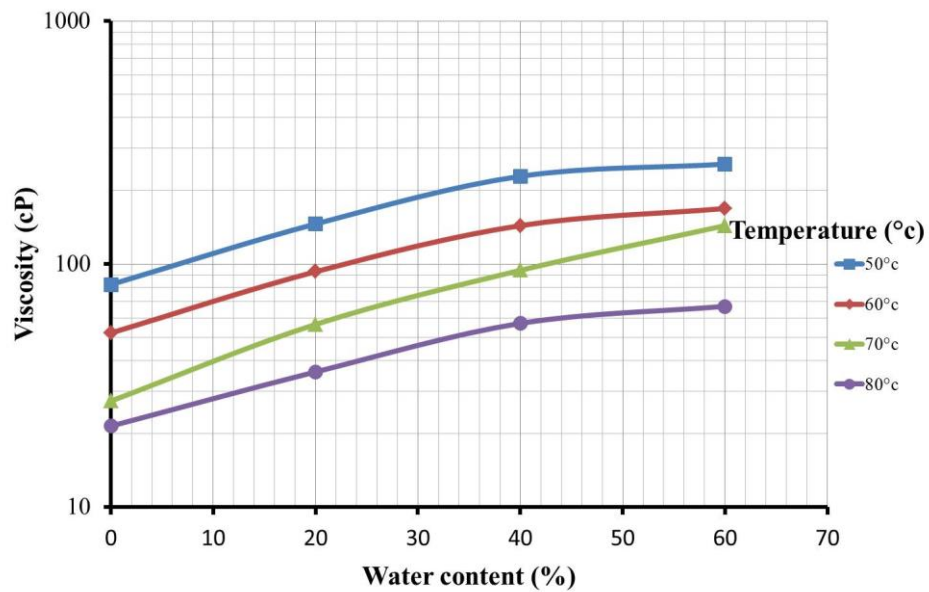


Figure 4.8 Effect of water content on viscosity at 30 s^{-1} Shear rate

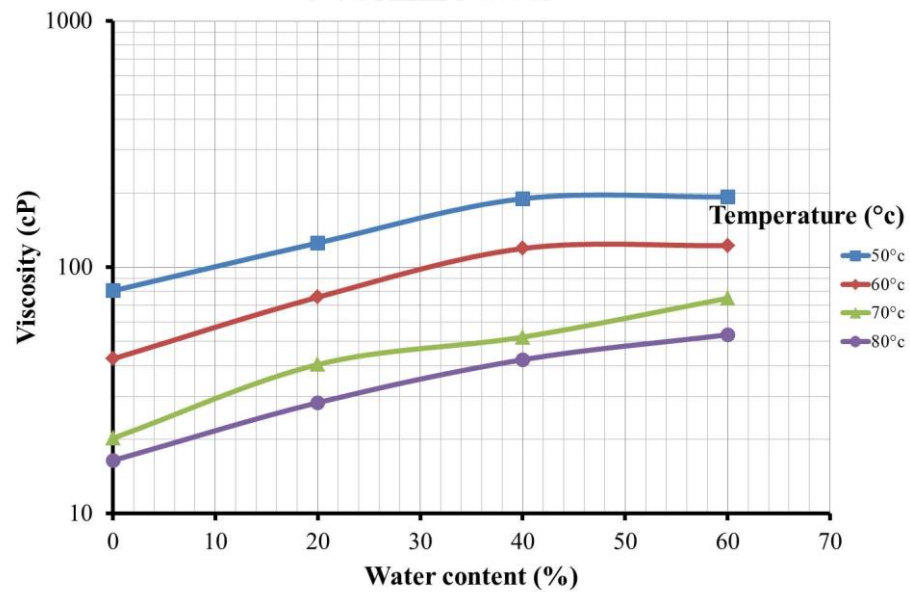


Figure 4.9 Effect of water content on viscosity at 60 s^{-1} Shear rate

The ranges of percent Deviation of viscosity at various water contents compare with original oil in each shear rate are 0.38percent-10.91percent. The higher percent Deviation at high water content than low water content.

4.4 Effect of shear rate on viscosity

The results of the effect of shear rate are shown in Table 4.1. Shear rate used for this study are 3.75, 7.5, 15, 30, 60 s^{-1} . As presented in Figure, the viscosity becomes lower with increasing shear rate. The shearing effects on the stability of the drop, oscillate in to smaller drops (Richardson, 1950). This phenomena can be explained from the break-up of water droplet to form smaller size as shown in next section. From this study presented this emulsion is Non-Newtonian fluid because increasing shear rate effect on decreasing viscosity.

The Figures 4.10 to 4.13 shows the viscosity of emulsion with various shear rate and water content from 50°C to 80°C. The results show that the viscosity is slightly decreased with increasing shear rate. At the high temperature, 70°C and 80°C, the viscosity extremely decreases as shown in the figures because of the effect of heat from high temperature which is presented in previous section.

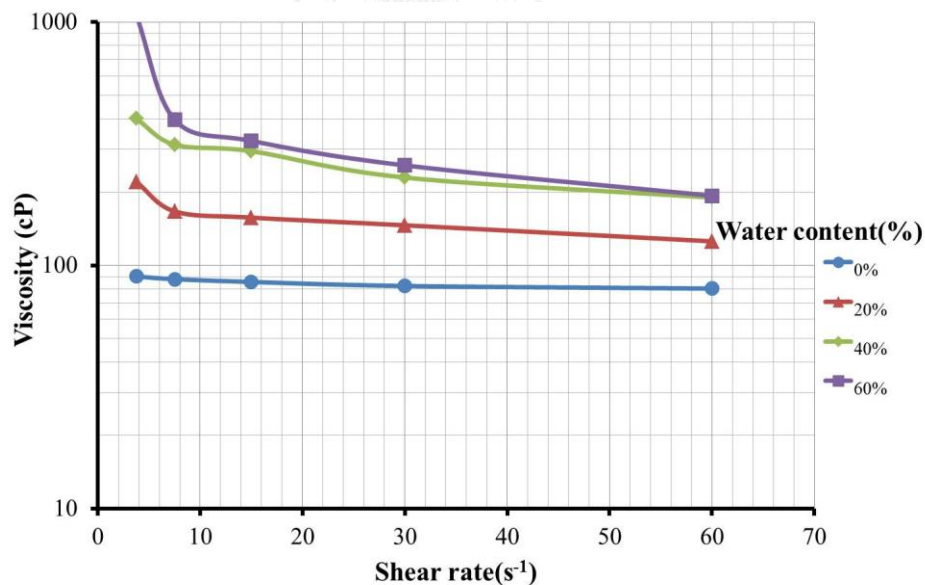


Figure 4.10 Effect of shear rate on viscosity at 50°C temperature.

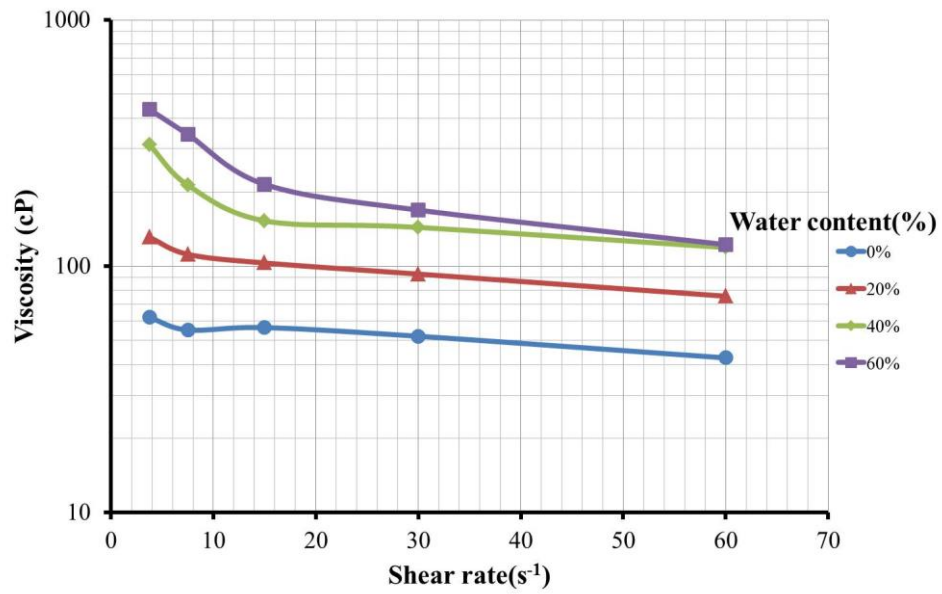


Figure 4.11 Effect of shear rate on viscosity at 60°C temperature.

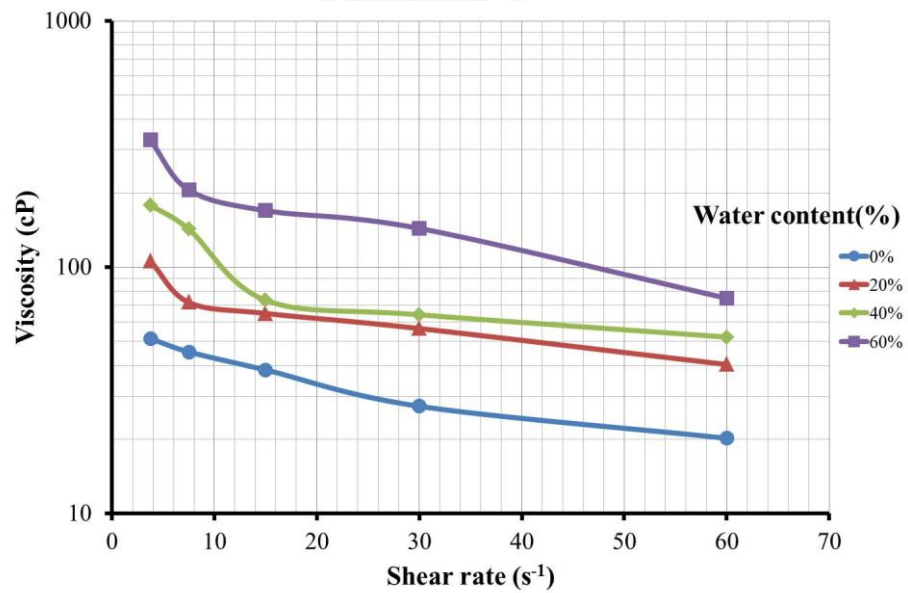


Figure 4.12 Effect of shear rate on viscosity at 70°C temperature.

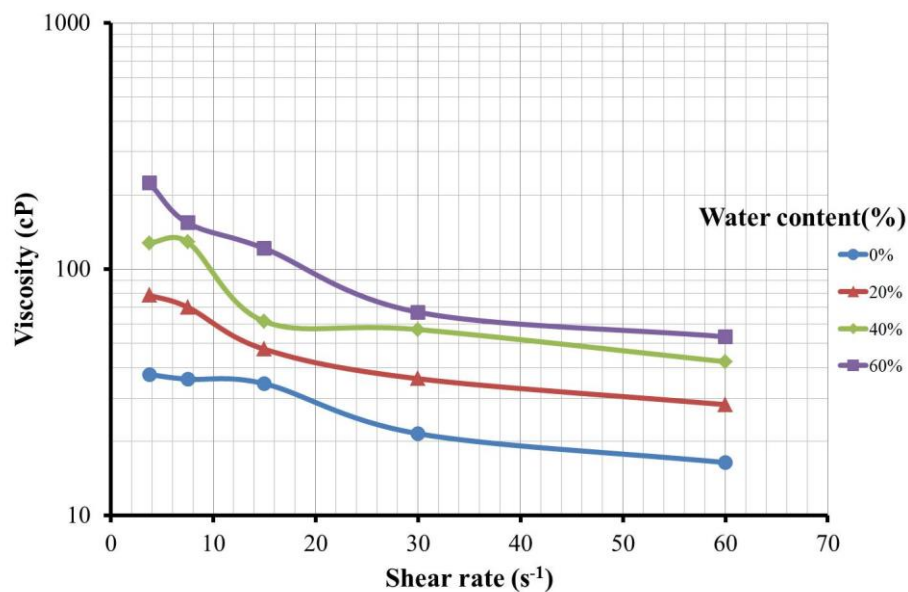


Figure 4.13 Effect of shear rate on viscosity at 80°C temperature.

4.5 Droplets size distribution

Droplets size distribution depends on oil and its emulsion type and conditions like water content, temperature and shear rate.

Figure 4.14, presents the water droplets dispersed in emulsion of oil with different water contents at 80°C and 15 s⁻¹ shear rate. (a), (b), (c) and (d) for water content at 0, 20, 40 and 60 percent, respectively. At 60 percent water content, the number of water droplets is more than others because the volume of water is higher.

For the effect of temperature on stability of emulsion is presented on Figure 4.15 (a), (b), (c) and (d) show the result of water droplets dispersed in emulsion of oil at 20 percent water content and 7.5 s⁻¹ shear rate with temperature 50, 60, 70 and 80°C, respectively. At high temperature, the droplets have higher energy from heat. And then the water droplets become smaller droplets. Emulsion with smaller droplets becomes stable emulsion.

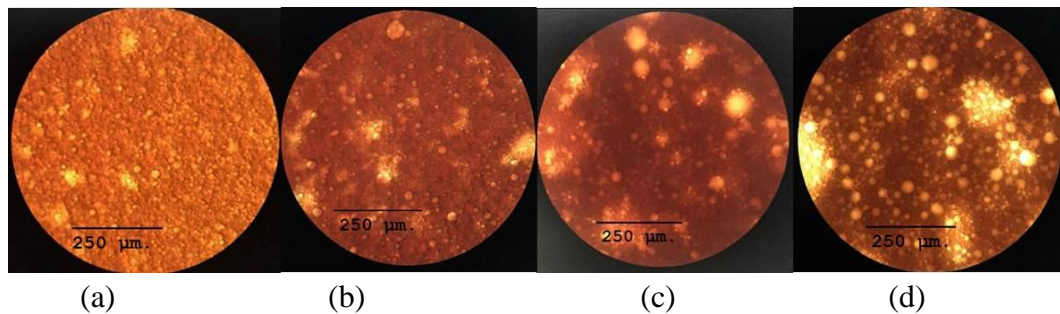


Figure 4.14 Microscopic observation of water droplet at 15 s^{-1} shear rate in water content 0percent (b) water content 20percent (c) water content 60percent and (d) water content 60percent at temperature 80°C

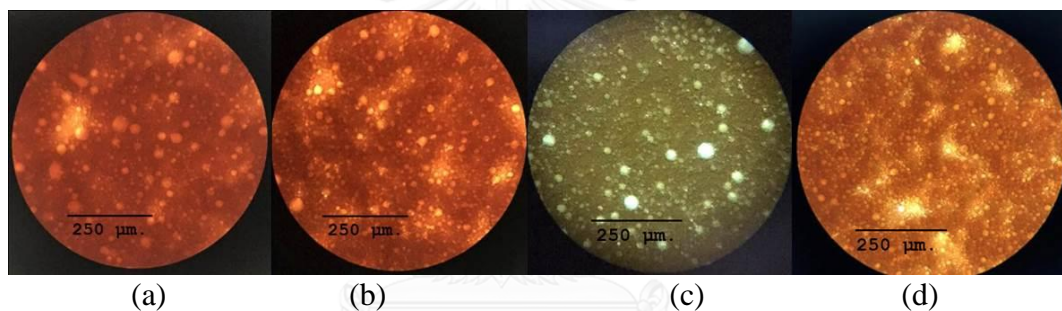


Figure 4.15 Microscopic observation of water droplet in 20 percent in temperature 50°C (b) temperature 60°C (c) temperature 70°C and (d) temperature 80°C at 7.5 s^{-1} shear rate.

For shear rate, it is obvious that the droplets become smaller with increasing shear rate when high shear rate is applied, the droplets of water split to small droplets thus making emulsion stable because interfacial tension and area of oil and water is increased. Figure 4.16 shows the result of water droplets dispersed in emulsion of oil with different shear rate at 70°C and 20percent water content.

Figure 4.19 to 4.21, shows the droplets size distribution at 20percent water content with different shear rates. At low shear rate, the water droplets distribute in many size as shown in figure 4.17 and 4.18.

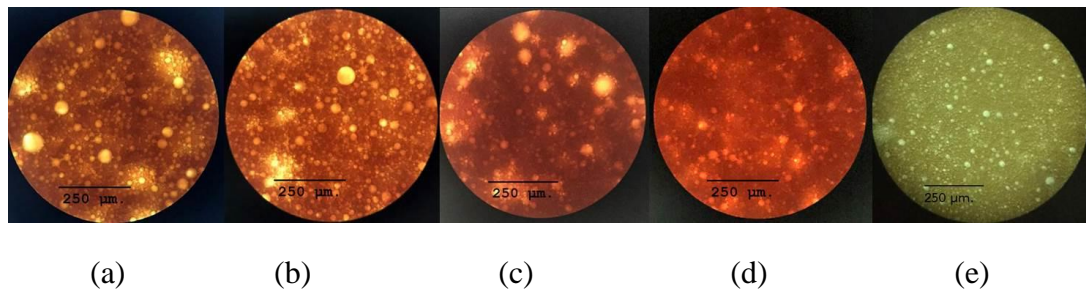


Figure 4.16 Microscopic observation of water droplet in 20percent in shear rate 3.75 s^{-1} (b) shear rate 7.5 s^{-1} (c) shear rate 15 s^{-1} (d) shear rate 30 s^{-1} and (e) shear rate 60 s^{-1} at 70°C temperature

At 15 s^{-1} to 60 s^{-1} shear rate, the droplets become distribute in smaller size and the size of droplets is less than 10 micron as shown in figure 4.19 to 4.21.

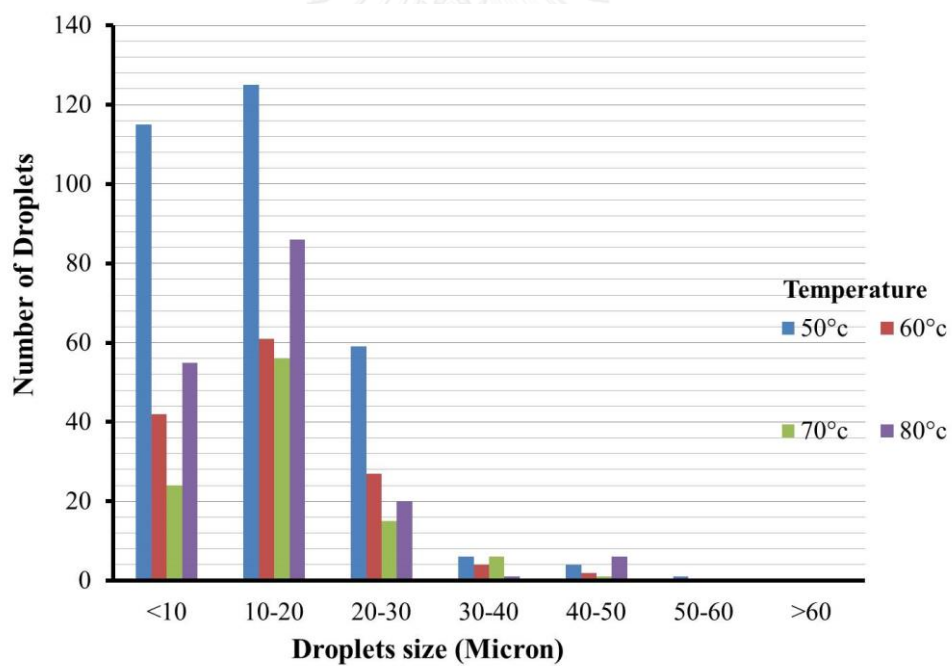


Figure 4.17 Droplets size distribution at 3.75 s^{-1} shear rate

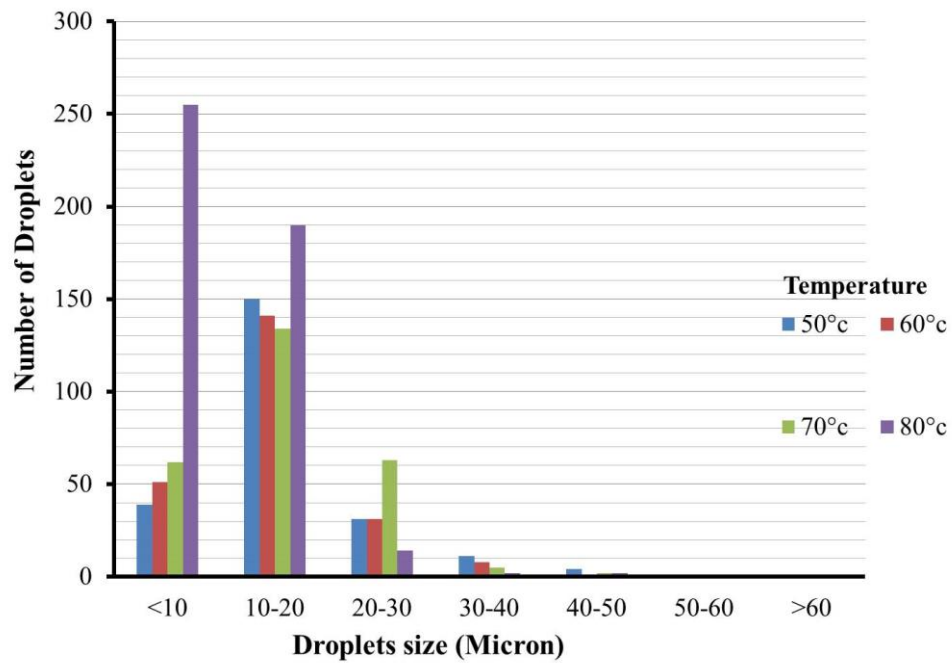


Figure 4.18 Droplets size distribution at 7.5 s^{-1} shear rate

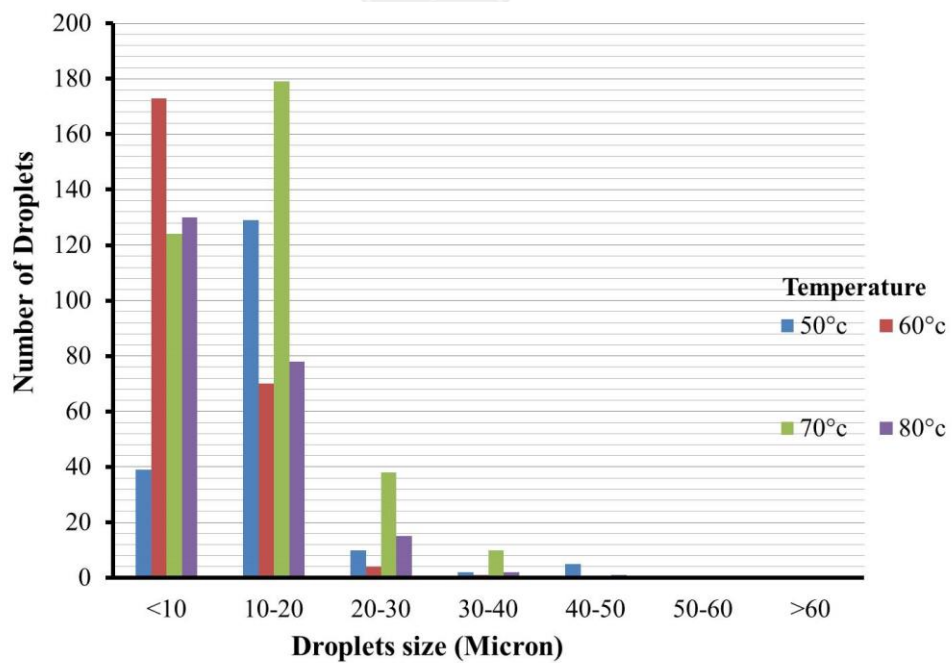


Figure 4.19 Droplets size distribution at 15 s^{-1} shear rate

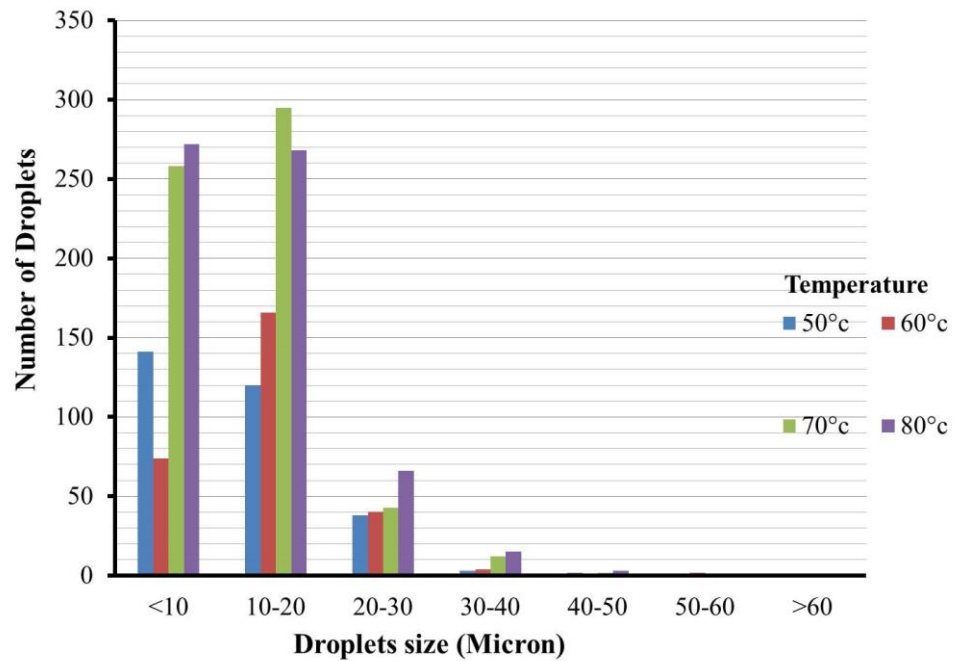


Figure 4.20 Droplets size distribution at 30 s⁻¹ shear rate

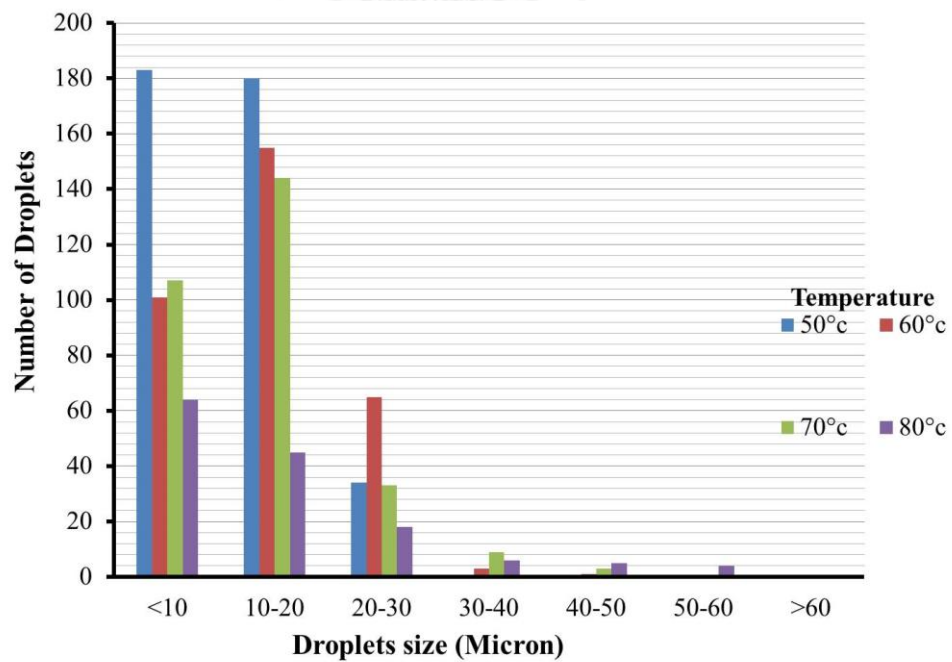


Figure 4.21 Droplets size distribution at 60 s⁻¹ shear rate

Correlation for predicting viscosity of emulsion

Ronningsen's Correlation;

$$\ln \eta_r = k_1 + k_2 t + k_3 + k_4 t \phi \quad (4.1)$$

Where η_r is relative viscosity, t is temperature, ϕ is water content and k_1, k_2, k_3, k_4 are constant of correlation.

From the experiment, there are five equations of Ronningsen's correlation. Each equation is shown in different shear rate because the correlation is only the function of temperature and water content.

The constants, k_1 - k_4 , can be calculated and presented in table 4.15

Table 4.2 The constants of Ronningsen's correlation from mathematical method.

Shear rate ($\dot{\gamma}$)	k_1	k_2	k_3	k_4
3.75	-0.09547803	0.00389691	0.05790337	-0.00041418
7.5	0.16498184	0.00050101	0.02898818	-0.00007802
15	0.35867019	-0.01979396	0.00681927	0.00021855
30	0.52025148	-0.00338547	0.00884986	0.00012565
60	0.44885440	-0.00183647	0.00136998	0.00018735

The comparison between experiment data and calculated data in each equation with different shear rate is shown in table 4.3 to 4.7. The range of percent difference is 0.55 -28.18.

Experimental data and predicted data from shear rate 3.75, 7.5, 15, 30 and 60 s^{-1} are compared and shown in Figures 4.22 to 4.26 respectively. The results presented experimental data get along well with calculated data as shown in Figures 4.22 to 4.26.

Table 4.3 experiment data and calculated data at 3.75s^{-1} shear rate equation.

Temperature (°c)	Water content (percent)	Viscosity (cP)		percent Difference
		Experiment	Calculated	
50	20	220.70	209.20	5.21
	40	401.20	440.18	9.72
	60	1072.00	926.18	13.60
60	20	131.20	137.92	5.12
	40	311.50	267.13	14.24
	60	433.90	517.39	19.24
70	20	106.01	109.42	3.22
	40	178.80	195.08	9.11
	60	328.30	347.79	5.94
80	20	78.48	76.20	2.91
	40	128.00	125.05	2.30
	60	224.30	205.22	8.51

Table 4.4 experiment data and calculated data at 7.5s^{-1} shear rate equation.

Temperature (°c)	Water content (percent)	Viscosity (cP)		percent Difference
		Experiment	Calculated	
50	20	166.80	175.42	5.17
	40	313.50	289.72	7.59
	60	397.20	478.50	20.47
60	20	111.90	109.05	2.55
	40	213.70	177.31	17.03
	60	343.30	288.32	16.02
70	20	72.04	88.72	23.15
	40	142.80	142.02	0.55
	60	206.10	227.35	10.31
80	20	70.20	69.26	1.34
	40	129.10	109.17	15.44
	60	154.20	172.05	11.58

Table 4.5 experiment data and calculated data at 15s^{-1} shear rate equation

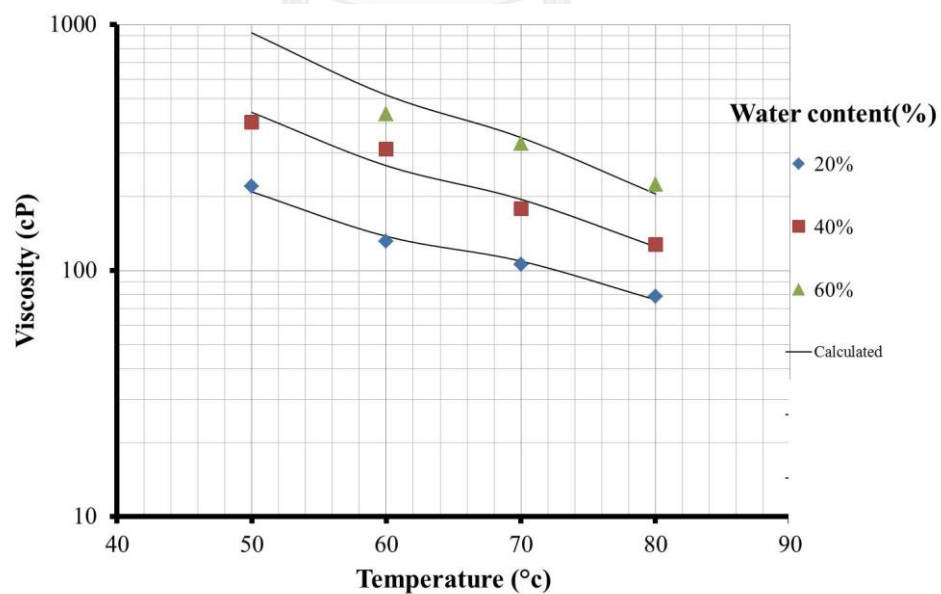
Temperature (°c)	Water content(percent)	Viscosity (cP)		percent Difference
		Experiment	Calculated	
50	20	157.20	176.40	12.21
	40	294.80	251.57	14.66
	60	324.90	358.76	10.42
60	20	103.20	99.72	3.37
	40	153.00	148.56	2.90
	60	215.23	221.32	2.83
70	20	65.00	59.06	9.14
	40	73.50	90.36	22.94
	60	169.90	140.63	17.23
80	20	47.36	44.59	5.85
	40	61.40	72.50	18.08
	60	121.50	117.88	2.98

Table 4.6 experiment data and calculated data at 30s^{-1} shear rate equation

Temperature (°c)	Water content(percent)	Viscosity (cP)		percent Difference
		Experiment	Calculated	
50	20	146.20	158.26	8.25
	40	229.75	214.19	6.77
	60	257.64	289.90	12.52
60	20	93.02	99.14	6.58
	40	143.90	137.59	4.38
	60	169.23	190.96	12.84
70	20	56.43	51.56	8.63
	40	94.20	73.38	22.10
	60	143.90	104.43	27.43
80	20	35.97	40.30	12.04
	40	56.97	59.82	5.00
	60	66.97	85.84	28.18

Table 4.7 experiment data and calculated data at 60s^{-1} shear rate equation.

Temperature (°c)	Water content(percent)	Viscosity (cP)		percent Difference
		Experiment	Calculated	
50	20	125.60	142.26	13.26
	40	189.92	176.34	7.15
	60	193.27	218.58	13.10
60	20	75.66	76.74	1.43
	40	119.20	98.75	17.16
	60	122.53	127.08	3.71
70	20	40.31	37.23	7.64
	40	52.09	49.74	4.51
	60	74.90	66.46	11.27
80	20	28.22	30.82	9.21
	40	42.17	42.75	1.38
	60	53.25	59.29	11.34

Figure 4.22 Experiment data and calculated data at 3.75s^{-1} shear rate.

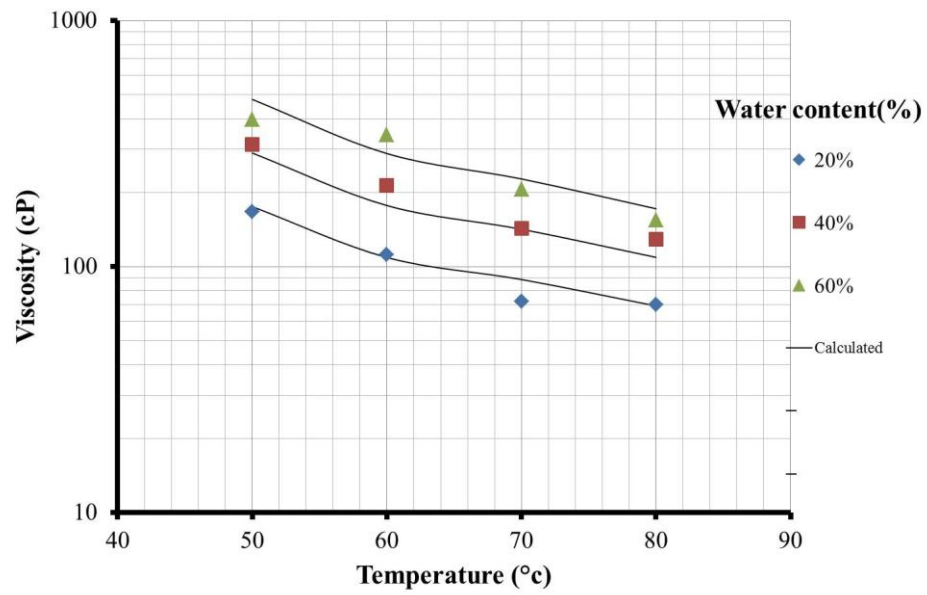


Figure 4.23 Experiment data and calculated data at 7.5s^{-1} shear rate

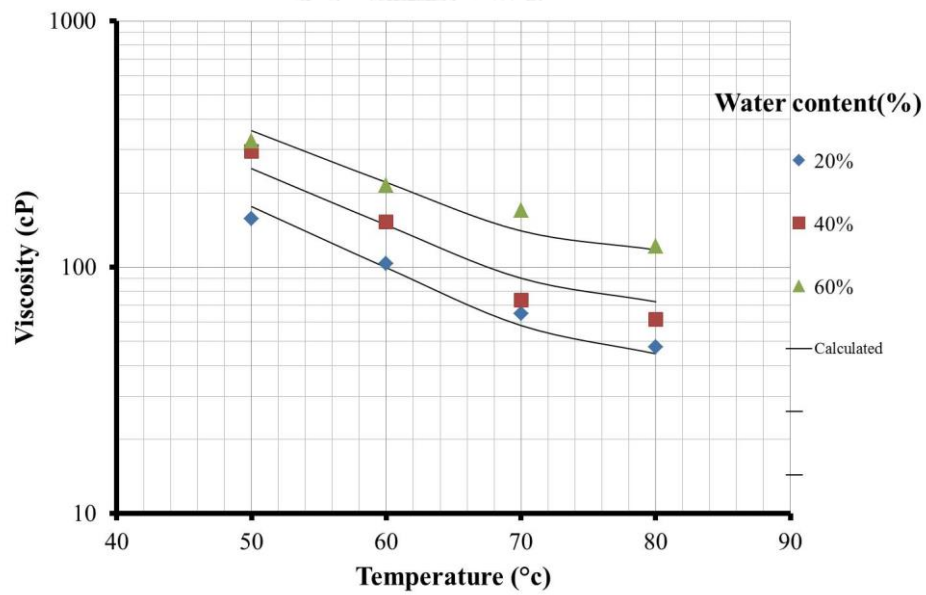


Figure 4.24 Experiment data and calculated data at 15s^{-1} shear rate.

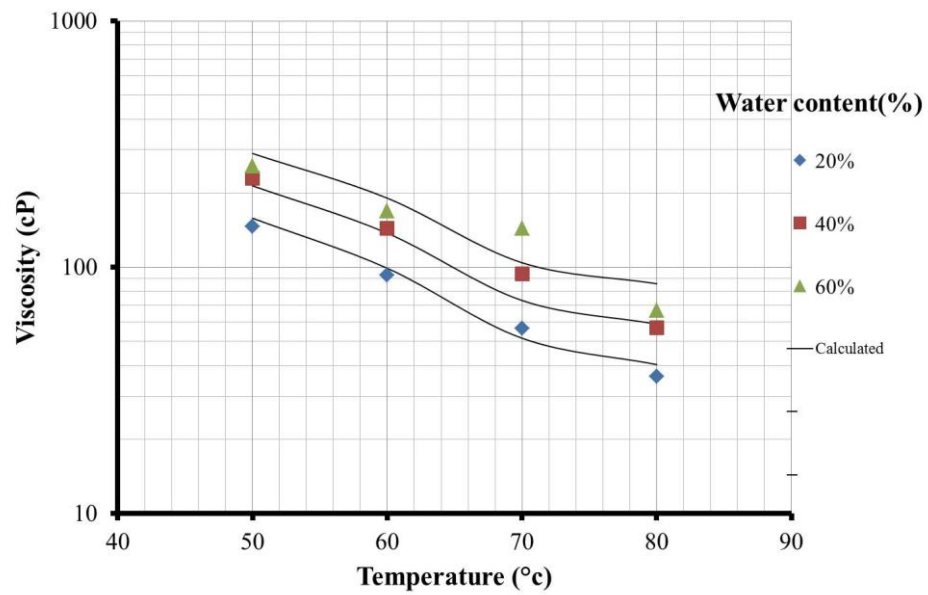


Figure 4.25 Experiment data and calculated data at 30s^{-1} shear rate

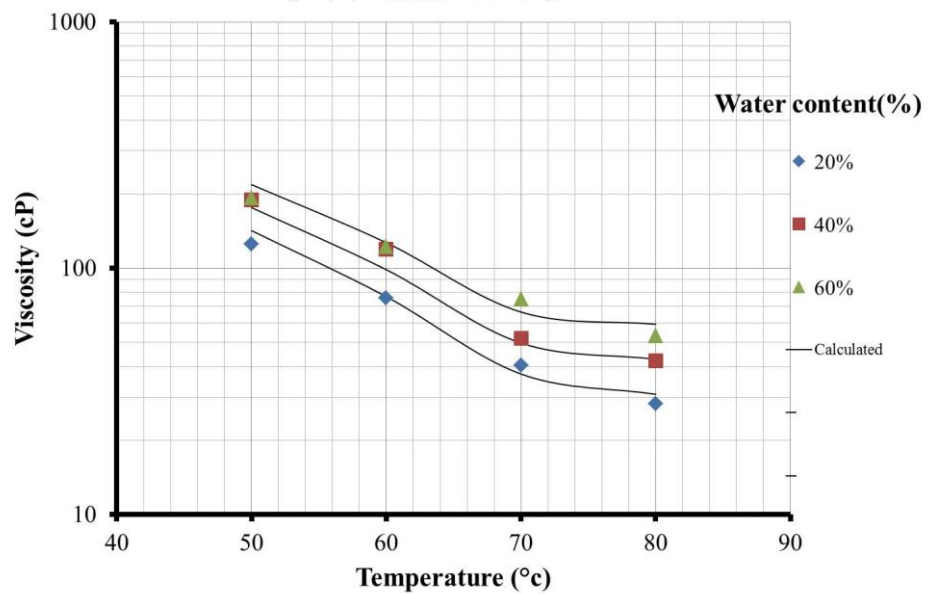


Figure 4.26 Experiment data and calculated data at 60s^{-1} shear rate

Farah's correlation

$$\ln(\ln(v + 0.7)) = k_1 + k_2V + k_3 \ln T + k_4V \ln T \quad (4.2)$$

Where v is relative viscosity, V is water content, T is temperature and k_1, k_2, k_3, k_4 are constants of correlation.

Each equation is shown in different shear rate because the correlation is the function of temperature and water content like Roningsen's correlation.

The constants, k_1 - k_4 , can be calculated and presented in Table 4.8.

Table 4.8 The constants of Farah's correlation from mathematical method.

Shear rate (s)	k_1	k_2	k_3	k_4
3.75	-0.08014666	0.05469839	0.04665192	0.00903238
7.5	-0.10284203	0.01934167	0.05206687	-0.00104794
15	3.59171253	-0.03441379	0.96975512	-0.01168630
30	0.24207253	-0.00911008	0.12360783	-0.00490164
60	-0.29959895	-0.01692001	-0.00777263	-0.00633851

The results presented experimental data get along well with calculated data as shown in Tables 4.9 to 4.13 and Figures 4.27 to 4.31. The range of percent difference is 0.02 – 29.89.

Table 4.9 Experiment data and calculated data at 3.75 s^{-1} shear rate equation.

Temperature (°c)	Water content(percent)	Viscosity (cP)		percent Difference
		Experiment	Calculated	
50	20	220.70	216.42	1.94
	40	401.20	414.44	3.30
	60	1072.00	988.06	7.83
60	20	131.20	140.42	7.03
	40	311.50	248.42	20.25
	60	433.90	520.43	19.94
70	20	106.01	110.80	5.42
	40	178.80	184.12	2.98
	60	328.30	349.94	6.59
80	20	78.48	77.32	1.48
	40	128.00	122.08	4.63
	60	224.30	214.93	4.18

Table 4.10 Experiment data and calculated data at 7.5 s^{-1} shear rate equation

Temperature (°c)	Water content(percent)	Viscosity (cP)		percent Difference
		Experiment	Calculated	
50	20	166.80	176.86	6.03
	40	313.50	278.72	11.09
	60	397.20	489.75	23.30
60	20	111.30	109.15	1.93
	40	213.70	170.25	20.33
	60	343.30	294.75	14.14
70	20	72.01	88.41	22.77
	40	142.80	136.72	4.26
	60	206.10	233.82	13.45
80	20	70.20	68.87	1.89
	40	129.10	105.73	18.10
	60	154.20	178.94	16.04

Table 4.11 Experiment data and calculated data at $15s^{-1}$ shear rate equation.

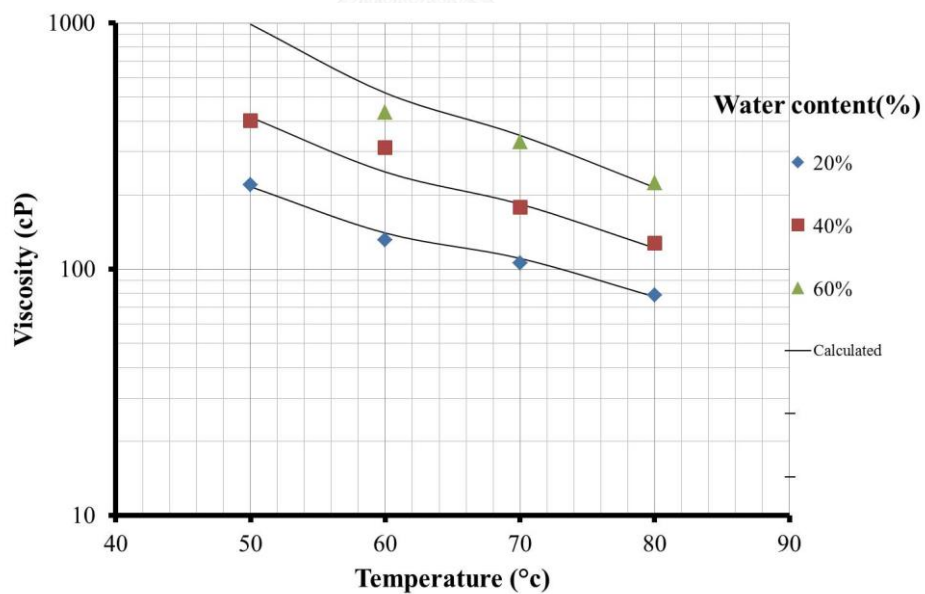
Temperature (°c)	Water content(percent)	Viscosity (cP)		percent Difference
		Experiment	Calculated	
50	20	157.20	178.35	13.45
	40	294.80	249.05	15.52
	60	324.90	367.99	13.26
60	20	103.20	98.66	4.40
	40	153.00	142.9	6.60
	60	215.23	221.81	3.06
70	20	65.00	58.42	10.12
	40	73.50	86.52	17.71
	60	169.90	139.97	17.62
80	20	47.36	46.85	1.08
	40	61.40	70.63	15.03
	60	121.50	117.89	2.97

Table 4.12 Experiment data and calculated data at $30s^{-1}$ shear rate equation

Temperature (°c)	Water content(percent)	Viscosity (cP)		percent Difference
		Experiment	Calculated	
50	20	146.20	157.50	7.73
	40	229.75	208.89	9.08
	60	257.64	288.71	12.06
60	20	93.02	98.92	6.34
	40	143.90	134.65	6.43
	60	169.23	192.60	13.81
70	20	56.43	51.62	8.52
	40	94.20	71.85	23.73
	60	143.90	105.87	26.43
80	20	35.97	40.53	12.68
	40	56.98	57.50	0.91
	60	66.98	87.00	29.89

Table 4.13 Experiment data and calculated data at 60s^{-1} shear rate equation

Temperature (°C)	Water content(percent)	Viscosity (cP)		percent Difference
		Experiment	Calculated	
50	20	125.60	140.13	11.57
	40	189.92	172.57	9.14
	60	193.27	217.32	12.44
60	20	75.66	76.52	1.14
	40	119.20	97.67	18.06
	60	122.53	128.61	4.96
70	20	40.31	37.40	7.22
	40	52.09	49.29	5.38
	60	74.90	67.58	9.77
80	20	28.22	31.40	11.27
	40	42.17	42.16	0.02
	60	53.25	60.01	12.69

Figure 4.27 Experiment data and calculated data at 3.7s^{-1} shear rate

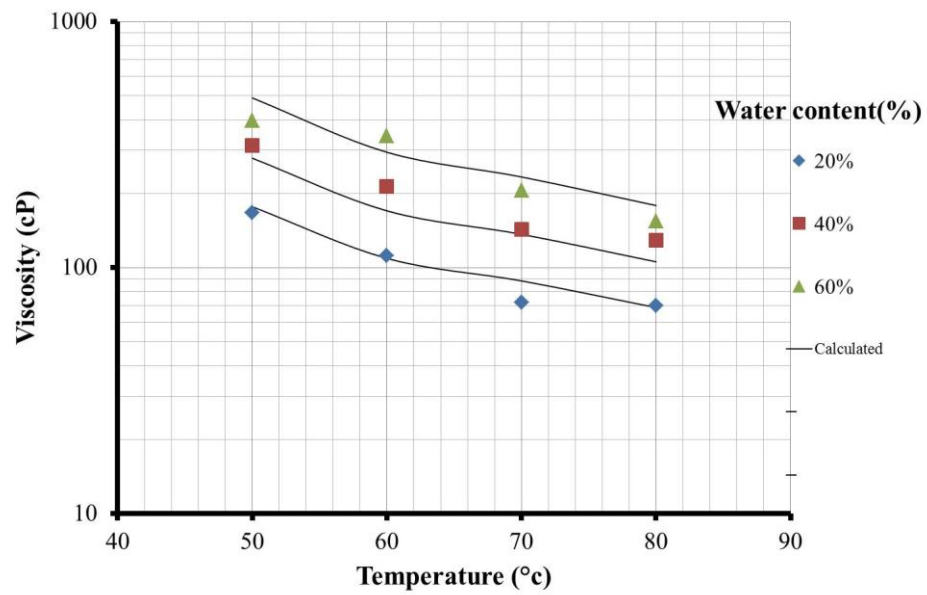


Figure 4.28 Experiment data and calculated data at 7.5s^{-1} shear rate

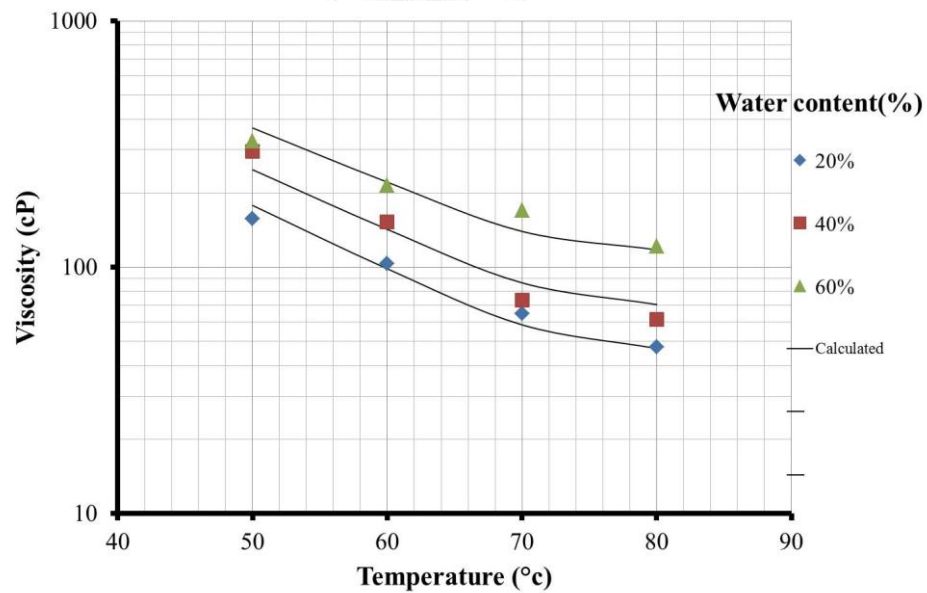


Figure 4.29 Experiment data and calculated data at 15s^{-1} shear rate

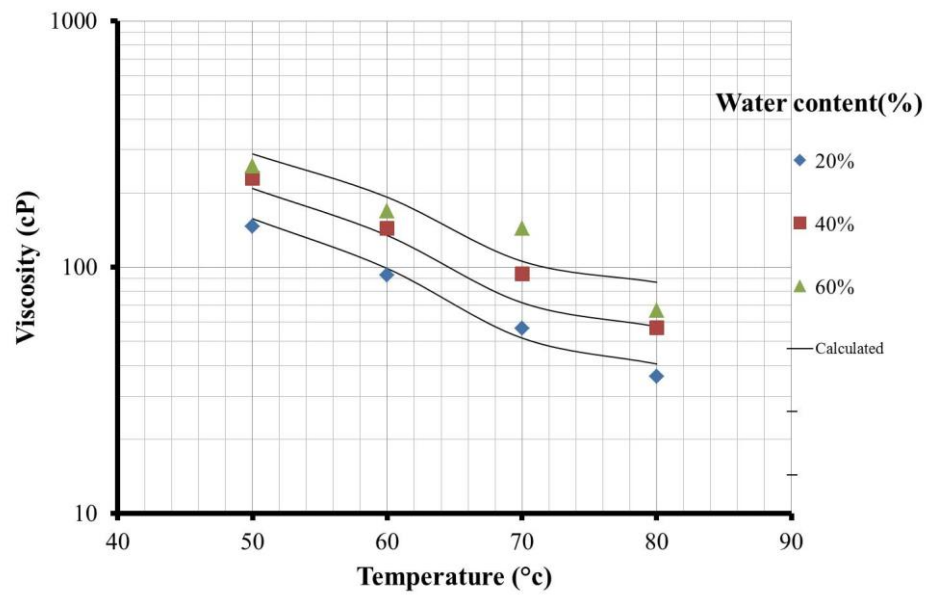


Figure 4.30 Experiment data and calculated data at 30s^{-1} shear rate

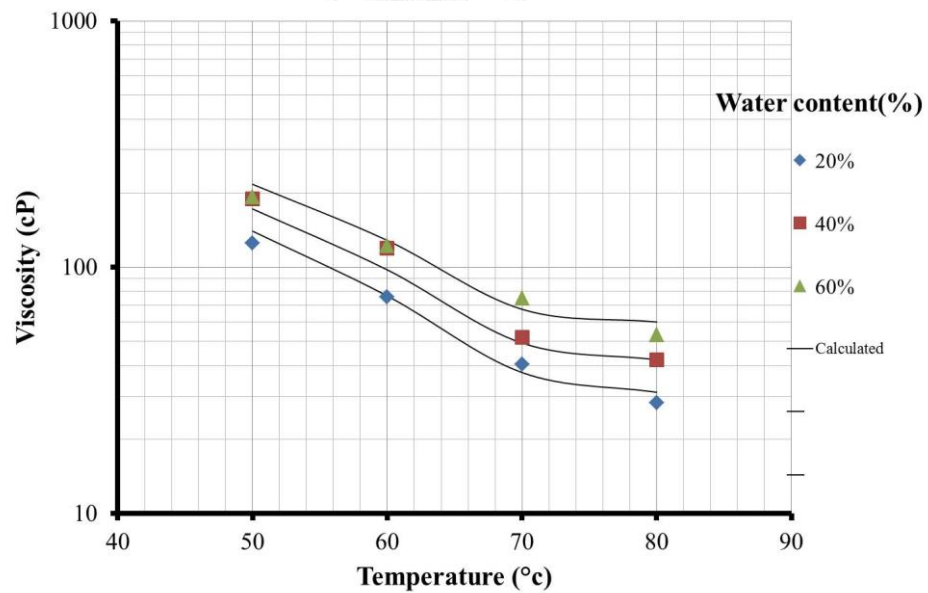


Figure 4.31 Experiment data and calculated data at 60s^{-1} shear rate

Al-Roomi's correlation

The parameters that Al-Roomi's correlation is used are temperature, water content and shear rate. So this correlation is good for this work.

$$\mu = a\gamma^b \exp(c\phi + \frac{d}{T}) \quad (4.3)$$

Where a, b, c and d are constant, μ is viscosity, γ is shear rate, ϕ is water content and T is temperature.

The develop Al-Roomi's correlation is taking natural logarithm (**ln**) into correlation and the equation become ;

$$\ln \eta = a + b \ln \gamma - c\phi + d/T \quad (4.4)$$

Where a, b, c and d are constant, μ is viscosity, γ is shear rate, ϕ is water content.

The constant, a-d, are calculated shown in Table 4.14.

Table 4.14 Constants for Al-Roomi's correlation.

a	2.20738065
b	-0.335761175
c	0.0244689669
d	163.009603

Al-Roomi's correlation is the function of temperature, shear rate, and water content. So from the experiment are developed equation should be;

$$\ln \eta = 2.20738065 - 0.335761175 \ln \gamma - 0.0244689669\phi + \frac{163.009603}{T} \quad (4.5)$$

The results presented experimental data get along well with calculated data as shown in Table 4.15. The range of percent difference is 0.07 – 68.83.

Table 4.15 Experiment data and calculated data of Al-Roomi's correlation

Temperature (°c)	Water content (percent)	Shear rate (s)	Viscosity (cP)		percent Difference
			Experiment	Calculated	
50	0	3.75	90.02	151.98	68.83
		7.5	87.83	120.43	37.12
		15	85.53	95.42	11.56
		30	82.32	75.61	8.15
		60	80.31	59.91	25.40
	20	3.75	220.70	247.93	12.34
		7.5	166.80	196.45	17.78
		15	157.20	155.66	0.98
		30	146.20	123.34	15.64
		60	125.60	97.73	22.19
	40	3.75	401.20	404.45	0.81
		7.5	313.50	320.48	2.23
		15	294.80	253.93	13.86
		30	229.75	201.21	12.42
		60	189.92	159.43	16.05
	60	3.75	1072.00	659.79	38.45
		7.5	392.20	522.79	33.30
		15	324.90	414.24	27.50
		30	257.64	328.23	27.40
		60	193.27	260.08	34.57
	0	3.75	62.01	88.27	42.35
		7.5	55.18	69.94	26.75
		15	56.41	55.42	1.76
		30	52.02	43.91	15.59
		60	42.50	34.80	18.12
		3.75	131.20	144.00	9.76
		7.5	111.90	114.10	1.97

60	20	15	103.20	90.41	12.39	
		30	93.02	71.64	22.98	
		60	75.66	56.76	24.98	
	40	3.75	311.50	234.90	24.59	
		7.5	213.70	186.13	12.90	
		15	153.00	147.48	3.61	
		30	143.90	116.86	18.79	
		60	119.20	92.60	22.32	
	60	3.75	433.90	383.20	11.68	
		7.5	343.30	303.63	11.59	
		15	215.23	240.59	11.78	
		30	169.23	190.63	12.65	
		60	122.53	151.05	23.28	
	70	0	3.75	51.40	59.88	16.50
			7.5	45.37	47.44	4.56
15			38.32	37.59	1.91	
30			27.29	29.79	9.16	
60			20.23	23.60	16.66	
20		3.75	106.01	97.68	7.86	
		7.5	72.04	77.40	7.44	
		15	65.00	61.33	5.65	
		30	56.43	48.59	13.89	
		60	40.31	38.50	4.49	
40		3.75	178.80	159.34	10.88	
		7.5	142.80	126.26	11.58	
		15	73.50	100.01	36.07	
		30	94.20	79.27	15.85	
		60	52.09	62.81	20.58	
60	3.75	328.3	259.94	20.82		
	7.5	206.1	205.96	0.07		
	15	169.90	163.20	3.94		

		30	143.90	129.31	10.14
		60	74.90	102.46	36.80
80	0	3.75	37.40	44.76	19.68
		7.5	35.80	35.46	0.95
		15	34.34	28.10	18.17
		30	21.52	22.26	3.44
		60	16.43	17.64	7.36
	20	3.75	78.48	73.01	6.97
		7.5	70.20	57.85	17.59
		15	47.36	45.84	3.21
		30	35.97	36.97	2.78
		60	28.22	28.78	1.98
	40	3.75	128.00	119.10	6.95
		7.5	129.10	94.37	26.90
		15	61.40	74.78	21.79
		30	56.97	59.25	4.00
		60	42.17	46.95	11.34
	60	3.75	224.30	194.29	13.38
		7.5	154.20	153.90	0.19
		15	121.50	121.98	0.40
		30	66.7	96.66	44.92
		60	53.25	76.59	43.83

Figure 4.32 to 4.35, presented the comparison between experimental data and predicted data. From this study the graph shown the points from high temperature data are nearing trend line like the result from Ronningsen and Farah correlations as shown in Figures 4.36 to 4.38.

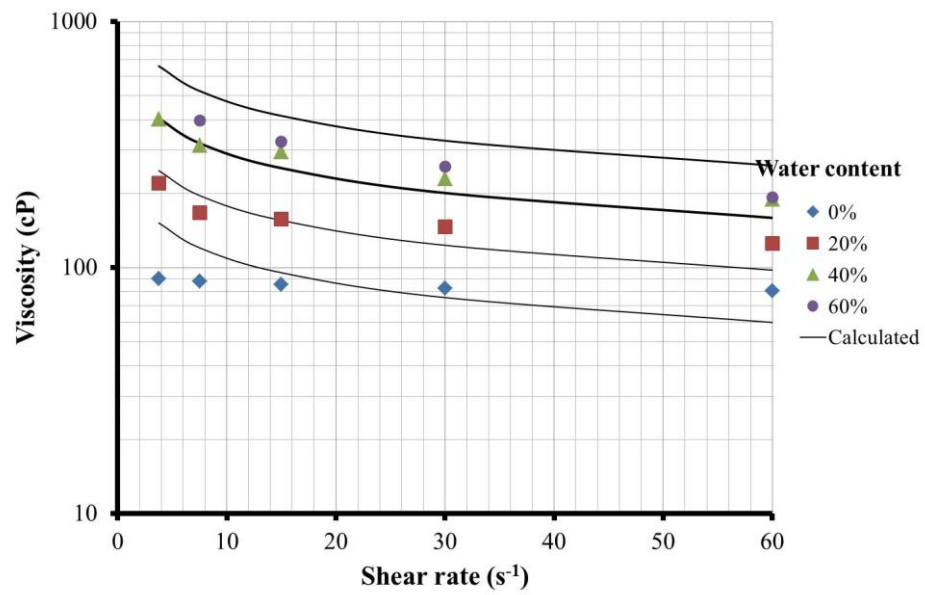


Figure 4.32 Experiment data and calculated data at 50°C temperature

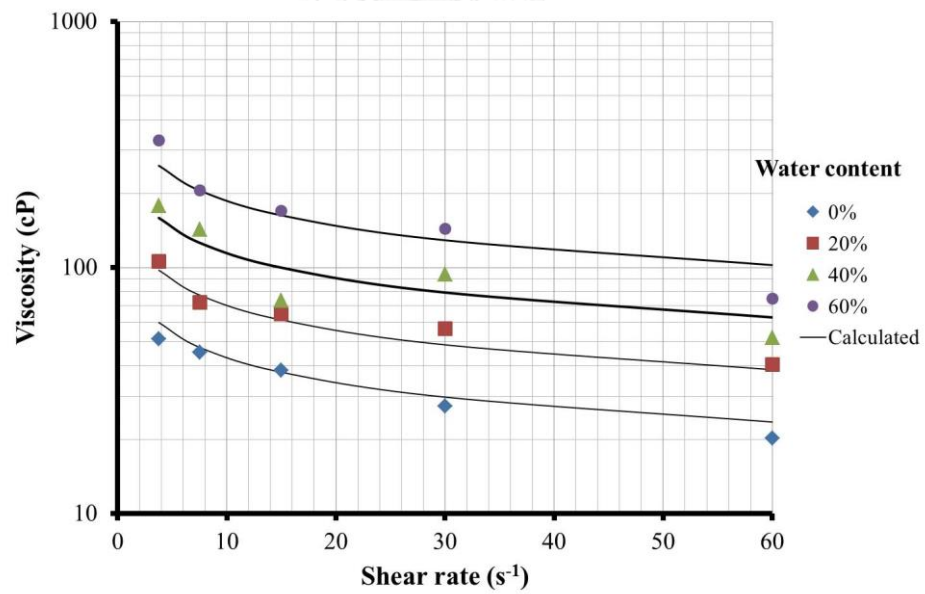


Figure 4.33 Experiment data and calculated data at 60°C temperature

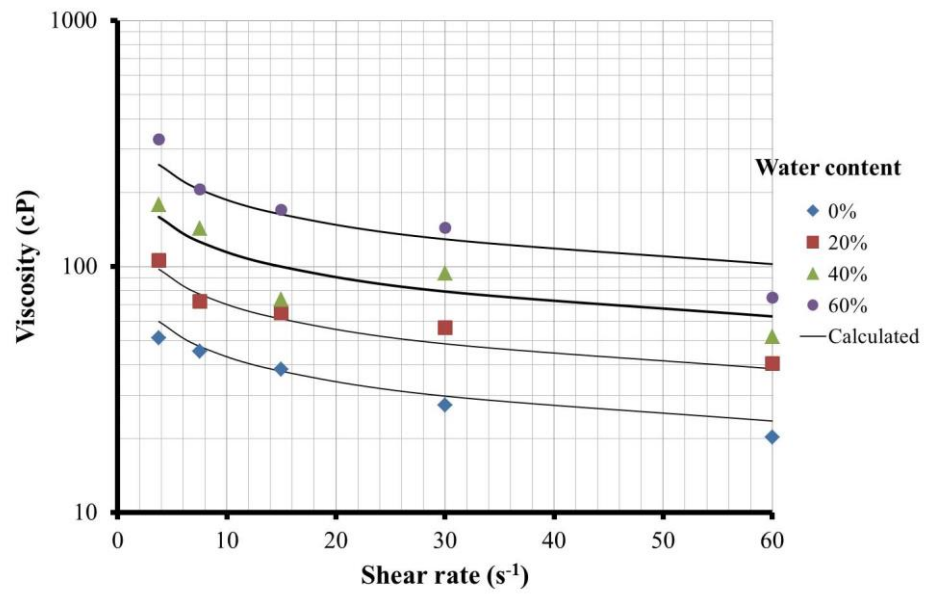


Figure 4.34 Experiment data and calculated data at 70°C temperature

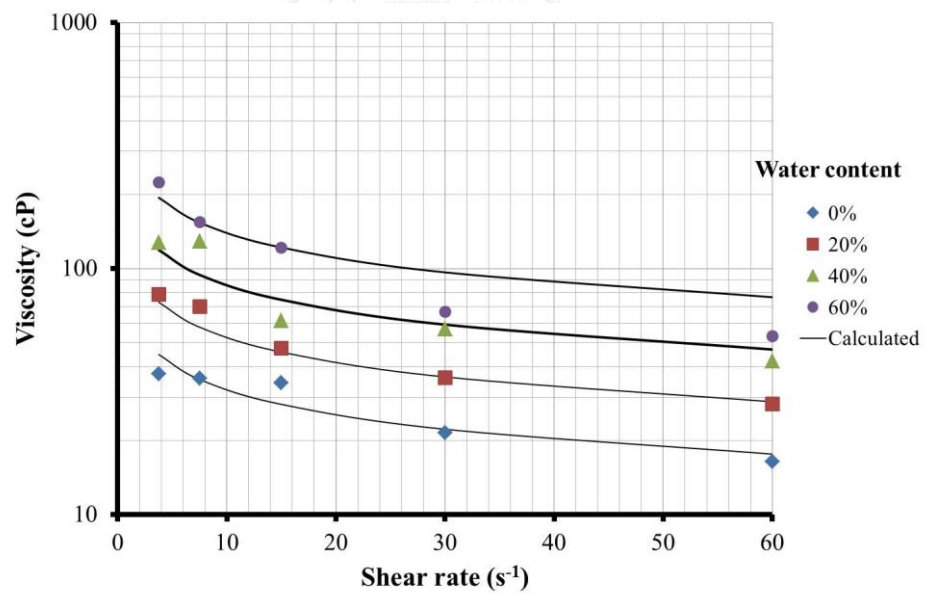


Figure 4.35 Experiment data and calculated data at 80°C temperature

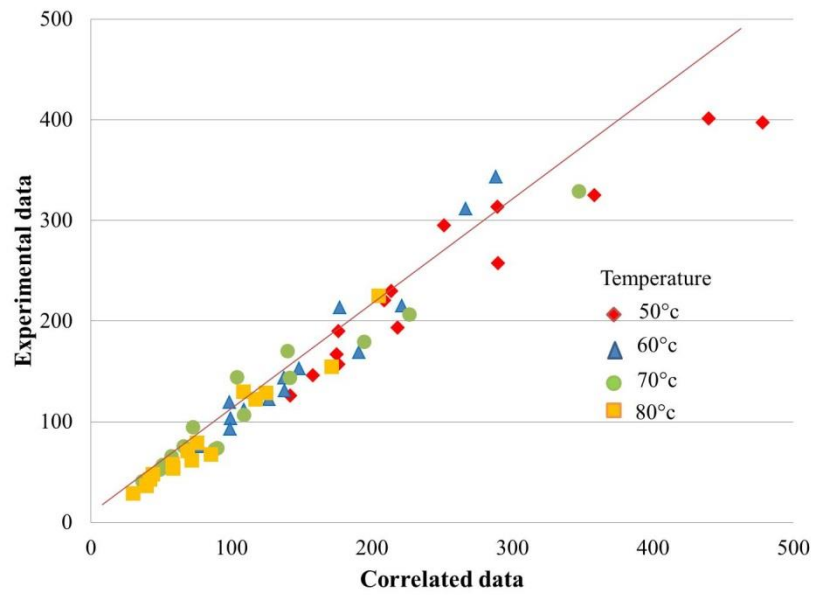


Figure 4.36 Experiment data and calculated data with Ronningsen's correlation

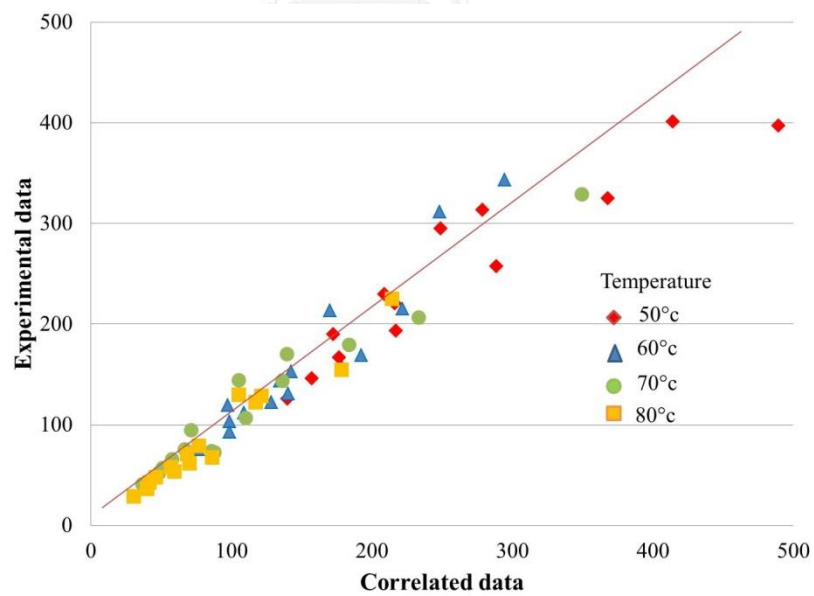


Figure 4.37 Experiment data and calculated data with Farah's correlation

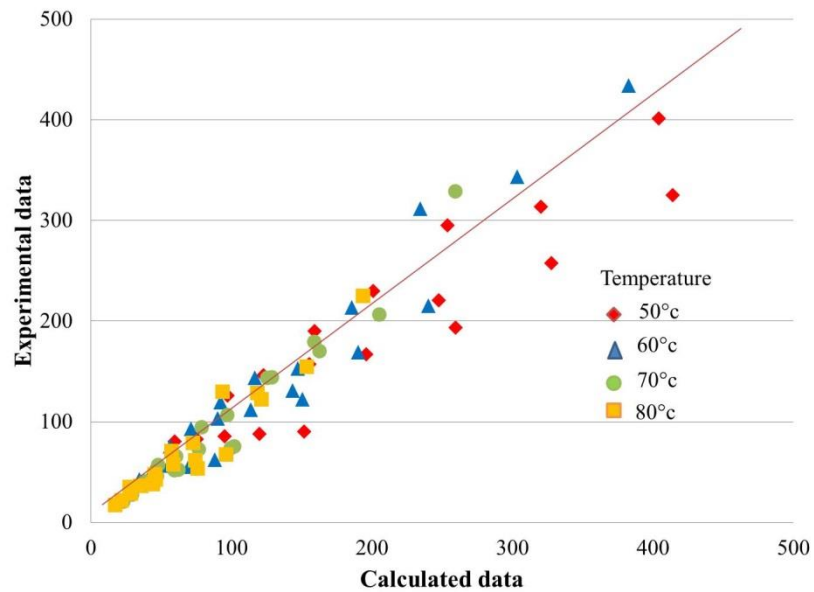


Figure 4.38 Experiment data and calculated data with Al-Roomi's correlation

Form this study Ronningsen' correlation, Farah's correlation and Al-Roomi's correlation are adopted for predicting the viscosity of emulsion from Fang oilfield in Thailand. So average absolute deviations (percent AAD) is used for compare between three correlation and shown in table 4.28 . Ronningsen' correlation is lowest percent AAD at 10.14. So Ronningsen' correlation should be chosen as the effective correlation for future work.

Table 4.16 percent of AAD of correlation

Correlation	Percent of AAD
Ronningsen	10.14
Farah	10.33
Al-Roomi	15.79

Chapter 5

Conclusions

From the study of the effect of parameters on viscosity of oil and its emulsion from Fang oilfield, Thailand .The parameters are temperature, water content, shear rate. Also, the effect of droplets and droplet size distribution of water and oil for emulsion are investigated to evaluate the emulsion stability. Moreover correlation developments for predicting the viscosity have been performed. Finally, the following conclusion can be presented.

1. Temperature is the most important parameters compare with water content and shear rate because temperature changes the viscosity of oil and its emulsion in highest value. Increasing temperature can decrease significantly the viscosity of oil and its emulsion. The viscosity extremely decrease as temperature in increase.
2. The viscosity becomes higher when water content is increased. At high percent of water content, the viscosity of emulsion greatly increase because volume of water droplets.
3. Shear rate has less effect of viscosity reduction. The larger the shear rate is applied, viscosity becomes lower. The emulsion shows Non-Newtonian fluid behavior at low temperature because its viscosity is a definition of shear rate.
4. Emulsion stability is studied by observing the droplet size. It is shown that at high temperature, droplet size is bigger and emulsion becomes less stable. On the other hand, high water content and shear rate can result in more smaller size of water droplet and make it more stable.

5. The average absolute deviations (AADs) of Ronningsen's correlation, Farah's correlation and Al-Roomi's correlation are 10.14percent, 10.33percent and 15.79percent respectively.
6. The correlation representing the experimental results has been developed to predict the viscosity for oil and its emulsion with 10.14 percent average absolute deviation of these results from Ronningsen's correlation give the lowest percentAAD.
7. The correlation can be used for future work to predict the viscosity of emulsion from Fang oilfield in Thailand.

Recommendation

1. Study more conditions and other parameters that effect on viscosity of oil and its emulsion. Such as pH, Viscosity of the continuous phase, Viscosity of the dispersed phase and Presence of solids in addition to dispersed liquid phase.

REFERENCES

- Farah, M. A., Oliveira, R. C., Caldas, J. N., & Rajagopal, K. (2005). Viscosity of water-in-oil emulsions: Variation with temperature and water volume fraction. *Journal of Petroleum Science and Engineering*, 48(3–4), 169-184. doi: <http://dx.doi.org/10.1016/j.petrol.2005.06.014>
- Fingas, M., & Fieldhouse, B. (2012). Studies on water-in-oil products from crude oils and petroleum products. *Marine Pollution Bulletin*, 64(2), 272-283. doi: <http://dx.doi.org/10.1016/j.marpolbul.2011.11.019>
- Ibrahim, S. (2011). Corrosion Inhibitors in the Oilfield. Retrieved 2016 May 26, 2016, from <https://isalama.wordpress.com/article/corrosion-inhibitors-in-the-oilfield-3uf3kbflnswt-4/>.
- Kokal, S. L., & Aramco, S. (2006). *Crude Oil Emulsions* (L. W. Lake Ed. Vol. 1). United States of America: Society of Petroleum Engineers.
- Krieger, I. M., & Dougherty, T. J. (1959). A Mechanism for Non-Newtonian Flow in Suspensions of Rigid Spheres. *Transactions of The Society of Rheology*, 3(1), 137-152. doi: [doi: http://dx.doi.org/10.1122/1.548848](http://dx.doi.org/10.1122/1.548848)
- Maneeintr, K., Sasaki, K., & Sugai, Y. (2013). *Japan Institute of Energy*, 92, 900-904.
- Neumann, H.-J., & Paczynska-Lahme, B. (1996). Stability and demulsification of petroleum emulsions. In H. J. Jacobasch (Ed.), *Interfaces, Surfactants and Colloids in Engineering* (pp. 101-104). Darmstadt: Steinkopff.
- Pumpfundamentals. (2010). About fluids. Retrieved 2016 May 26, 2016, from http://www.pumpfundamentals.com/about_fluids.htm
- Ronningsen, H. P. (1995). *Correlations for predicting Viscosity of W/O-Emulsions based on North Sea Crude Oils*.
- Schramm, L. L. (1992). *Emulsions Fundamentals and Applications in the Petroleum Industry* Washington,DC: American Chemical Society.
- Sciences, P. (2011). Emulsion Stability and Testing. Retrieved 2016 May 26, 2016, from <http://www.particlesciences.com/news/technical-briefs/2011/emulsion-stability-and-testing.html>
- Sinterface. (2016). Fundamentals of interfacial science. Retrieved 2016 May 26, from http://www.sinterface.com/service/fundamentals/interfacial_science/index.html#

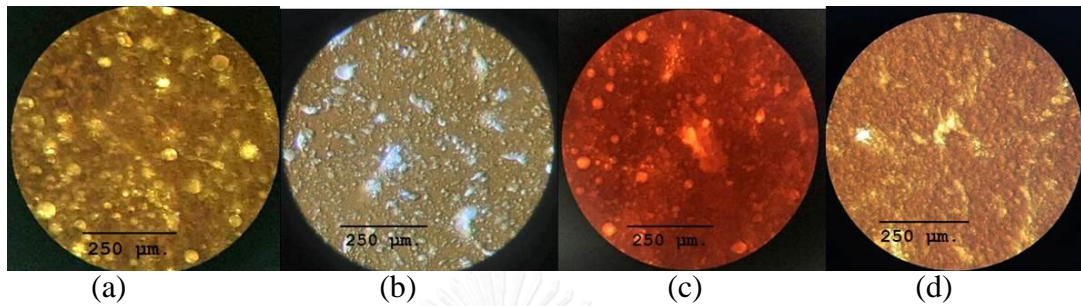
APPENDIX



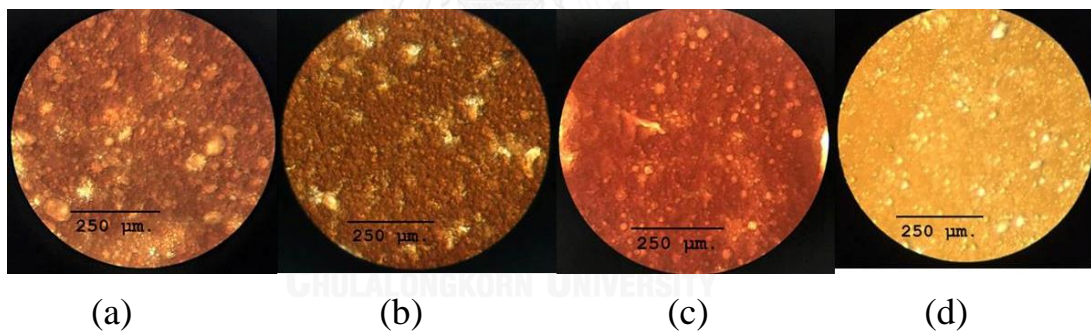
จุฬาลงกรณ์มหาวิทยาลัย
CHULALONGKORN UNIVERSITY

1. Droplets size distribution with difference temperature.

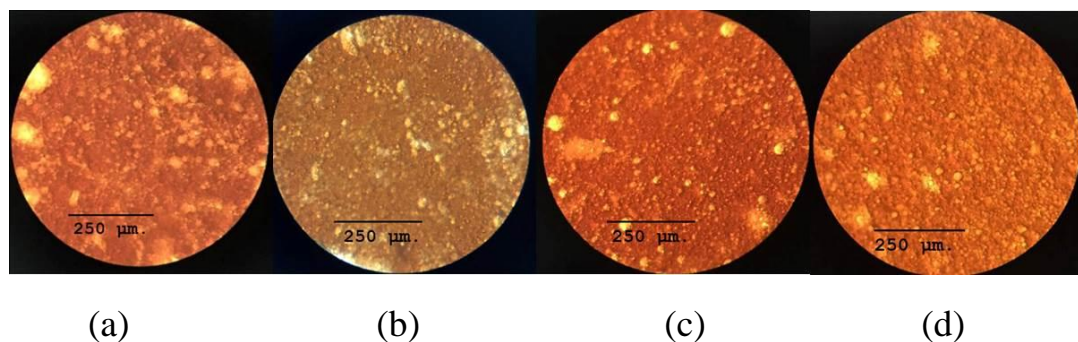
Microscopic observation of water droplet in 0percent in(a) temperature 50°C (b) temperature 60°C (c) temperature 70°C and (d) temperature 80°C at 3.75 s^{-1} shear rate



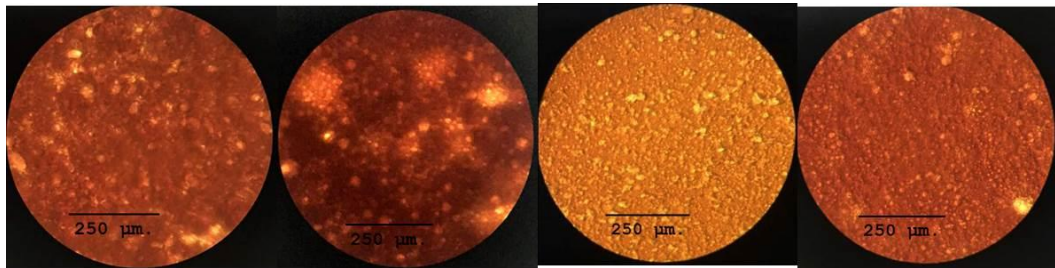
Microscopic observation of water droplet in 0percent in(a) temperature 50°C (b) temperature 60°C (c) temperature 70°C and (d) temperature 80°C at 7.5 s^{-1} shear rate



Microscopic observation of water droplet in 0percent in(a) temperature 50°C (b) temperature 60°C (c) temperature 70°C and (d) temperature 80°C at 15 s^{-1} shear rate



Microscopic observation of water droplet in 0percent in(a) temperature 50°C (b) temperature 60°C (c) temperature 70°C and (d) temperature 80°C at 30 s⁻¹ shear rate



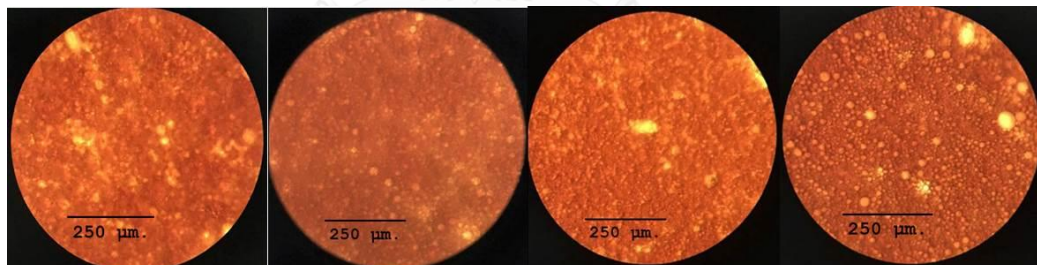
(a)

(b)

(c)

(d)

Microscopic observation of water droplet in 0percent in(a) temperature 50°C (b) temperature 60°C (c) temperature 70°C and (d) temperature 80°C at 60 s⁻¹ shear rate

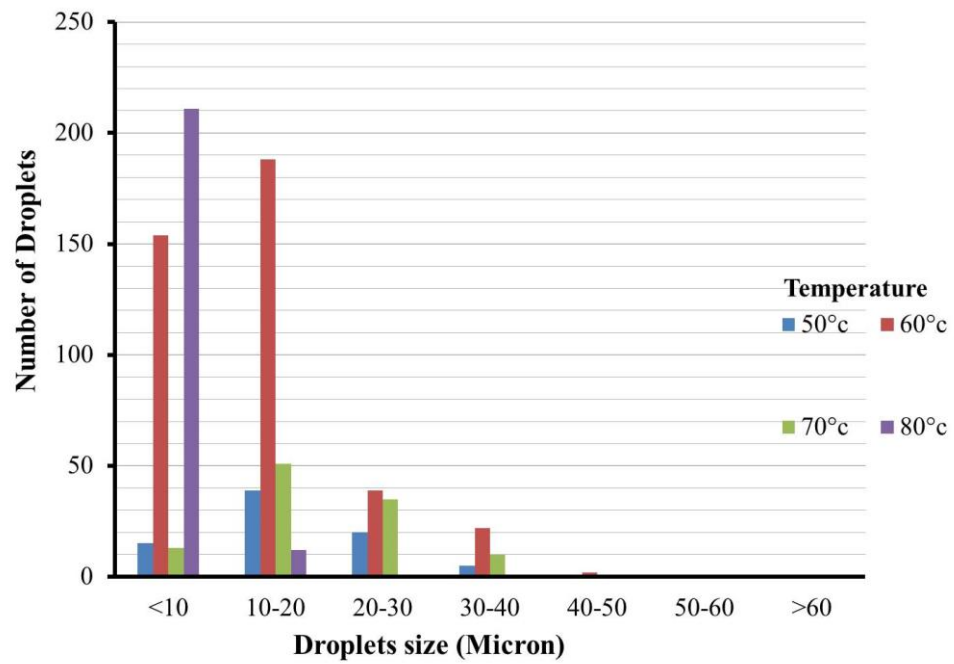
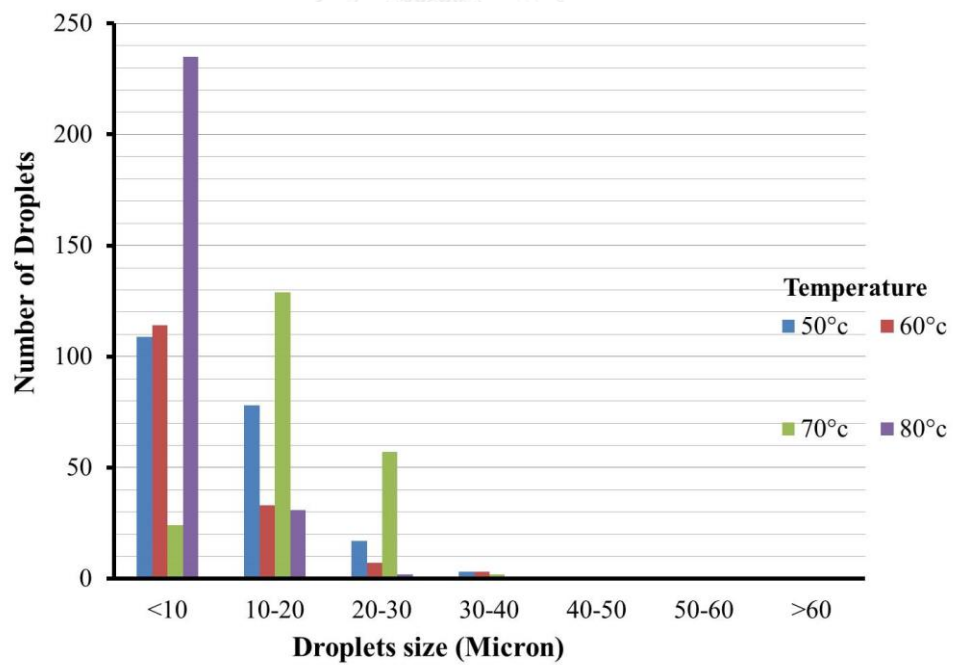


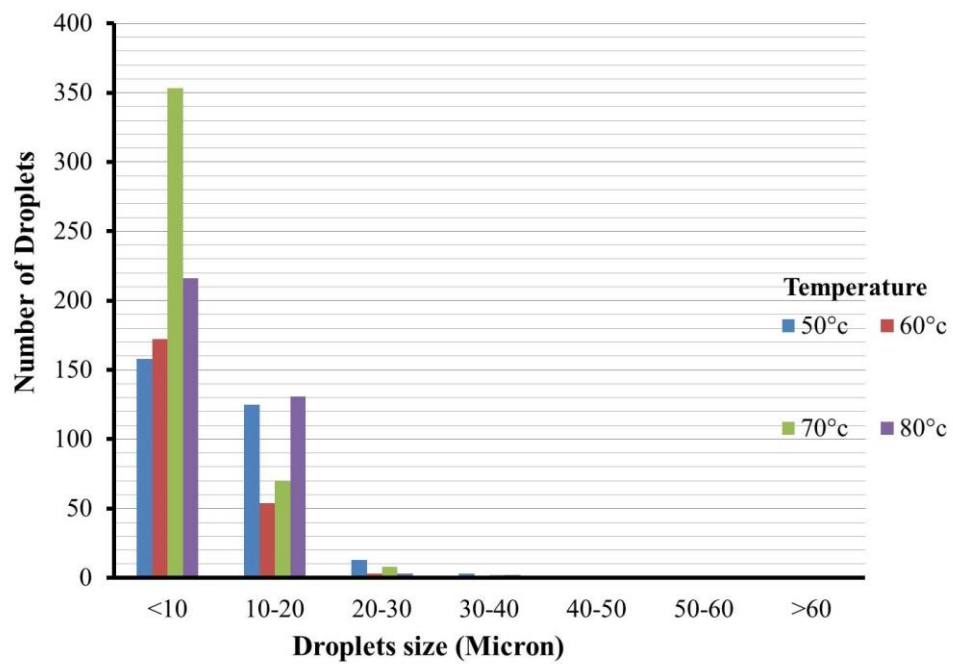
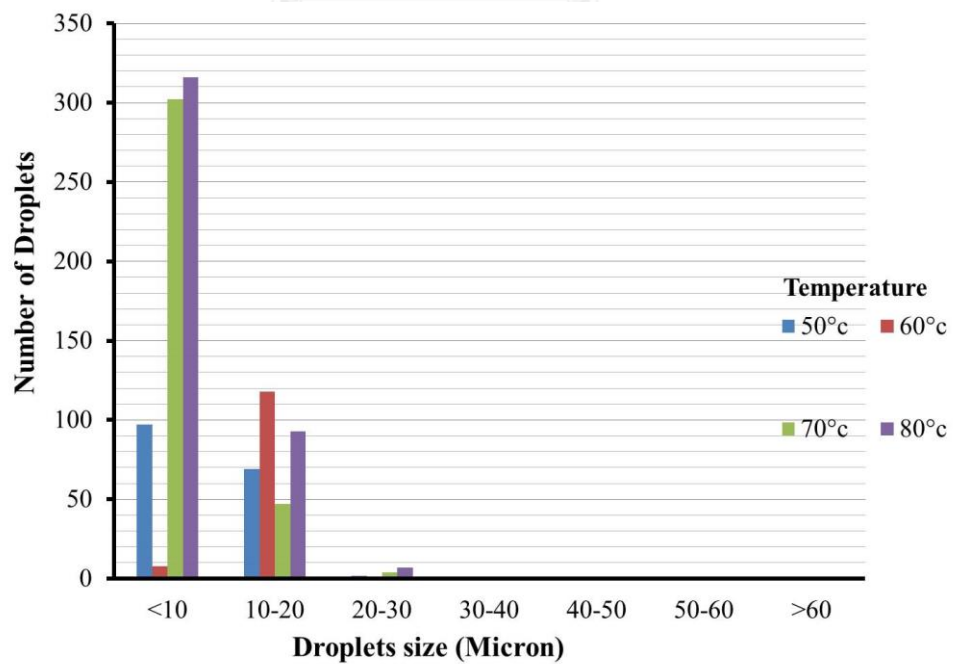
(a)

(b)

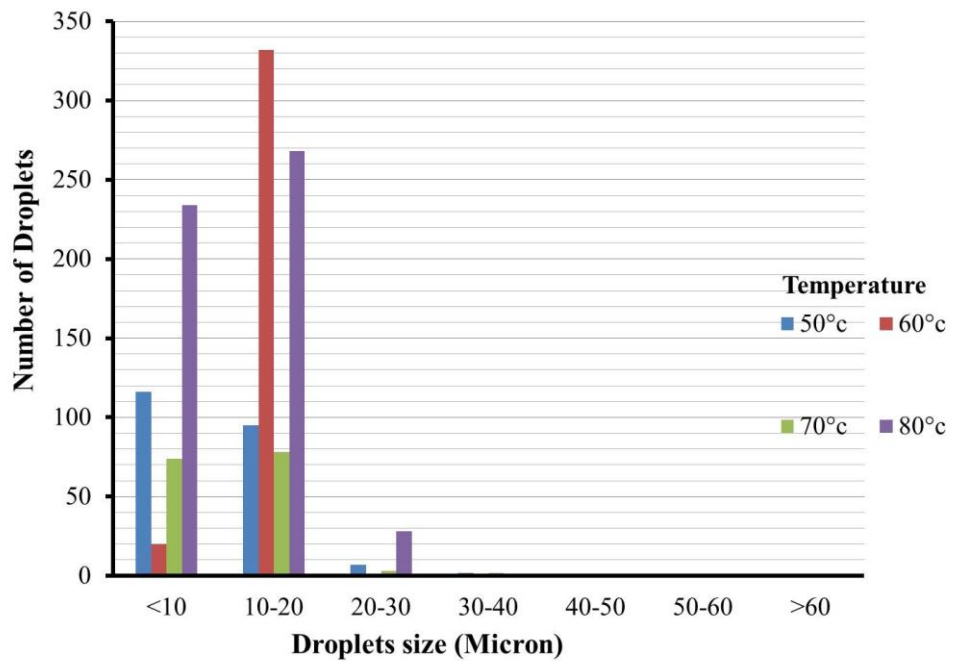
(c)

(d)

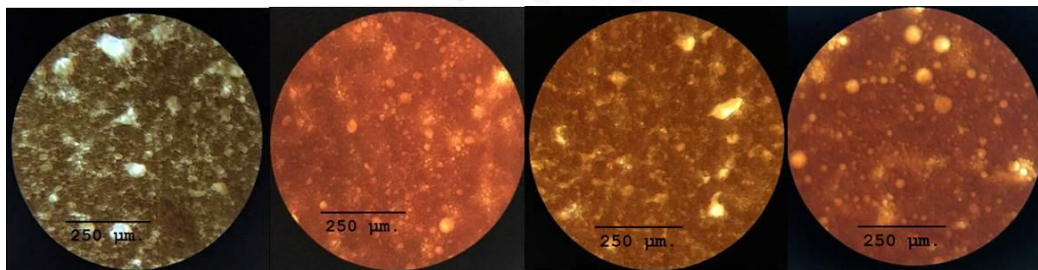
Droplets size distribution at 3.75 s^{-1} shear rateDroplets size distribution at 7.5 s^{-1} shear rate

Droplets size distribution at 15 s⁻¹ shear rateDroplets size distribution at 30 s⁻¹ shear rate

Droplets size distribution at 60 s^{-1} shear rate



Microscopic observation of water droplet in 20percent in (a) temperature 50°C (b) temperature 60°C (c) temperature 70°C and (d) temperature 80°C at 3.75 s^{-1} shear rate



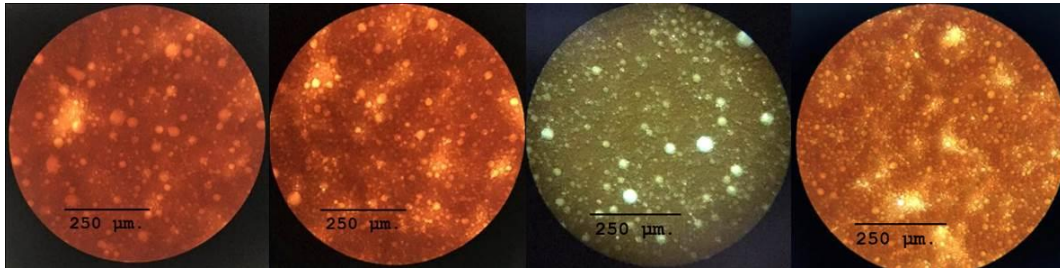
(b)

(b)

(c)

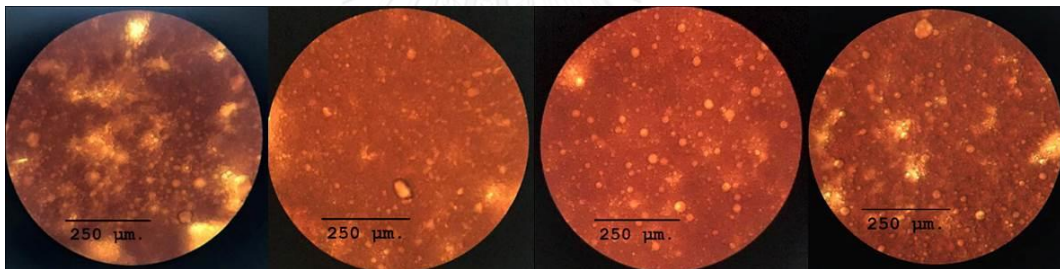
(d)

Microscopic observation of water droplet in 20percent in(a) temperature 50°C (b) temperature 60°C (c) temperature 70°C and (d) temperature 80°C at 7.5 s^{-1} shear rate



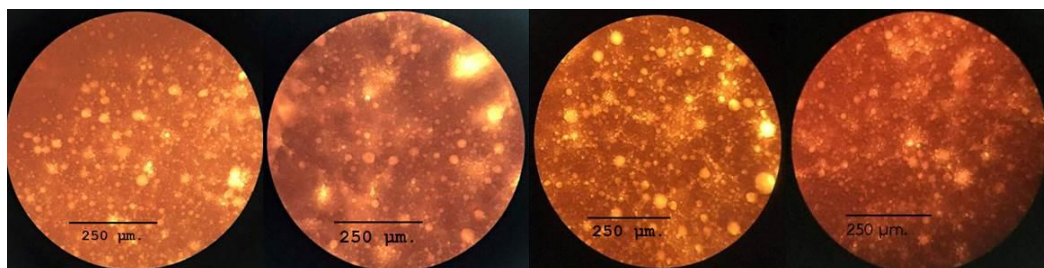
(a) (b) (c) (d)

Microscopic observation of water droplet in 20percent in(a) temperature 50°C (b) temperature 60°C (c) temperature 70°C and (d) temperature 80°C at 15 s^{-1} shear rate



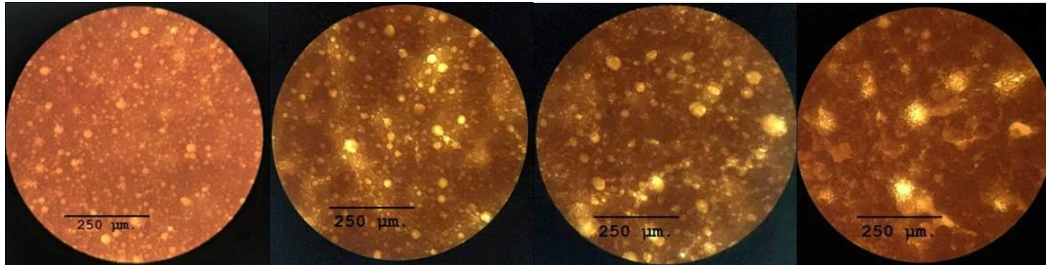
(a) (b) (c) (d)

Microscopic observation of water droplet in 20percent in(a) temperature 50°C (b) temperature 60°C (c) temperature 70°C and (d) temperature 80°C at 30 s^{-1} shear rate



(a) (b) (c) (d)

Microscopic observation of water droplet in 20percent in(a) temperature 50°C (b) temperature 60°C (c) temperature 70°C and (d) temperature 80°C at 60 s⁻¹ shear rate



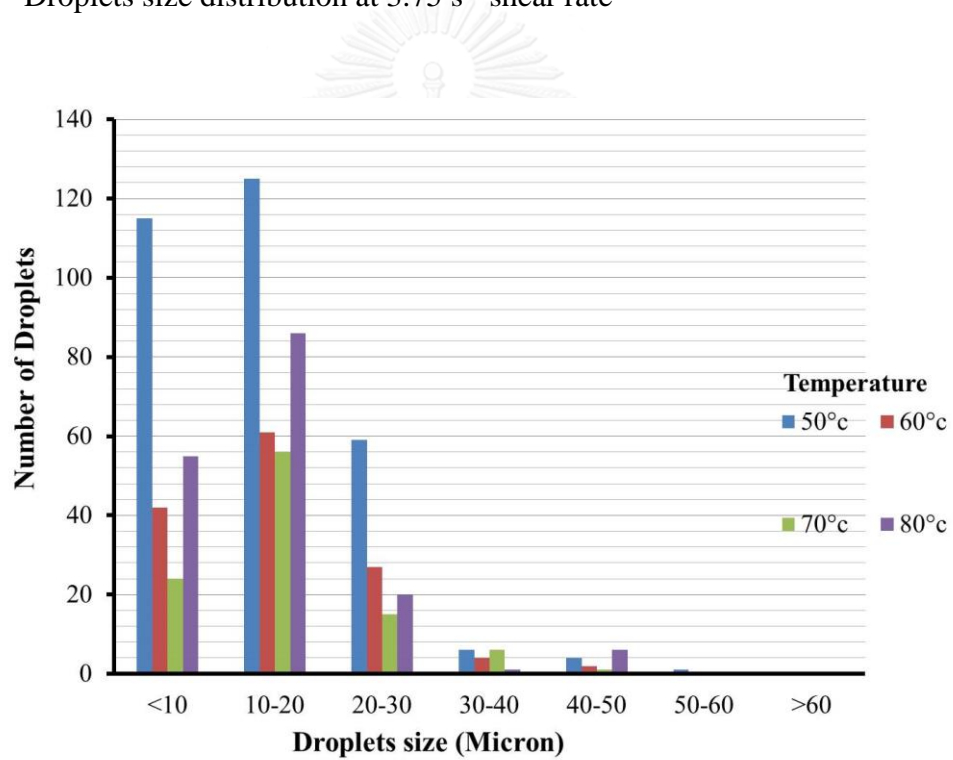
(a)

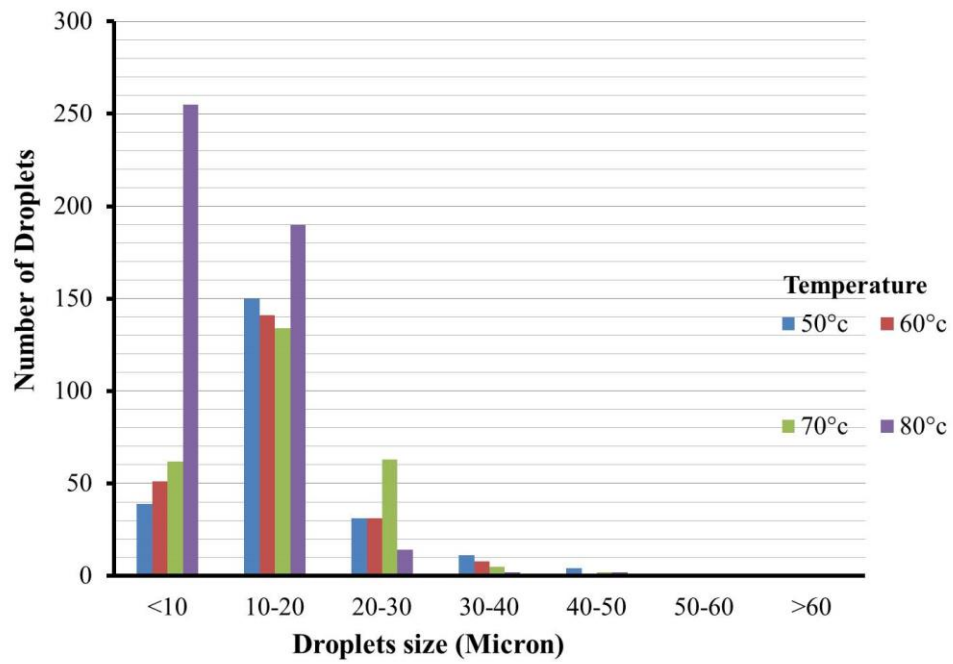
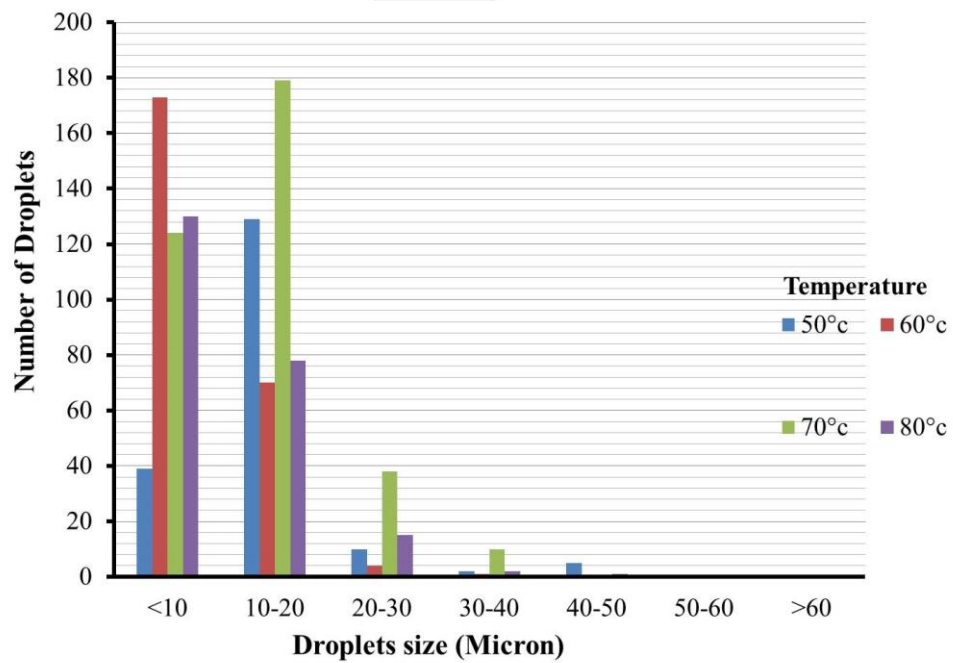
(b)

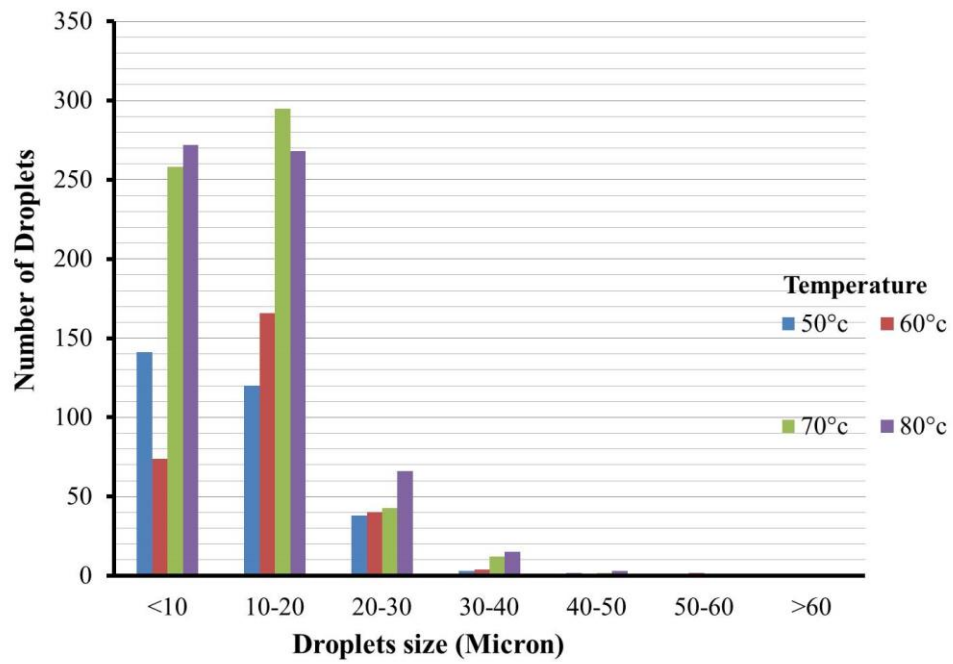
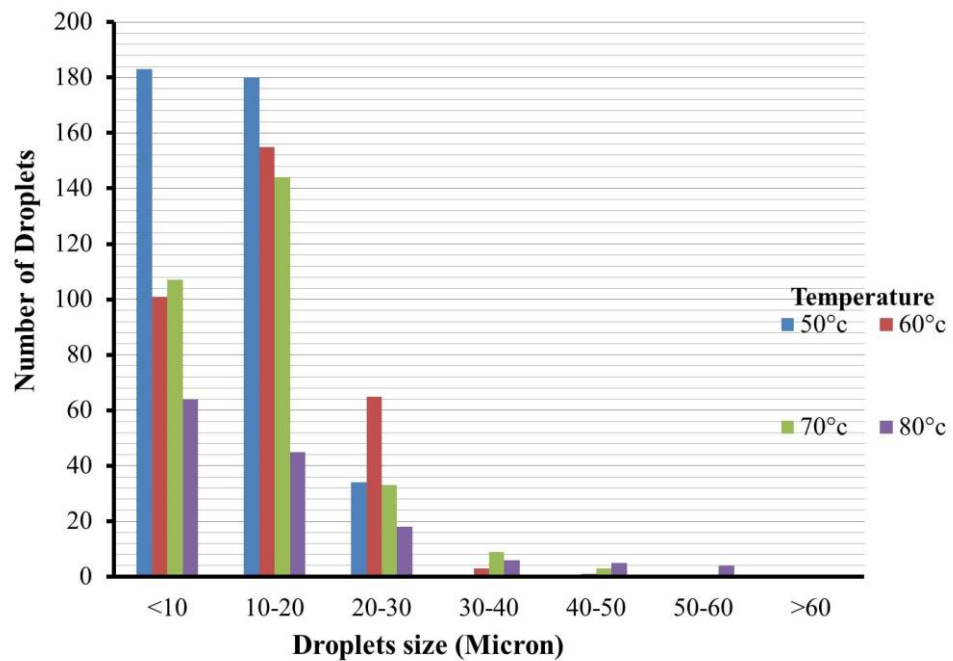
(c)

(d)

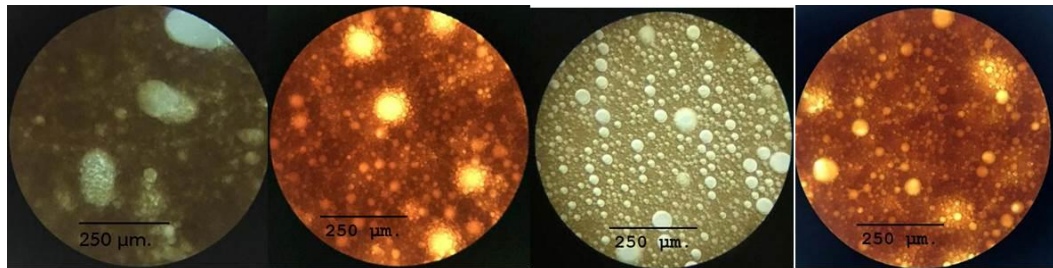
Droplets size distribution at 3.75 s⁻¹ shear rate



Droplets size distribution at 7.5 s^{-1} shear rateDroplets size distribution at 15 s^{-1} shear rate

Droplets size distribution at 30 s⁻¹ shear rateDroplets size distribution at 60 s⁻¹ shear rate

Microscopic observation of water droplet in 40percent in(a) temperature 50°C (b) temperature 60°C (c) temperature 70°C and (d) temperature 80°C at 3.75 s^{-1} shear rate



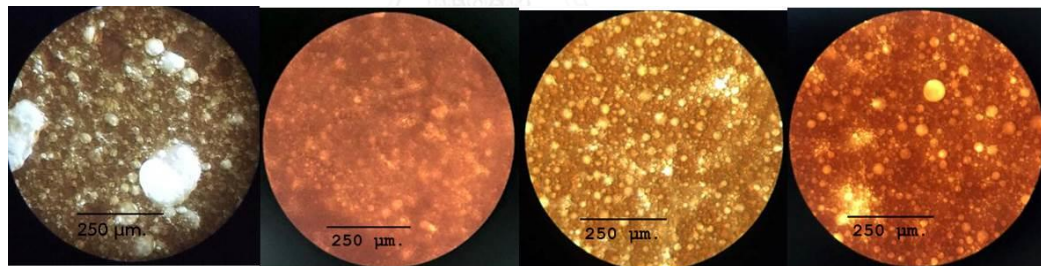
(a)

(b)

(c)

(d)

Microscopic observation of water droplet in 40percent in(a) temperature 50°C (b) temperature 60°C (c) temperature 70°C and (d) temperature 80°C at 7.5 s^{-1} shear rate



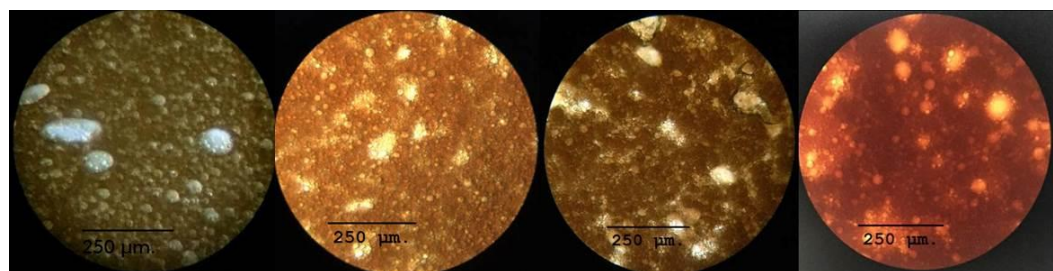
(a)

(b)

(c)

(d)

Microscopic observation of water droplet in 40percent in(a) temperature 50°C (b) temperature 60°C (c) temperature 70°C and (d) temperature 80°C at 15 s^{-1} shear rate



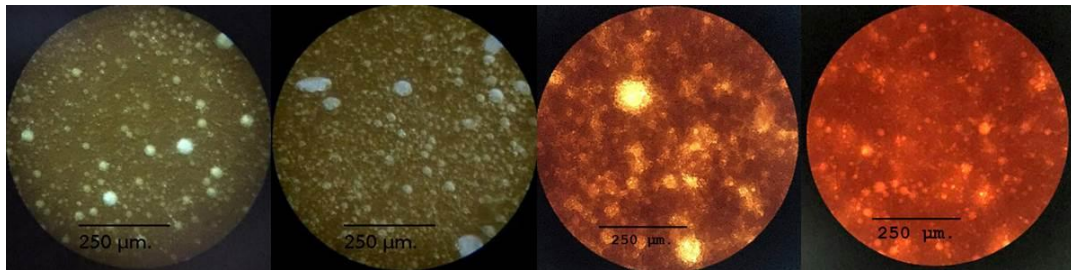
(a)

(b)

(c)

(d)

Microscopic observation of water droplet in 40percent in(a) temperature 50°C (b) temperature 60°C (c) temperature 70°C and (d) temperature 80°C at 30 s^{-1} shear rate



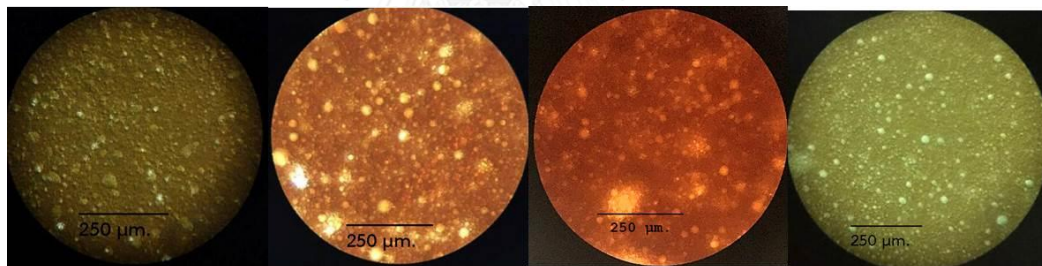
(a)

(b)

(c)

(d)

Microscopic observation of water droplet in 40percent in(a) temperature 50°C (b) temperature 60°C (c) temperature 70°C and (d) temperature 80°C at 60 s^{-1} shear rate

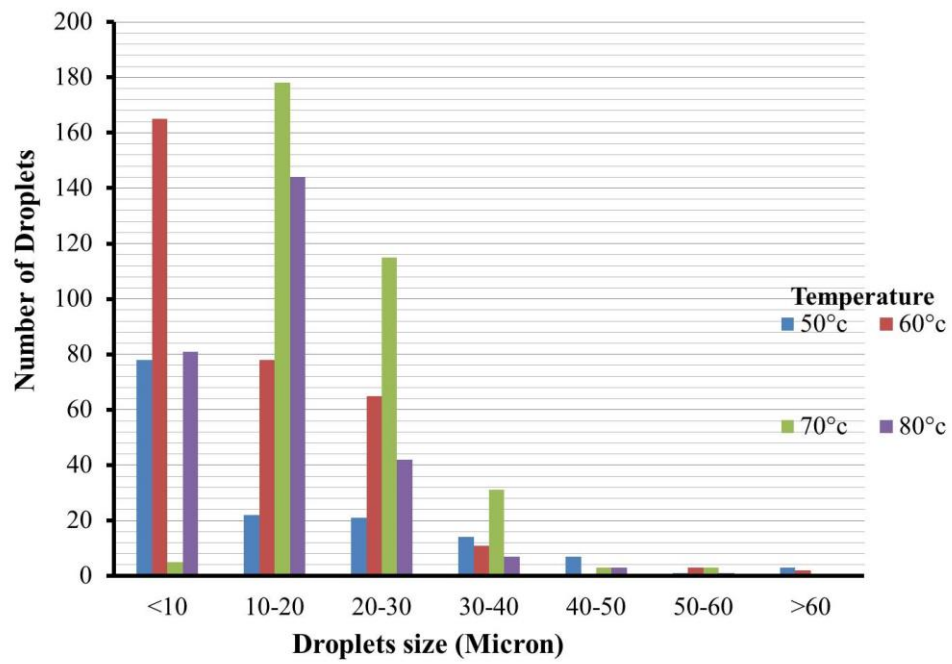
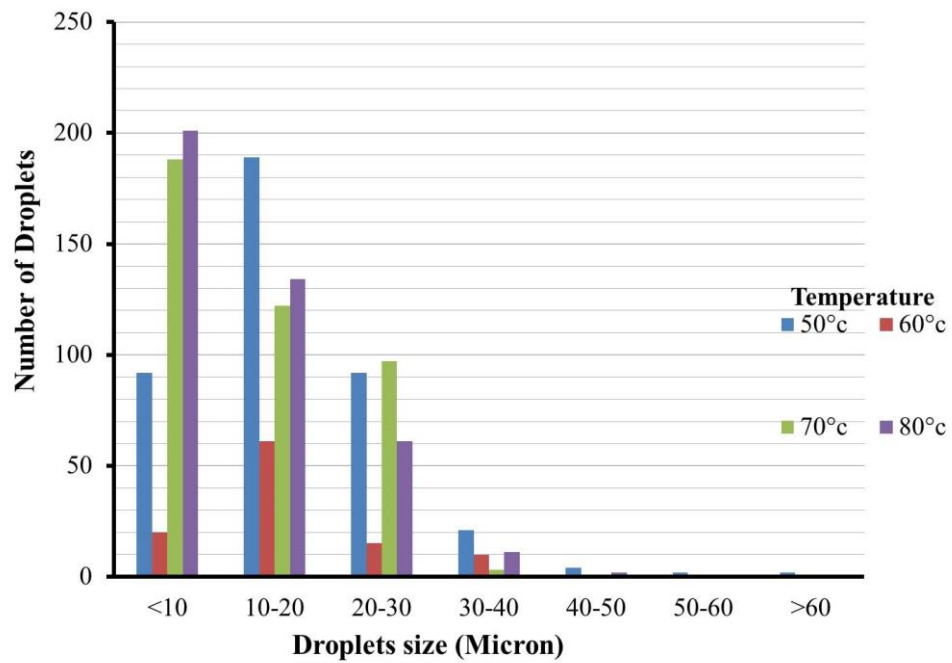


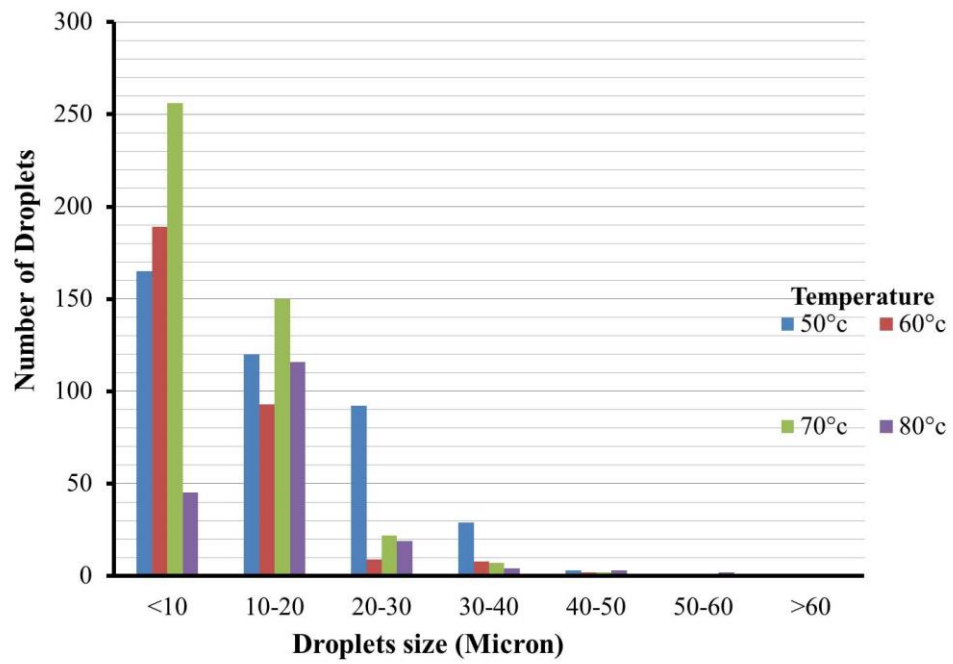
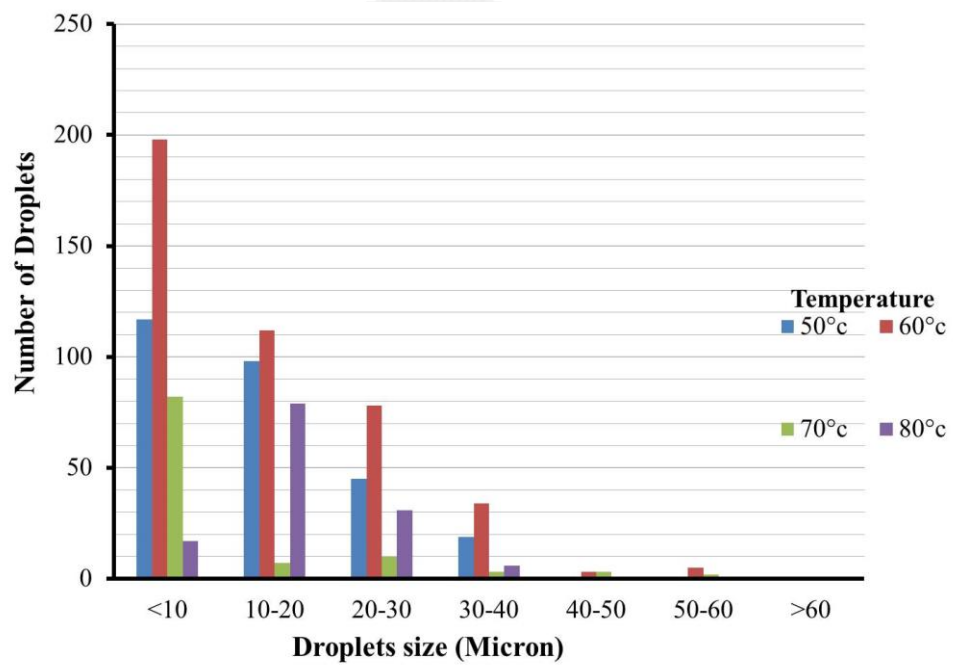
(a)

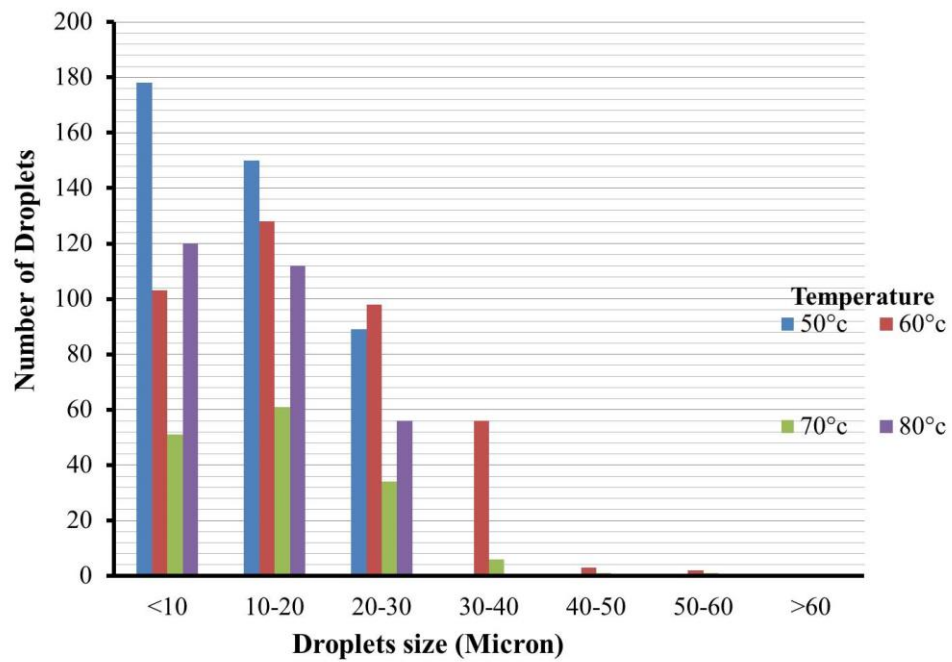
(b)

(c)

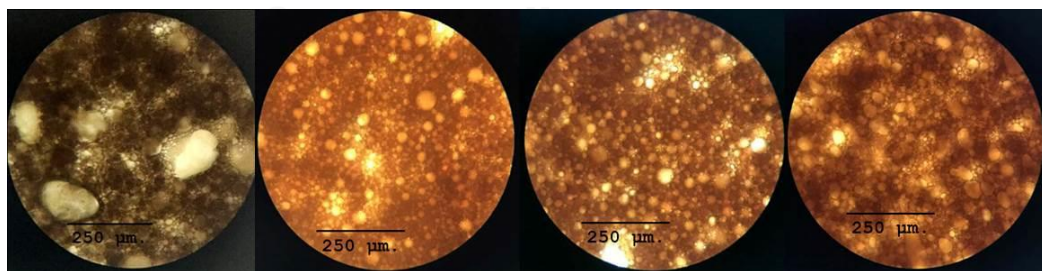
(d)

Droplets size distribution at 3.75 s^{-1} shear rateDroplets size distribution at 7.5 s^{-1} shear rate

Droplets size distribution at 15 s⁻¹ shear rateDroplets size distribution at 30 s⁻¹ shear rate

Droplets size distribution at 60 s^{-1} shear rate

Microscopic observation of water droplet in 60percent in (a) temperature 50°C (b) temperature 60°C (c) temperature 70°C and (d) temperature 80°C at 3.75 s^{-1} shear rate



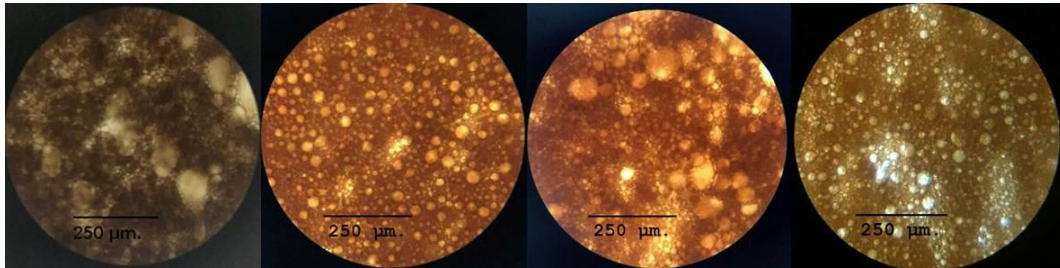
(a)

(b)

(c)

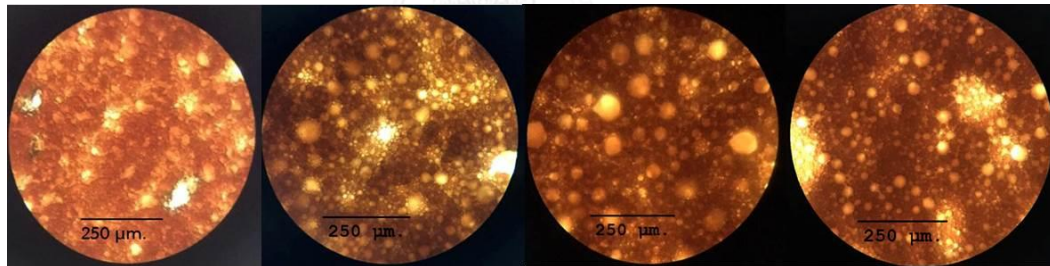
(d)

Microscopic observation of water droplet in 60percent in(a) temperature 50°C (b) temperature 60°C (c) temperature 70°C and (d) temperature 80°C at 7.5 s^{-1} shear rate



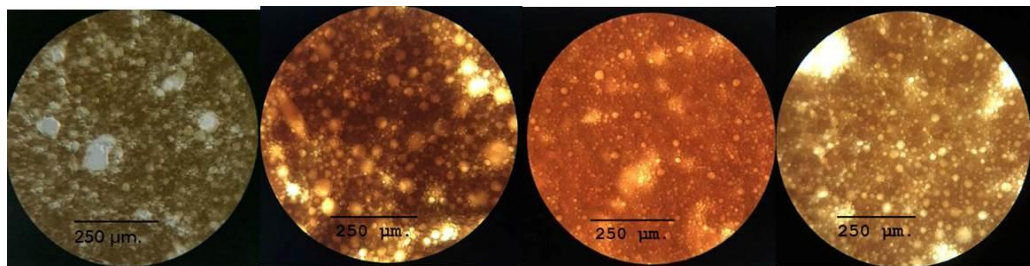
(a) (b) (c) (d)

Microscopic observation of water droplet in 60percent in(a) temperature 50°C (b) temperature 60°C (c) temperature 70°C and (d) temperature 80°C at 15 s^{-1} shear rate



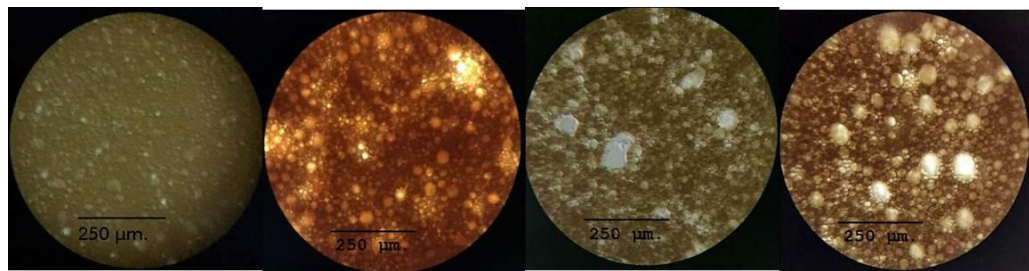
(a) (b) (c) (d)

Microscopic observation of water droplet in 60percent in(a) temperature 50°C (b) temperature 60°C (c) temperature 70°C and (d) temperature 80°C at 30 s^{-1} shear rate



(a) (b) (c) (d)

Microscopic observation of water droplet in 60percent in(a) temperature 50°C (b) temperature 60°C (c) temperature 70°C and (d) temperature 80°C at 60 s⁻¹ shear rate



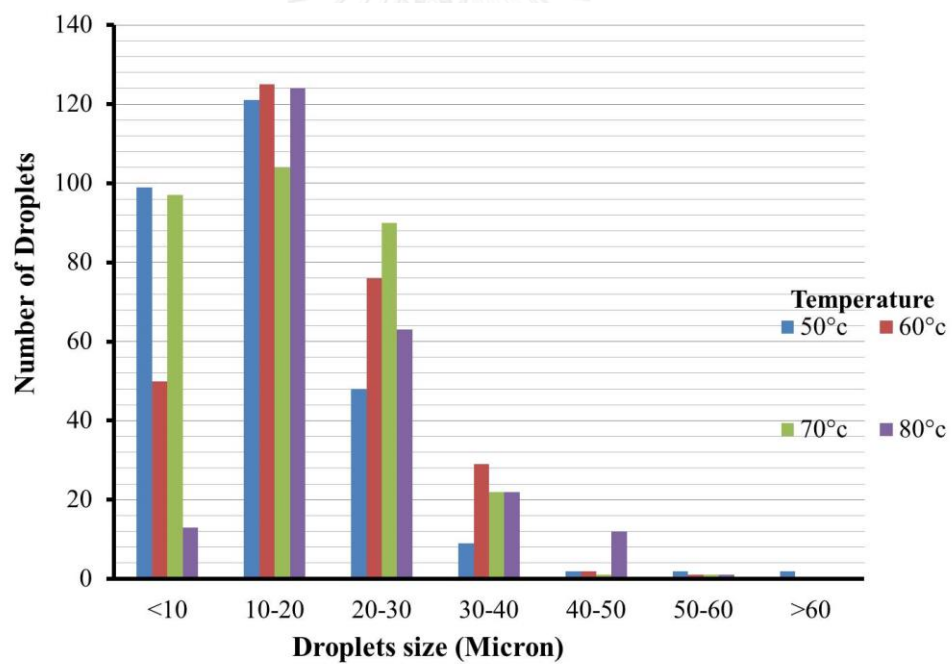
(a)

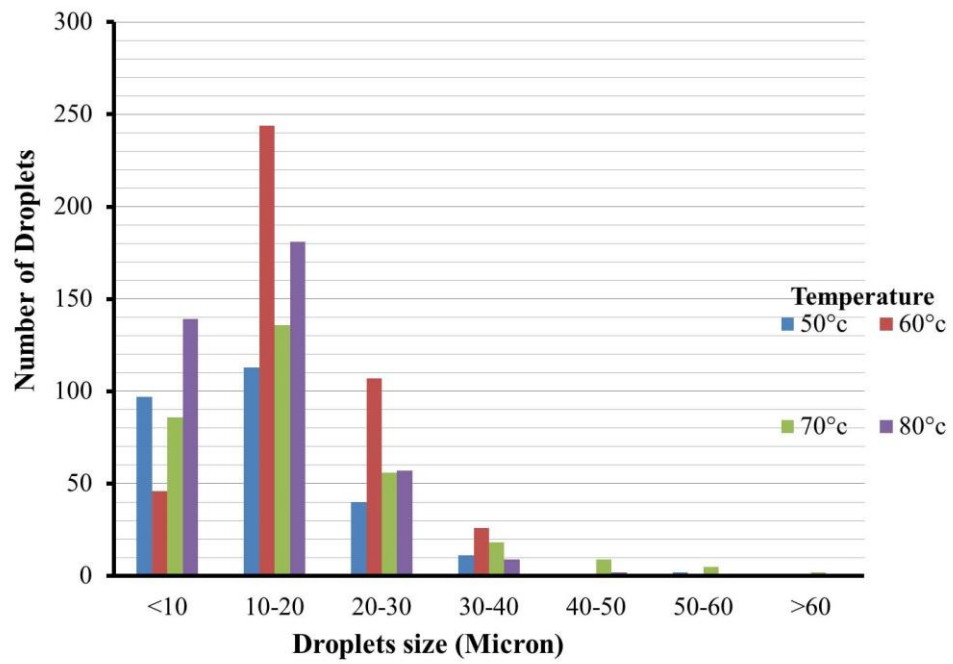
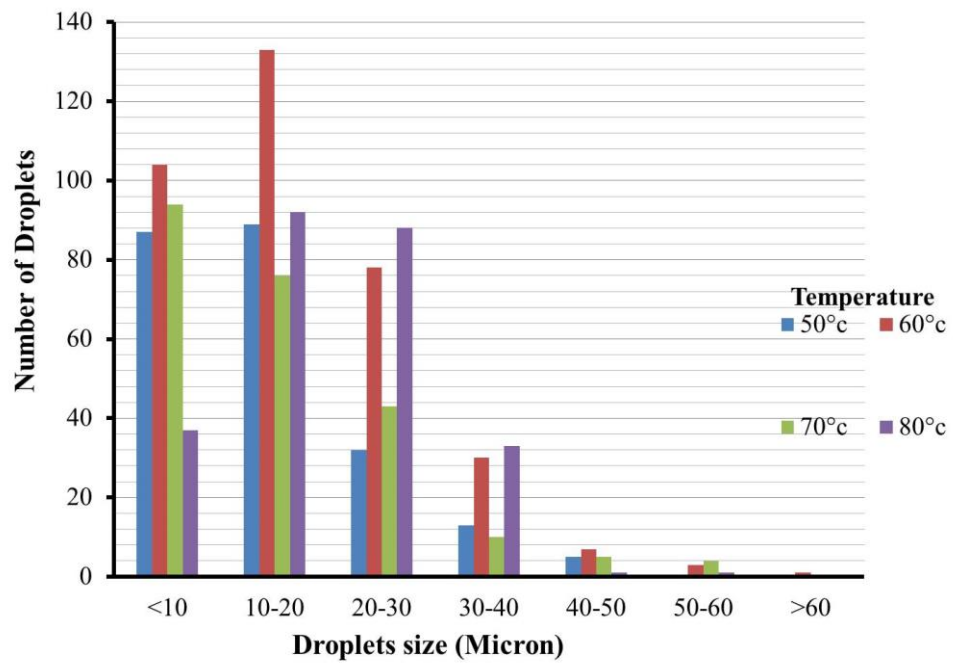
(b)

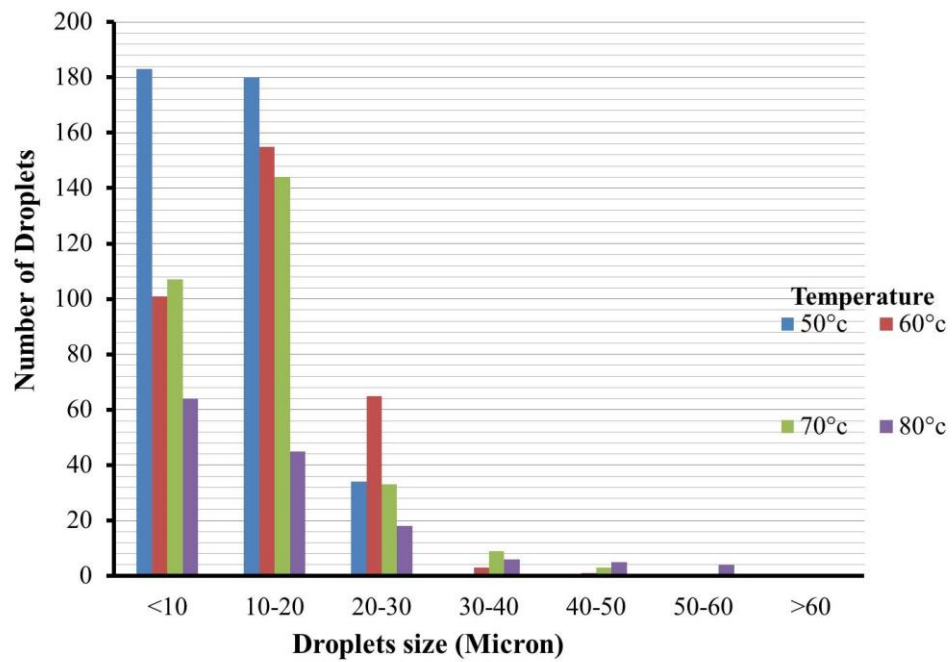
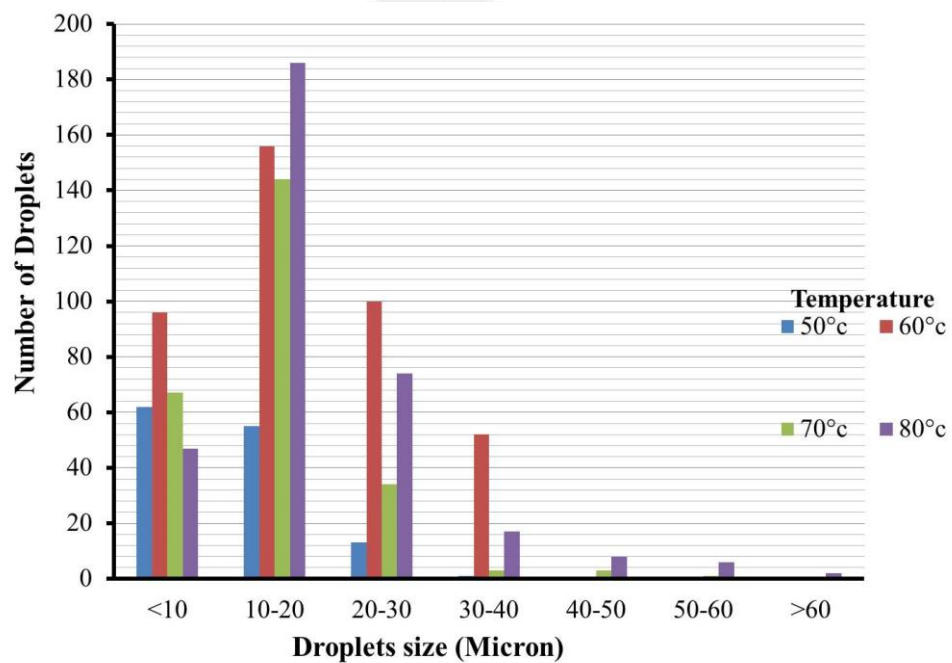
(c)

(d)

Droplets size distribution at 3.75 s⁻¹ shear rate

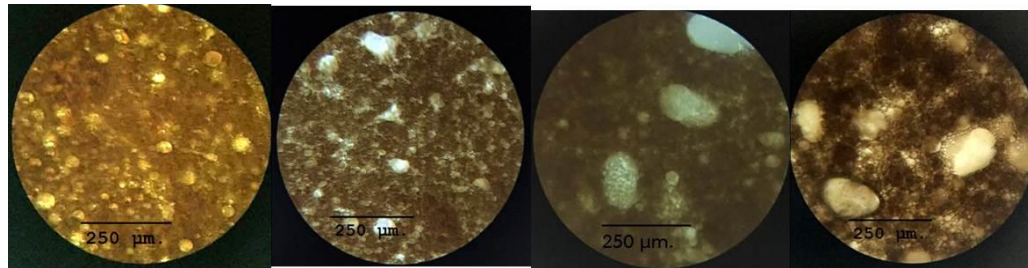


Droplets size distribution at 7.5 s^{-1} shear rateDroplets size distribution at 15 s^{-1} shear rate

Droplets size distribution at 30 s^{-1} shear rateDroplets size distribution at 60 s^{-1} shear rate

2. Droplets size distribution with difference water content.

Microscopic observation of temperature 50°C in(a) water content 0percent (b) water content 20percent (c) water content 30percent and (d) water content 60percent at 3.75 s⁻¹ shear rate



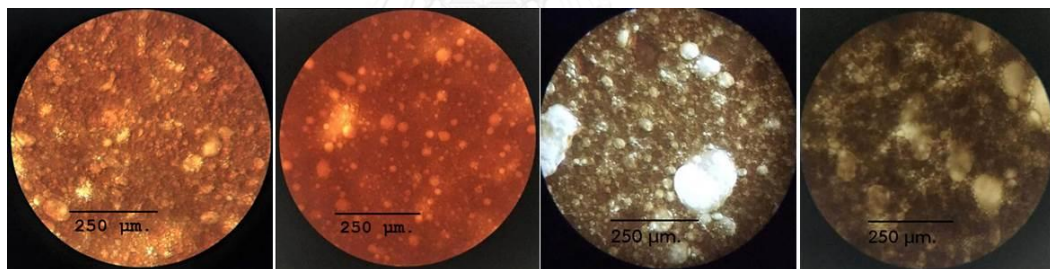
(a)

(b)

(c)

(d)

Microscopic observation of temperature 50°C in(a) water content 0percent (b) water content 20percent (c) water content 30percent and (d) water content 60percent at 7.5 s⁻¹ shear rate



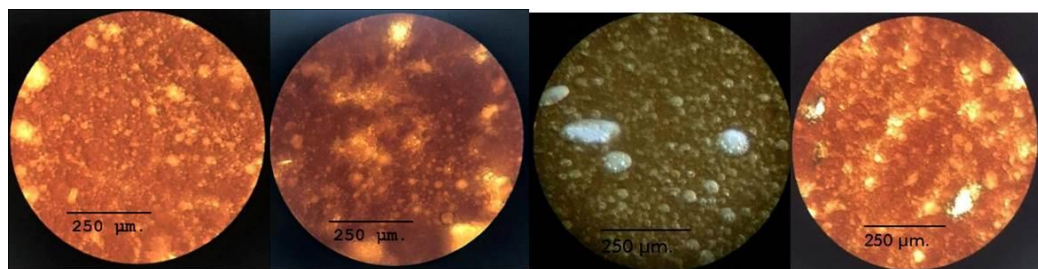
(a)

(b)

(c)

(d)

Microscopic observation of temperature 50°C in(a) water content 0percent (b) water content 20percent (c) water content 30percent and (d) water content 60percent at 15 s⁻¹ shear rate



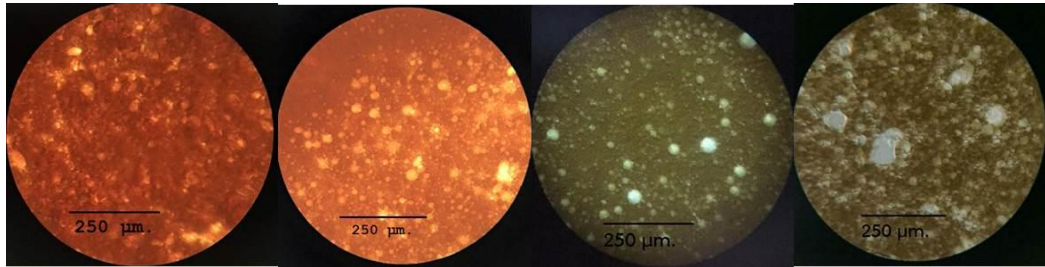
(a)

(b)

(c)

(d)

Microscopic observation of temperature 50°C in(a) water content 0percent (b) water content 20percent (c) water content 30percent and (d) water content 60percent at 30 s⁻¹ shear rate



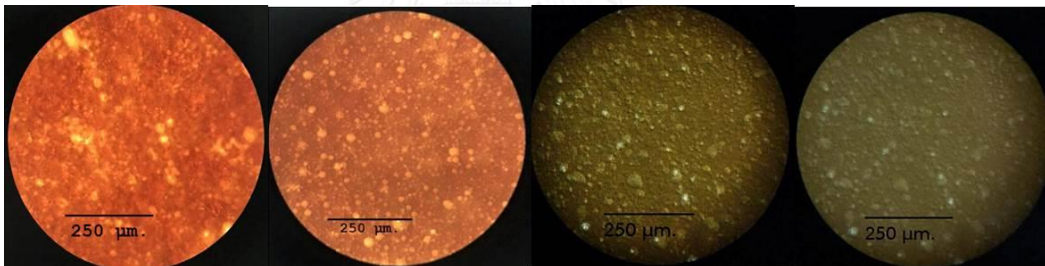
(a)

(b)

(c)

(d)

Microscopic observation of temperature 50°C in(a) water content 0percent (b) water content 20percent (c) water content 30percent and (d) water content 60percent at 60 s⁻¹ shear rate

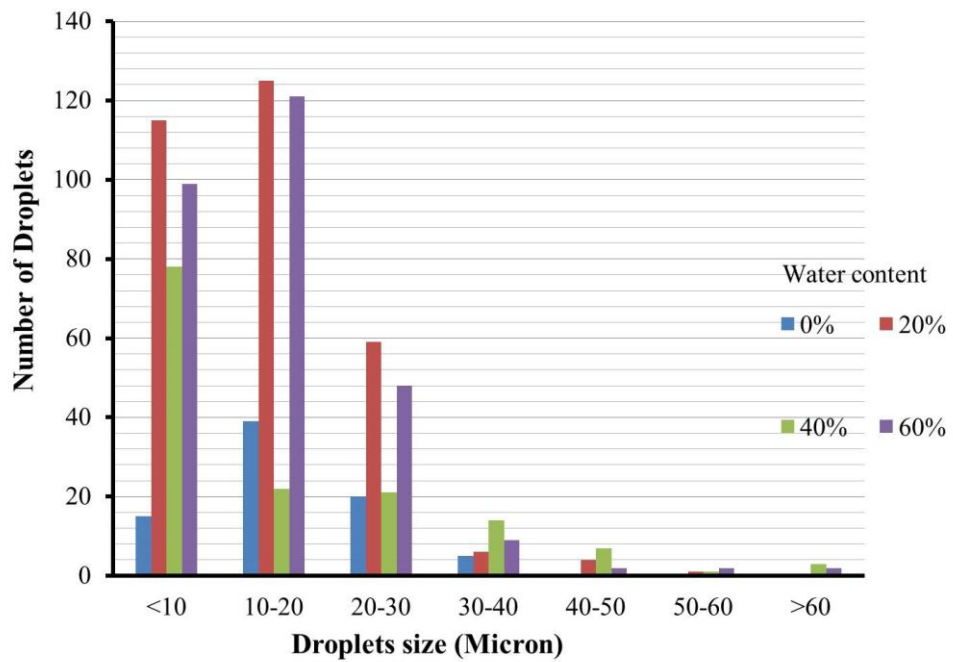
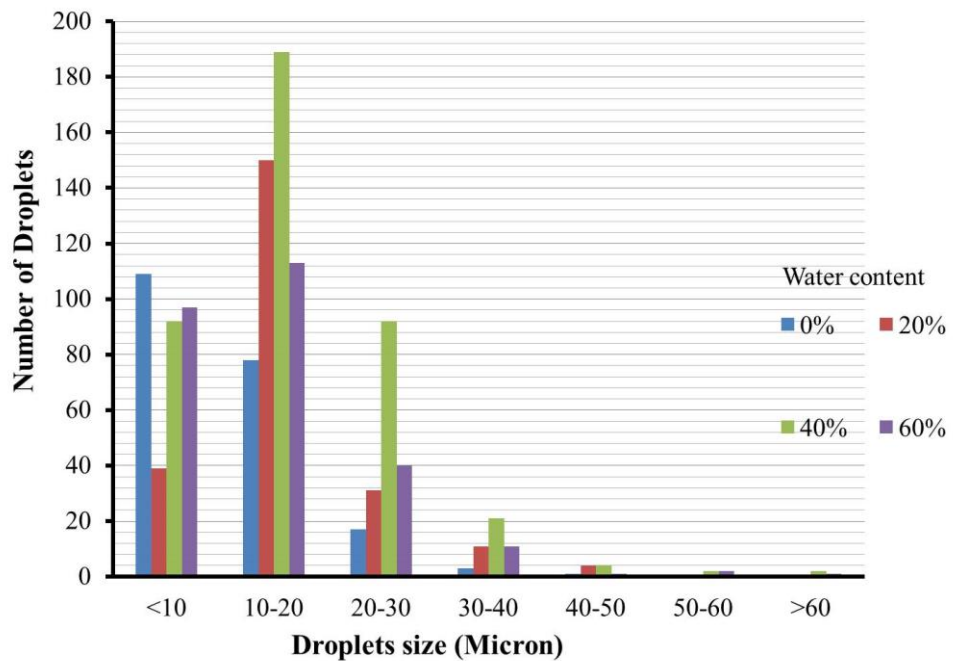


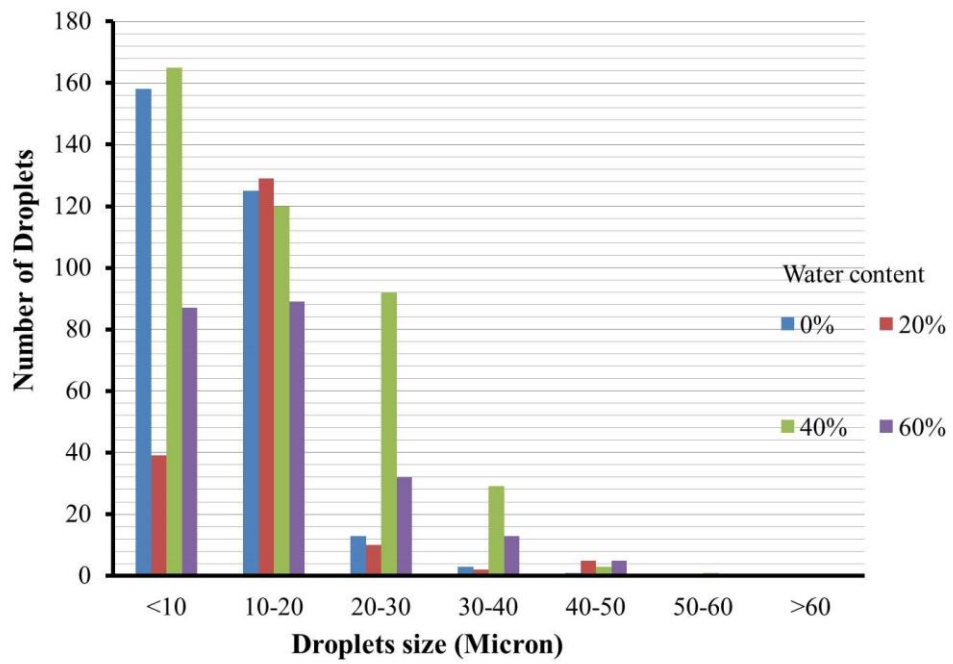
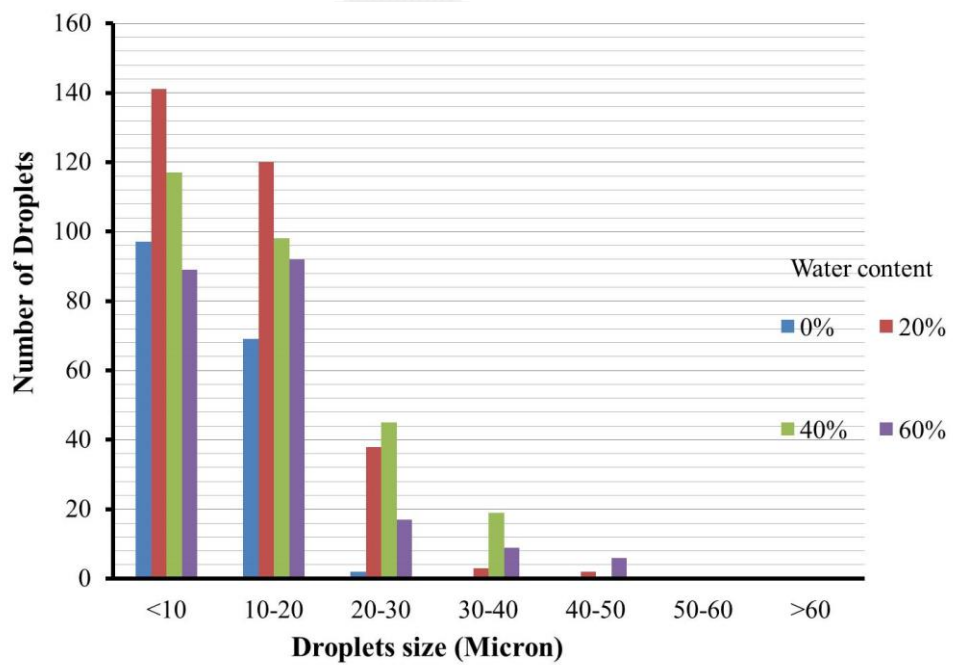
(a)

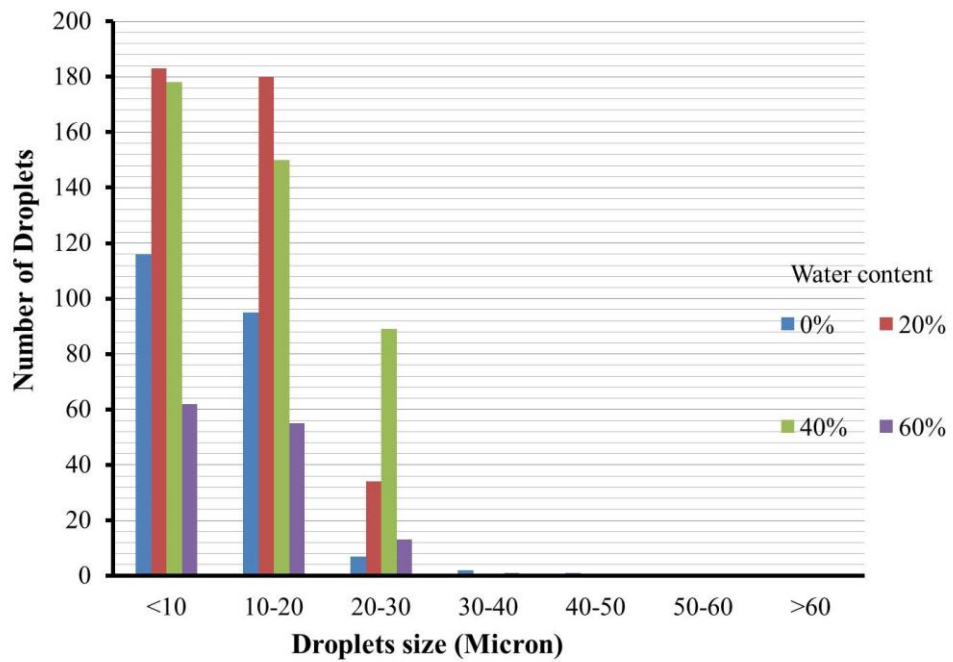
(b)

(c)

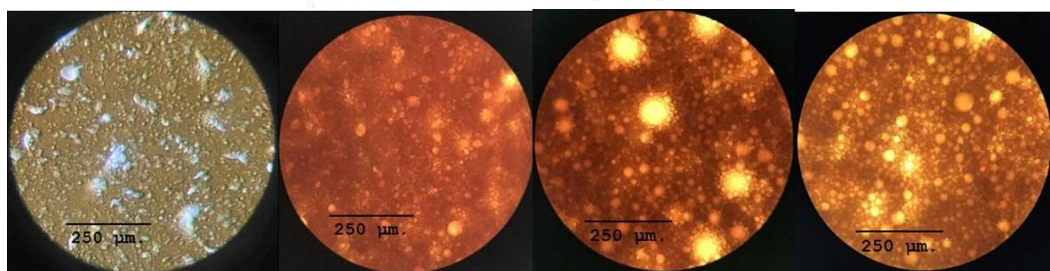
(d)

Droplets size distribution at 3.75 s^{-1} shear rateDroplets size distribution at 7.5 s^{-1} shear rate

Droplets size distribution at 15 s^{-1} shear rateDroplets size distribution at 30 s^{-1} shear rate

Droplets size distribution at 60 s^{-1} shear rate

Microscopic observation of temperature 60°C in (a) water content 0percent (b) water content 20percent (c) water content 30percent and (d) water content 60percent at 3.75 s^{-1} shear rate



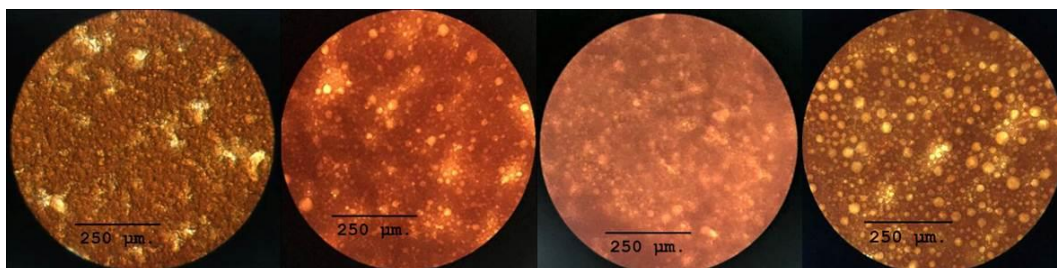
(a)

(b)

(c)

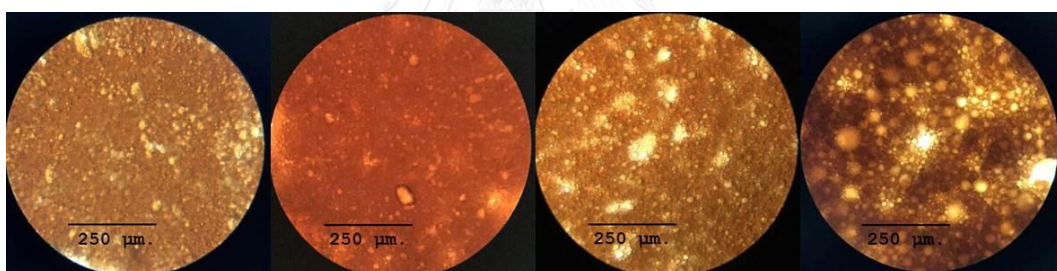
(d)

Microscopic observation of temperature 60°C in(a) water content 0percent (b) water content 20percent (c) water content 30percent and (d) water content 60percent at 7.5 s⁻¹ shear rate



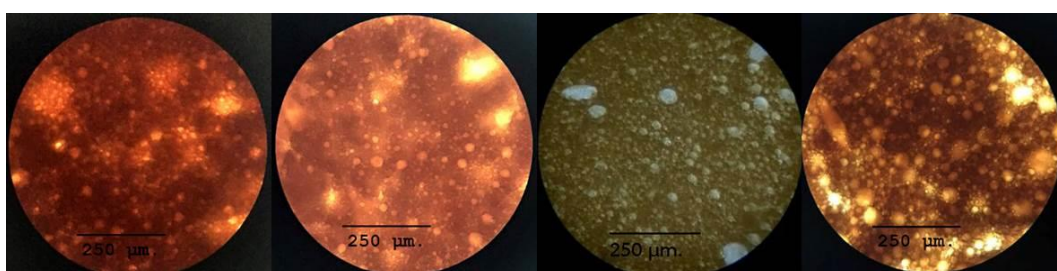
(a) (b) (c) (d)

Microscopic observation of temperature 60°C in(a) water content 0percent (b) water content 20percent (c) water content 30percent and (d) water content 60percent at 15 s⁻¹ shear rate



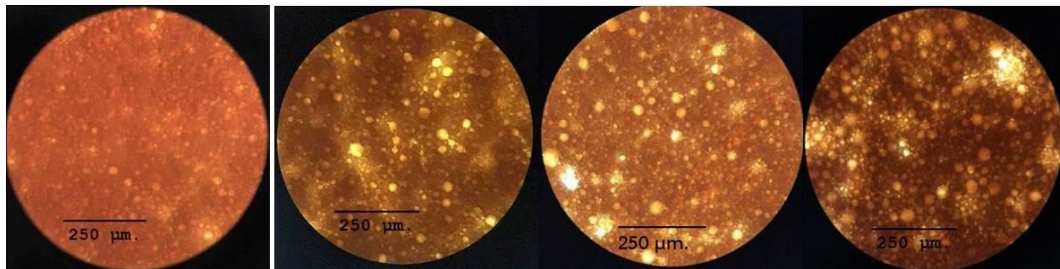
(a) (b) (c) (d)

Microscopic observation of temperature 60°C in(a) water content 0percent (b) water content 20percent (c) water content 30percent and (d) water content 60percent at 30 s⁻¹ shear rate



(a) (b) (c) (d)

Microscopic observation of temperature 60°C in (a) water content 0percent (b) water content 20percent (c) water content 30percent and (d) water content 60percent at 60 s⁻¹ shear rate



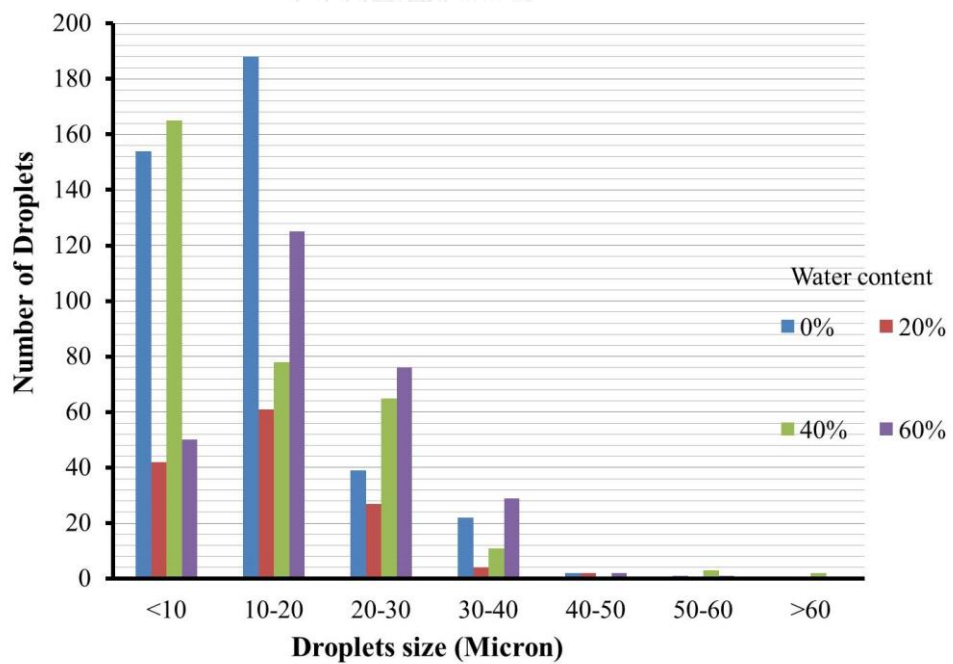
(a)

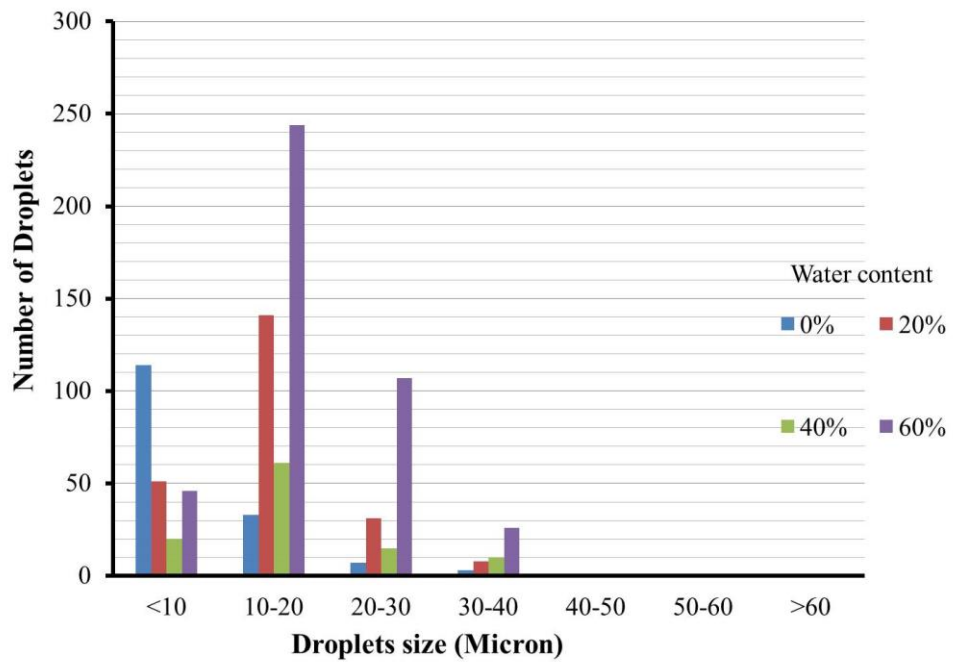
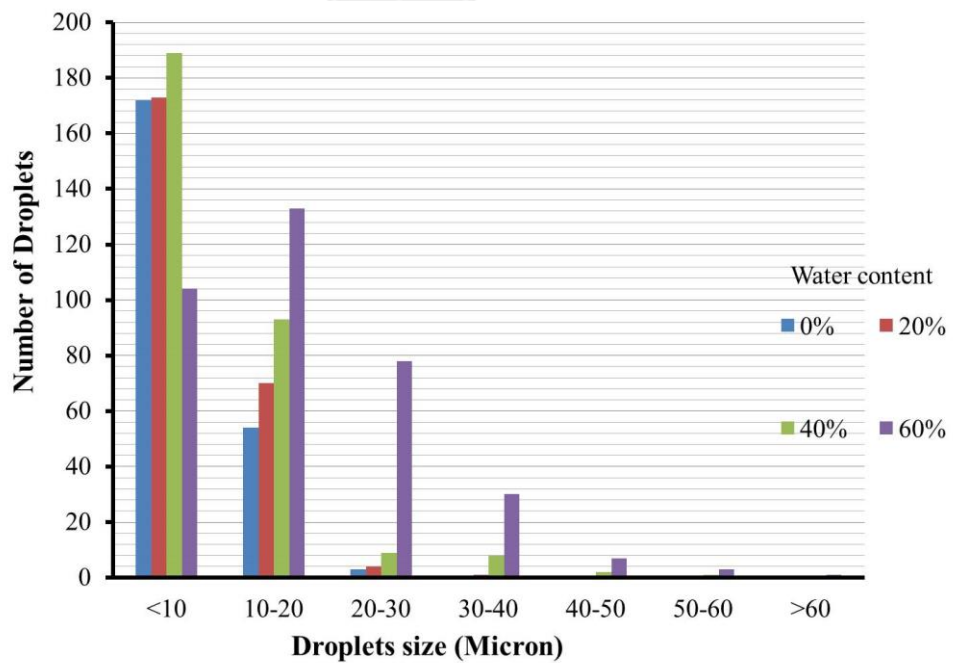
(b)

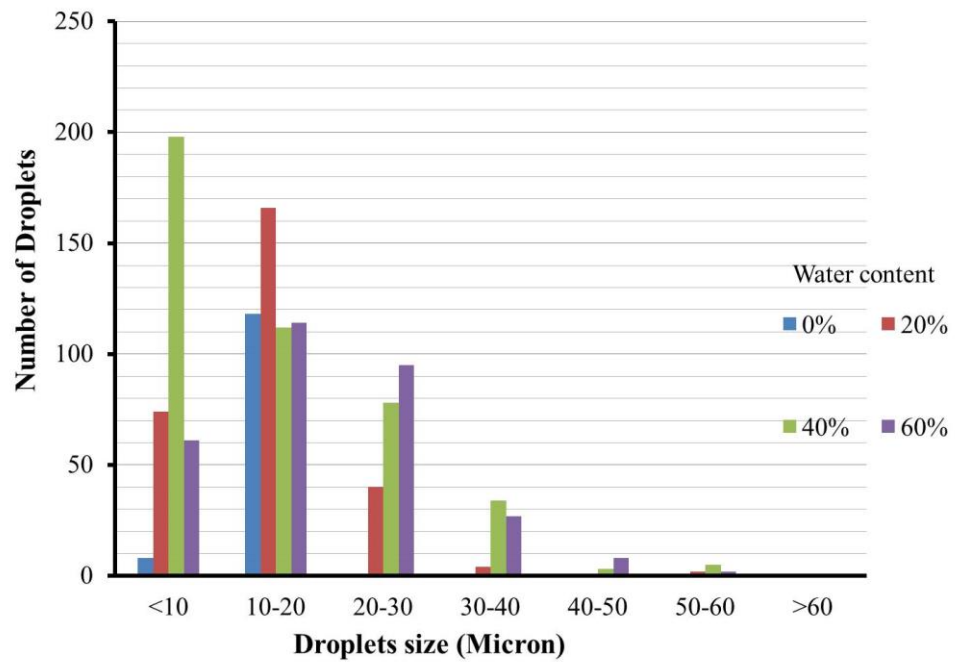
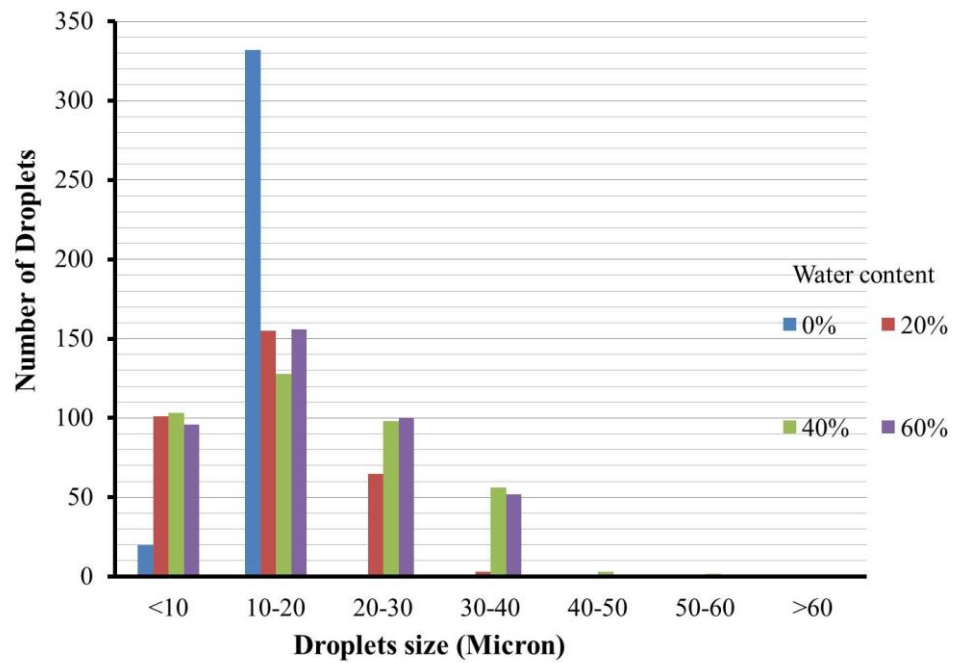
(c)

(d)

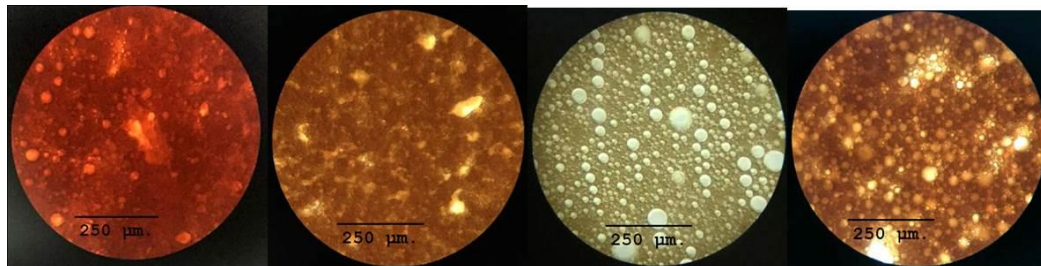
Droplets size distribution at 3.75 s⁻¹ shear rate



Droplets size distribution at 7.5 s^{-1} shear rateDroplets size distribution at 15 s^{-1} shear rate

Droplets size distribution at 30 s^{-1} shear rateDroplets size distribution at 60 s^{-1} shear rate

Microscopic observation of temperature 70°C in(a) water content 0percent (b) water content 20percent (c) water content 30percent and (d) water content 60percent at 3.75 s⁻¹ shear rate



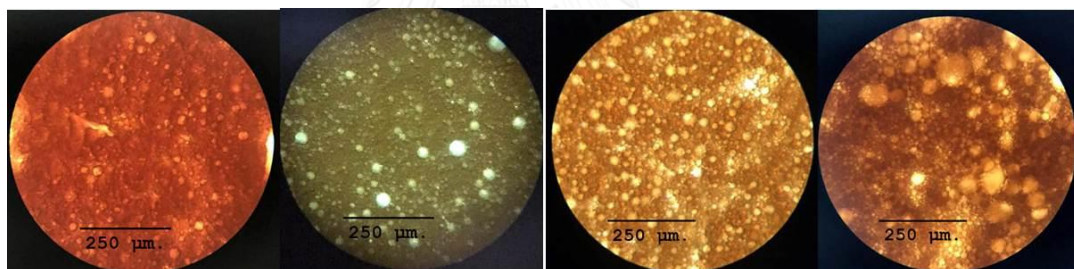
(a)

(b)

(c)

(d)

Microscopic observation of temperature 70°C in(a) water content 0percent (b) water content 20percent (c) water content 30percent and (d) water content 60percent at 7.5 s⁻¹ shear rate



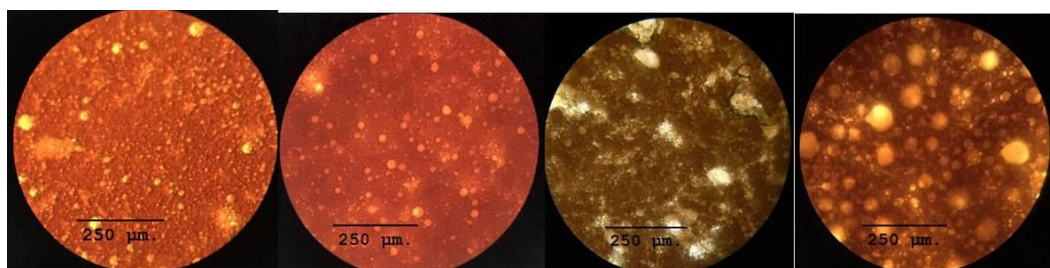
(a)

(b)

(c)

(d)

Microscopic observation of temperature 70°C in(a) water content 0percent (b) water content 20percent (c) water content 30percent and (d) water content 60percent at 15 s⁻¹ shear rate



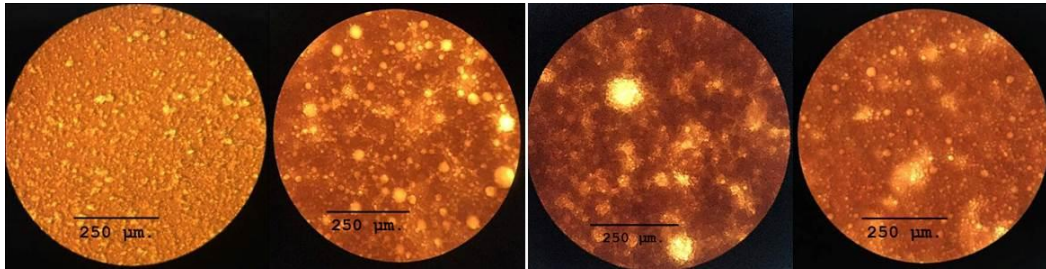
(a)

(b)

(c)

(d)

Microscopic observation of temperature 70°C in(a) water content 0percent (b) water content 20percent (c) water content 30percent and (d) water content 60percent at 30 s⁻¹ shear rate



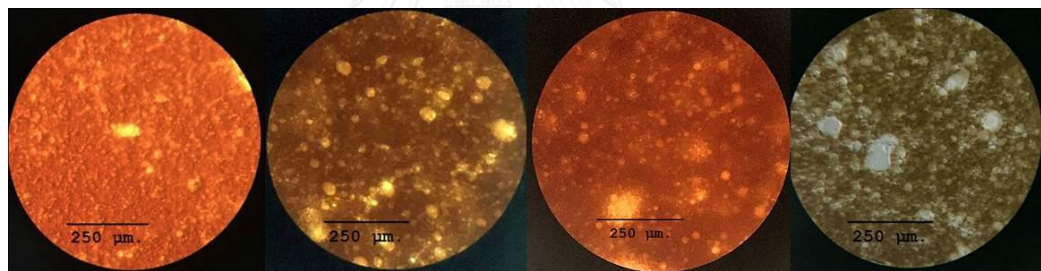
(a)

(b)

(c)

(d)

Microscopic observation of temperature 70°C in(a) water content 0percent (b) water content 20percent (c) water content 30percent and (d) water content 60percent at 60 s⁻¹ shear rate

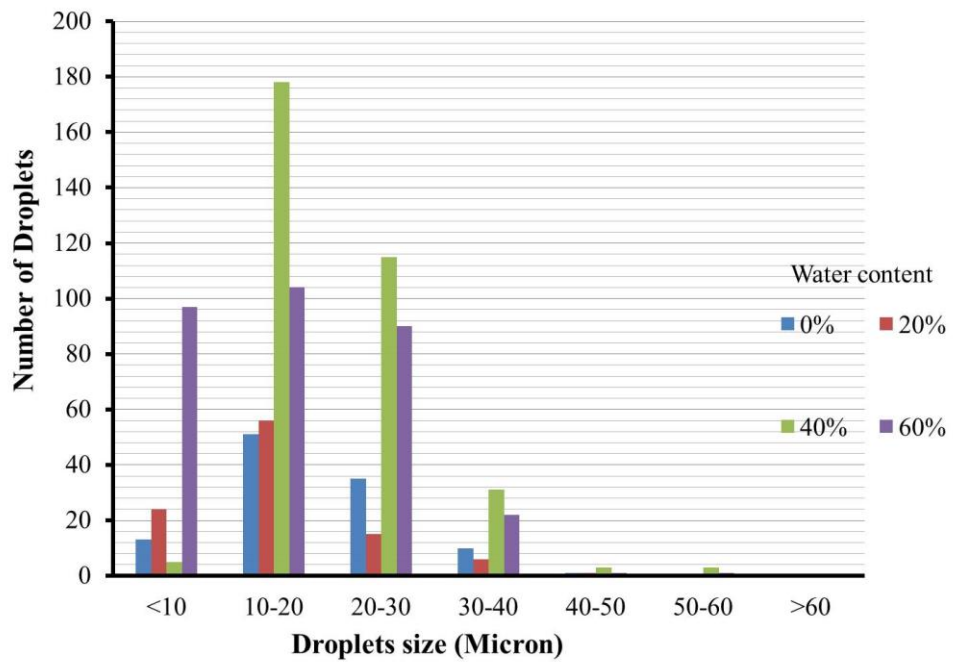
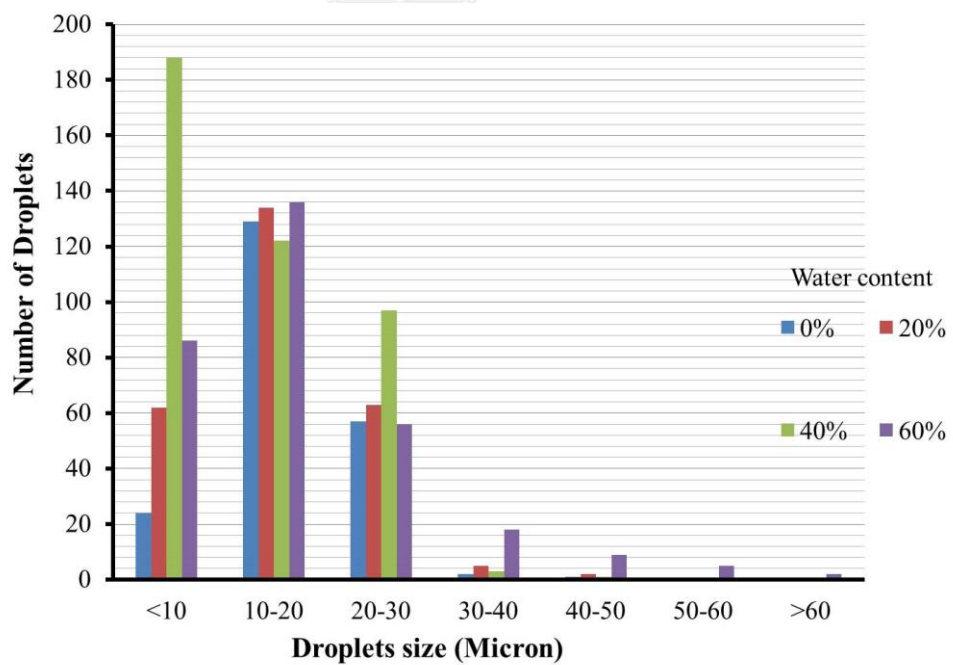


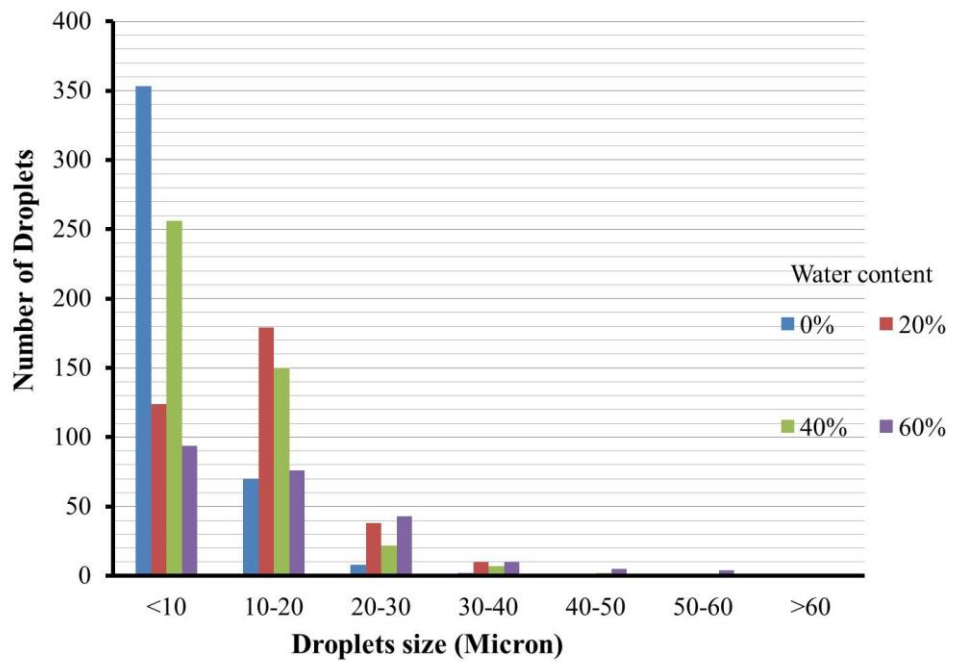
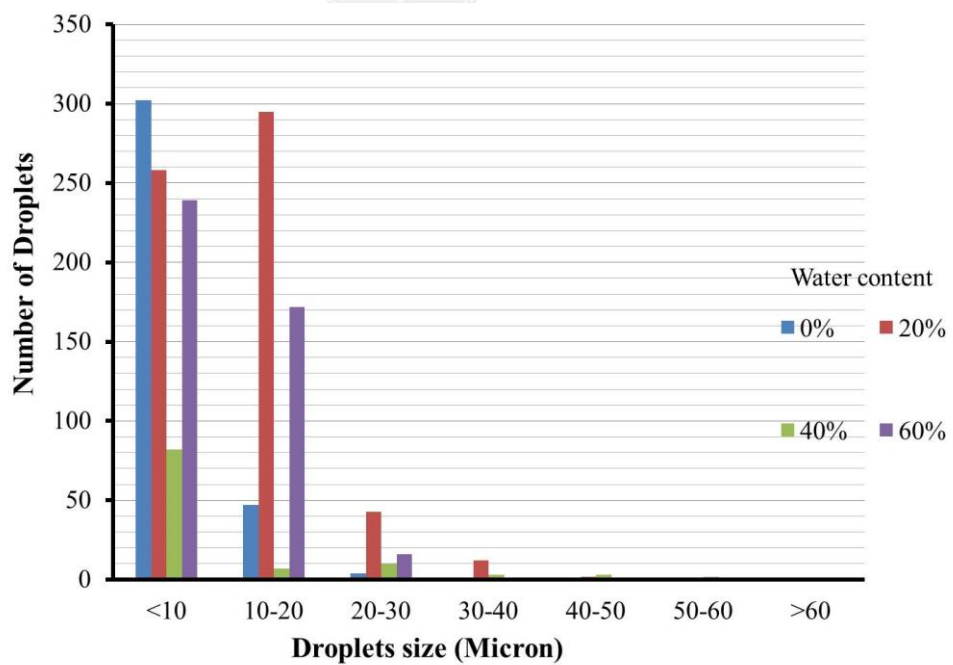
(a)

(b)

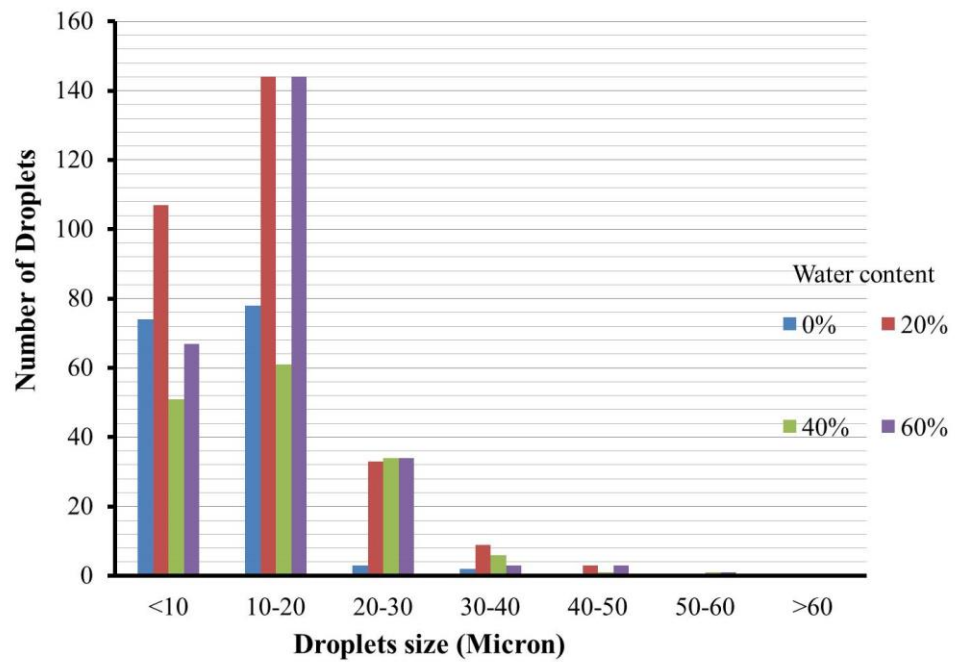
(c)

(d)

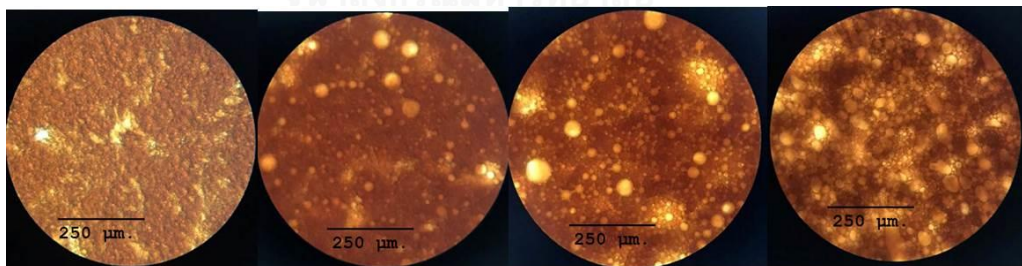
Droplets size distribution at 3.75 s^{-1} shear rateDroplets size distribution at 7.5 s^{-1} shear rate

Droplets size distribution at 15 s^{-1} shear rateDroplets size distribution at 30 s^{-1} shear rate

Droplets size distribution at 60 s^{-1} shear rate



Microscopic observation of temperature 80°C in (a) water content 0percent (b) water content 20percent (c) water content 30percent and (d) water content 60percent at 3.75 s^{-1} shear rate



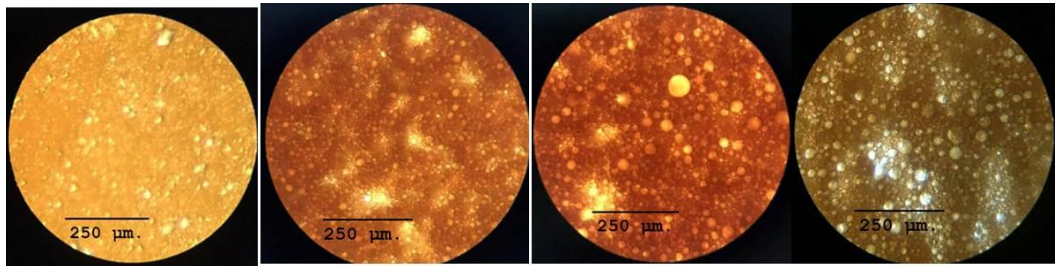
(a)

(b)

(c)

(d)

Microscopic observation of temperature 80°C in(a) water content 0percent (b) water content 20percent (c) water content 30percent and (d) water content 60percent at 7.5 s⁻¹ shear rate



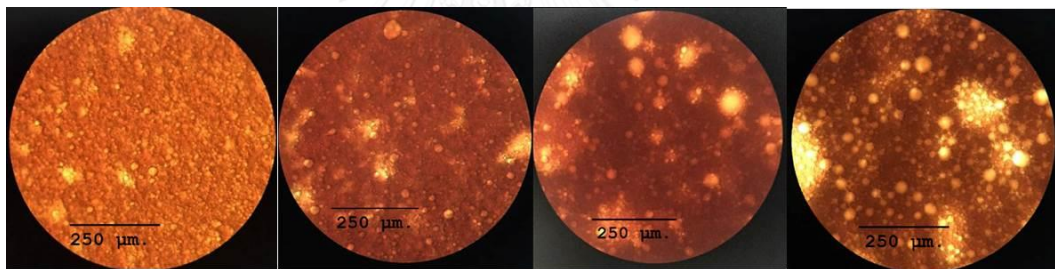
(a)

(b)

(c)

(d)

Microscopic observation of temperature 80°C in(a) water content 0percent (b) water content 20percent (c) water content 30percent and (d) water content 60percent at 15 s⁻¹ shear rate



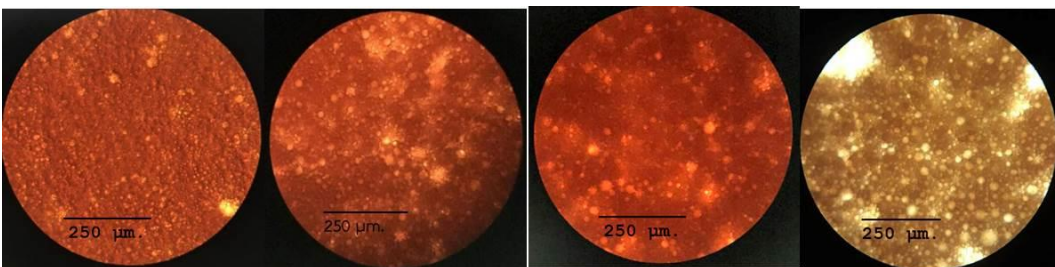
(a)

(b)

(c)

(d)

Microscopic observation of temperature 80°C in(a) water content 0percent (b) water content 20percent (c) water content 30percent and (d) water content 60percent at 30 s⁻¹ shear rate



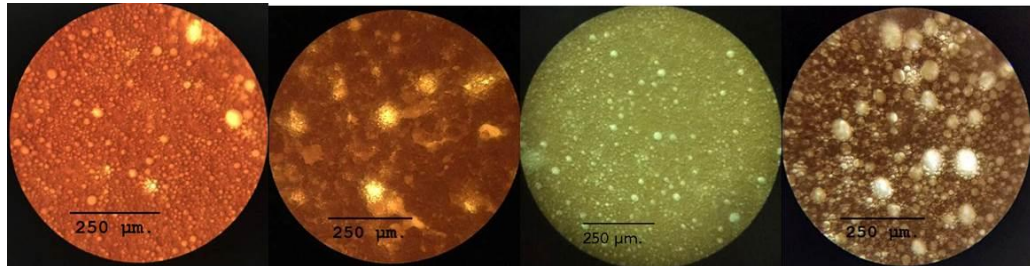
(a)

(b)

(c)

(d)

Microscopic observation of temperature 80°C in (a) water content 0percent (b) water content 20percent (c) water content 30percent and (d) water content 60percent at 60 s⁻¹ shear rate



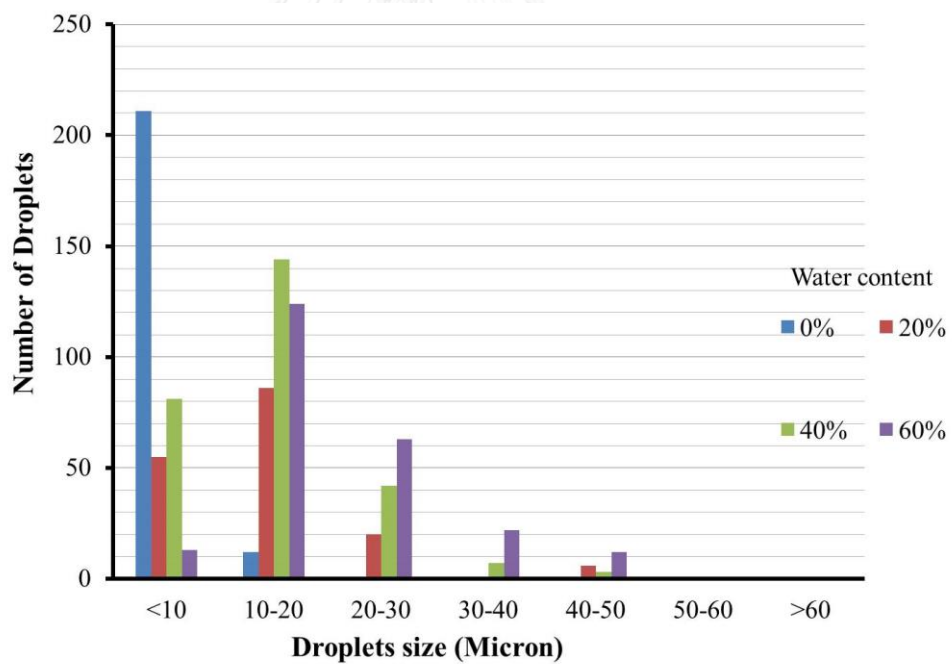
(a)

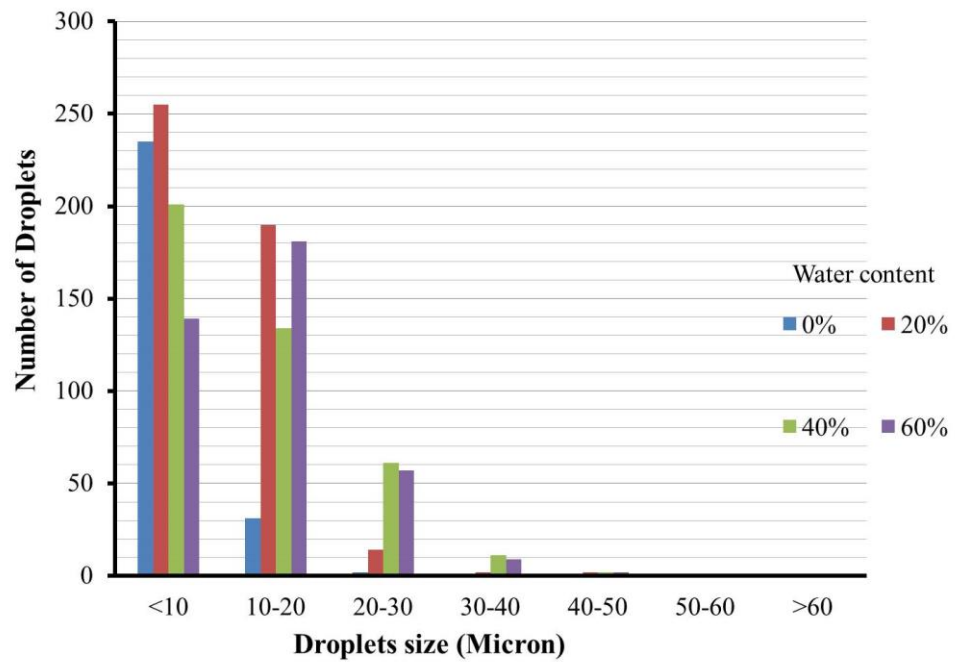
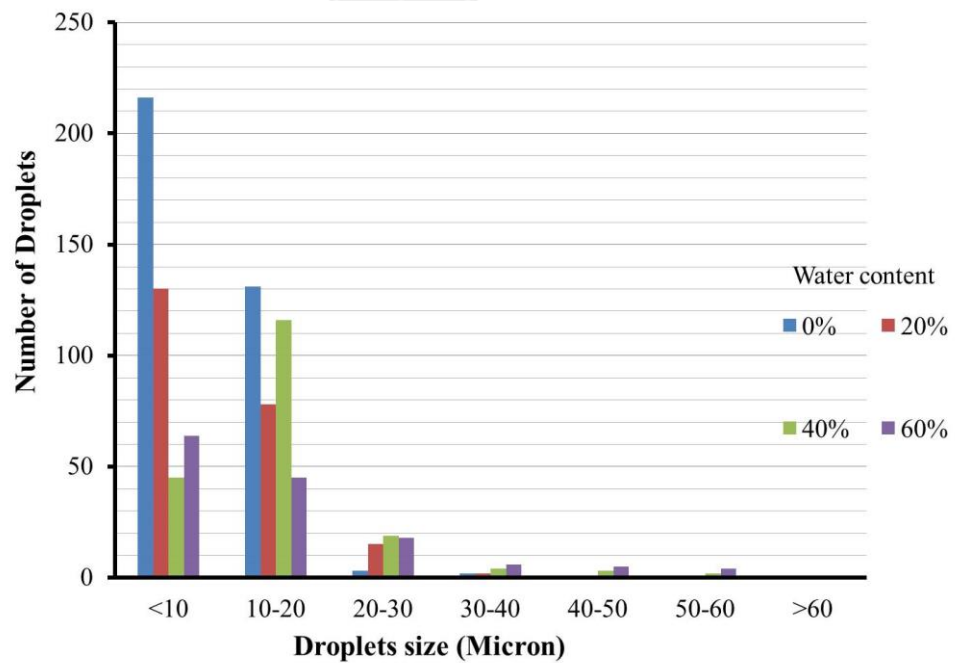
(b)

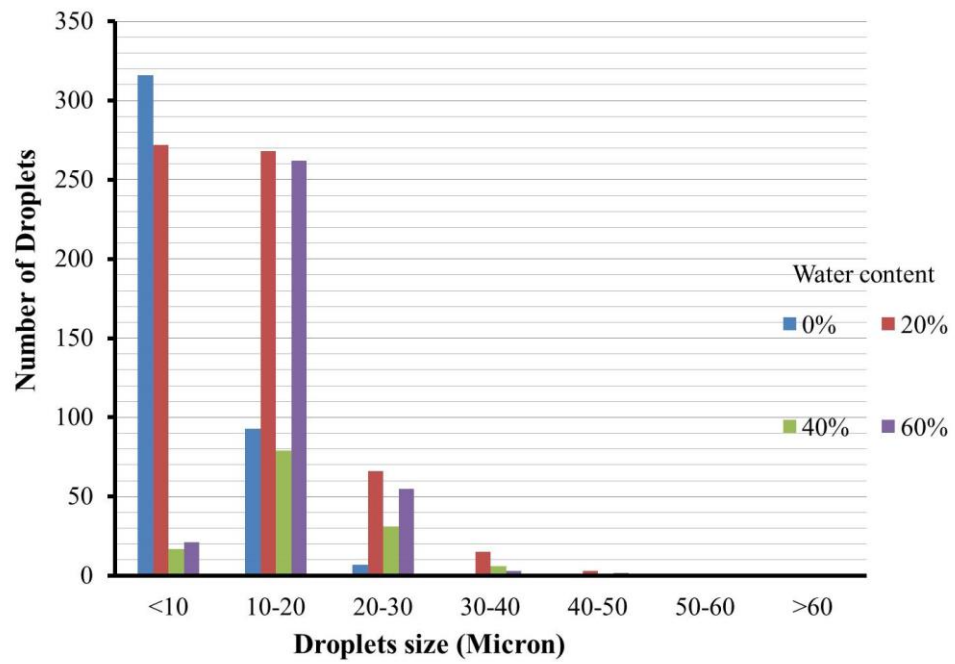
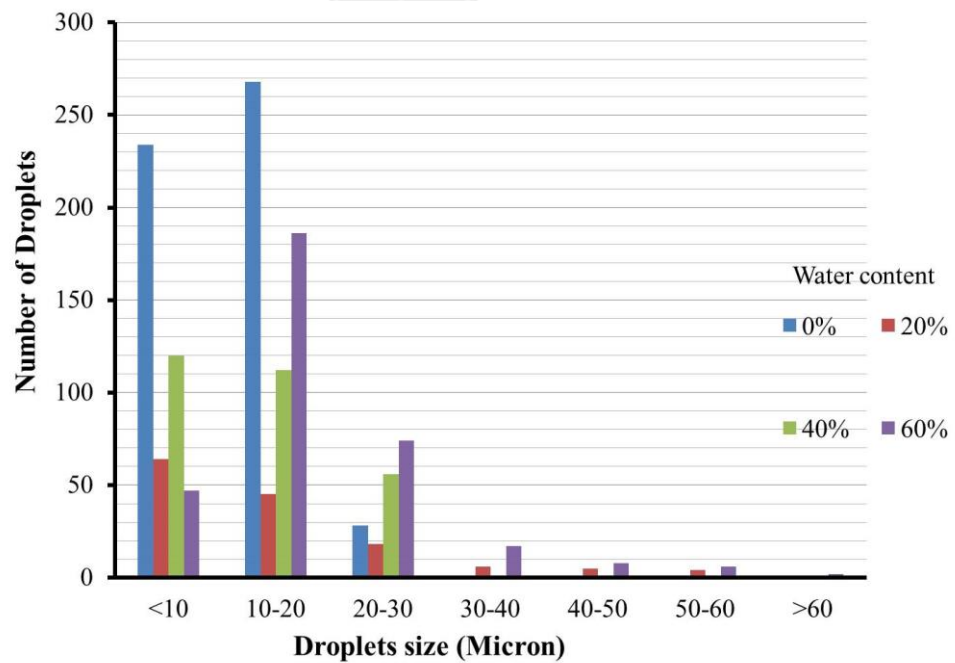
(c)

(d)

Droplets size distribution at 3.75 s⁻¹ shear rate

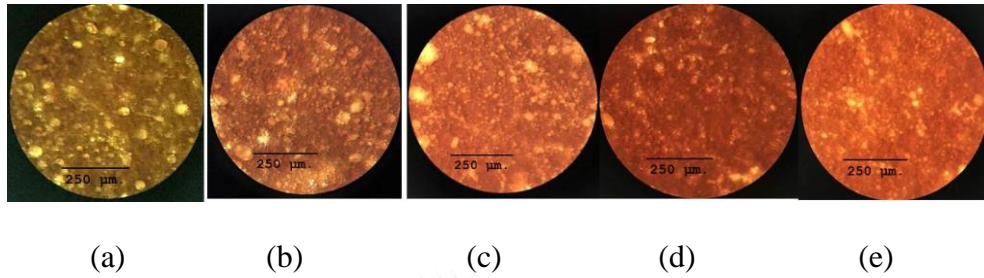


Droplets size distribution at 7.5 s^{-1} shear rateDroplets size distribution at 15 s^{-1} shear rate

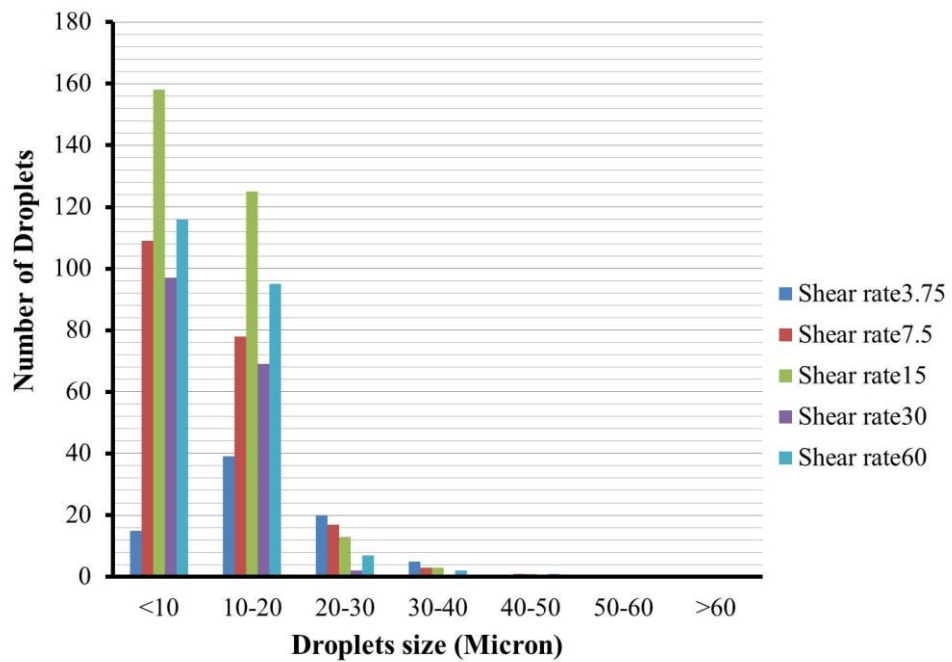
Droplets size distribution at 30 s⁻¹ shear rateDroplets size distribution at 60 s⁻¹ shear rate

3. Droplets size distribution with difference shear rate.

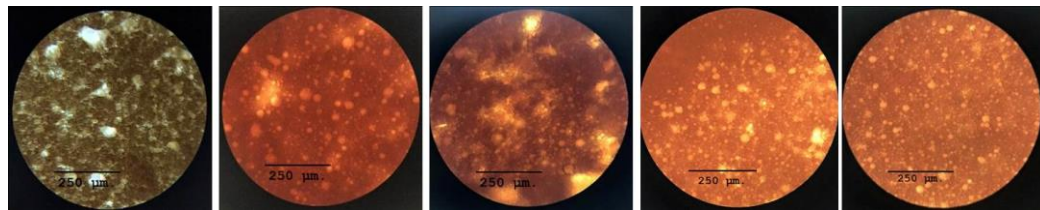
Microscopic observation of temperature 50°C in (a) shear rate 3.75 s^{-1} (b) shear rate 7.5 s^{-1} (c) shear rate 15 s^{-1} (d) shear rate 30 s^{-1} and (e) shear rate 60 s^{-1} at 0 percent water content.



Droplets size distribution at 0 percent water content

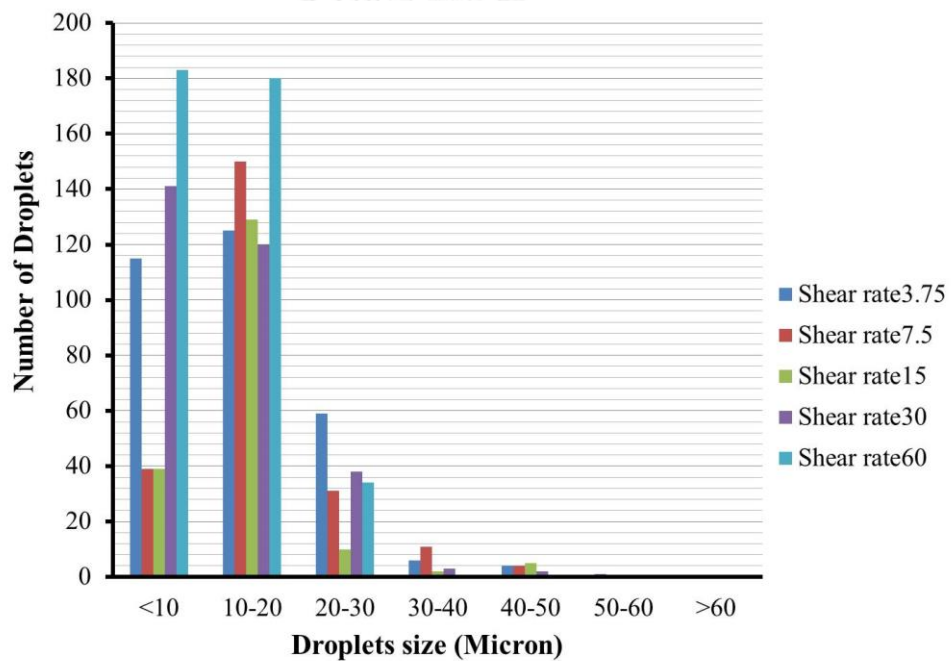


Microscopic observation of temperature 50°C in (a) shear rate 3.75 s⁻¹ (b) shear rate 7.5 s⁻¹ (c) shear rate 15 s⁻¹ (d) shear rate 30 s⁻¹ and (e) shear rate 60 s⁻¹ at 20 percent water content.

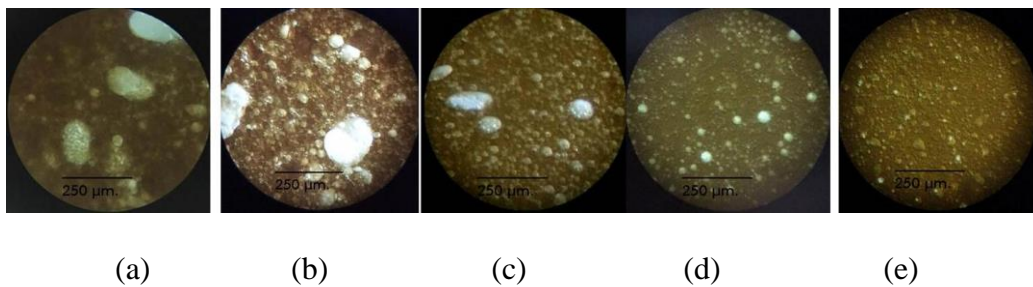


(b) (b) (c) (d) (e)

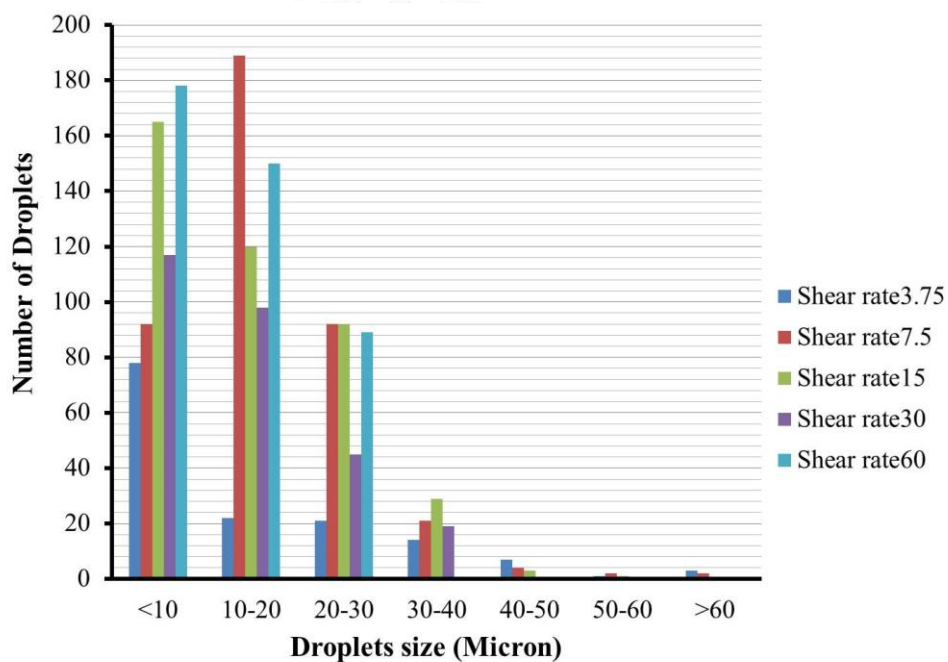
Droplets size distribution at 20 percent water content



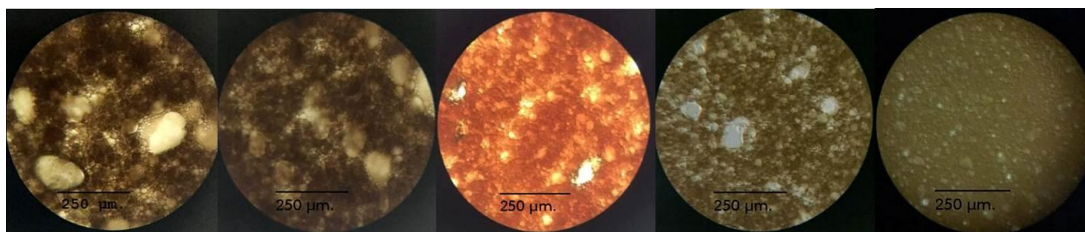
Microscopic observation of temperature 50°C in (a) shear rate 3.75 s⁻¹ (b) shear rate 7.5 s⁻¹ (c) shear rate 15 s⁻¹ (d) shear rate 30 s⁻¹ and (e) shear rate 60 s⁻¹ at 40 percent water content.



Droplets size distribution at 40 percent water content

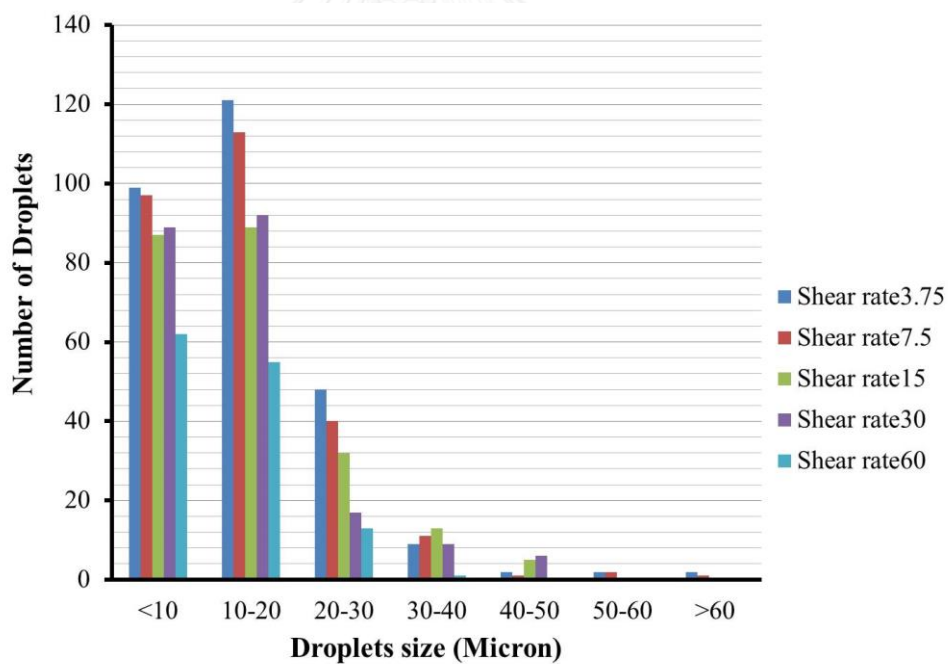


Microscopic observation of temperature 50°C in (a) shear rate 3.75 s⁻¹ (b) shear rate 7.5 s⁻¹ (c) shear rate 15 s⁻¹ (d) shear rate 30 s⁻¹ and (e) shear rate 60 s⁻¹ at 60 percent water content.

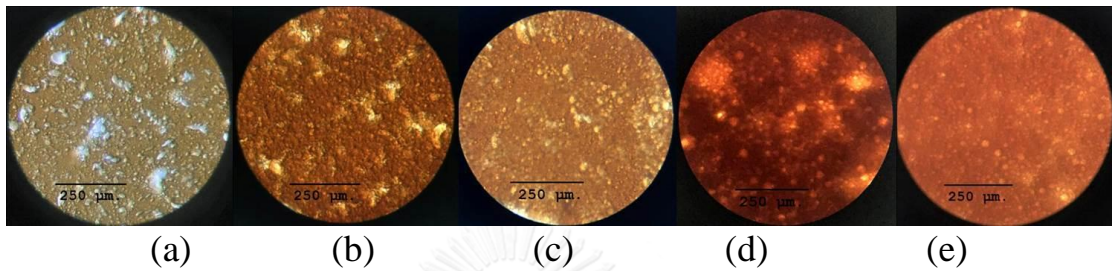


(a) (b) (c) (d) (e)

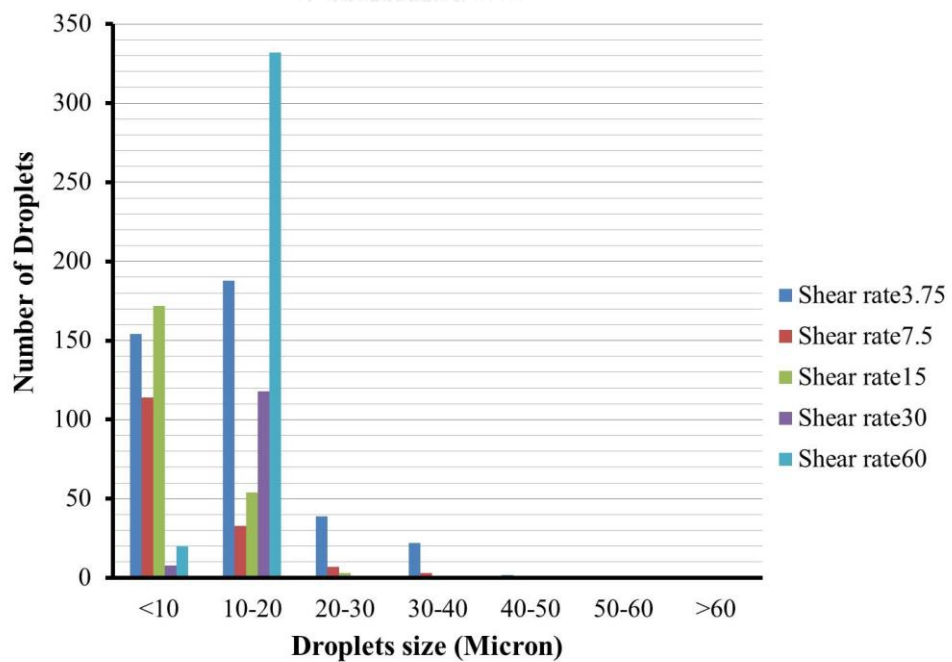
Droplets size distribution at 60 percent water content



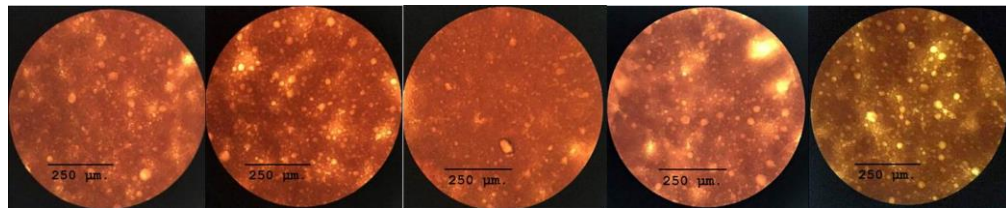
Microscopic observation of temperature 60°C in (a) shear rate 3.75 s⁻¹ (b) shear rate 7.5 s⁻¹ (c) shear rate 15 s⁻¹ (d) shear rate 30 s⁻¹ and (e) shear rate 60 s⁻¹ at 0 percent water content.



Droplets size distribution at 0 percent water content

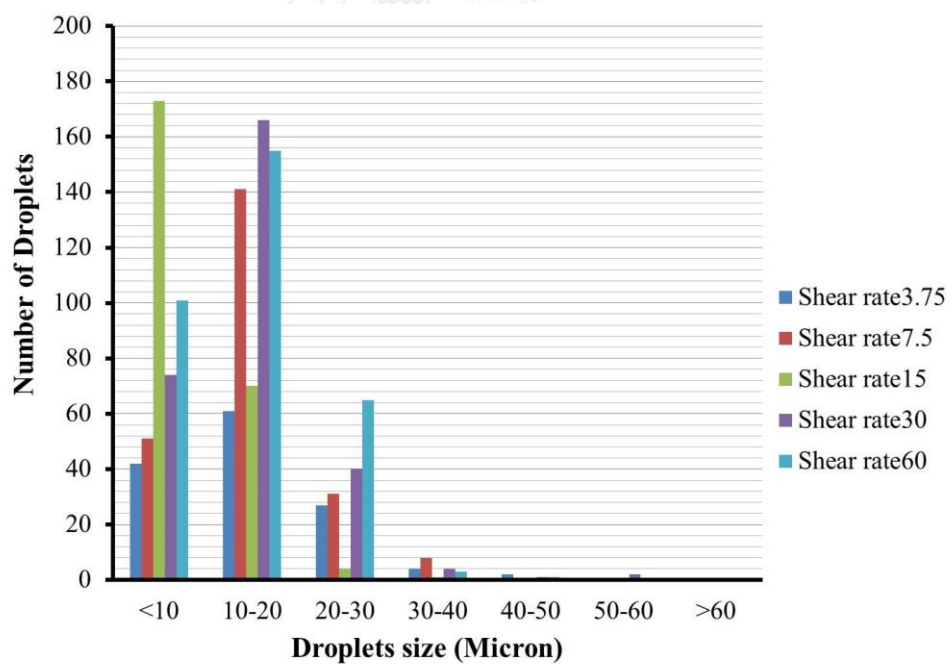


Microscopic observation of temperature 60°C in (a) shear rate 3.75 s⁻¹ (b) shear rate 7.5 s⁻¹ (c) shear rate 15 s⁻¹ (d) shear rate 30 s⁻¹ and (e) shear rate 60 s⁻¹ at 20 percent water content.

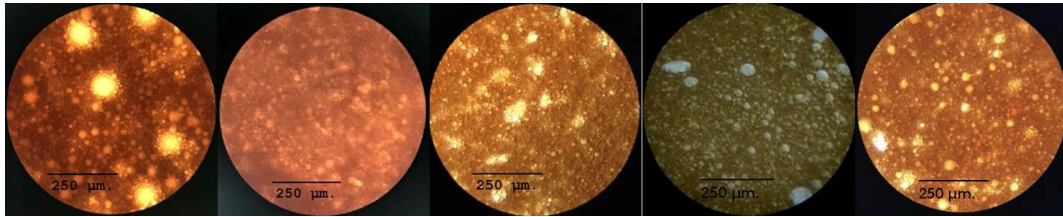


(a) (b) (c) (d) (e)

Droplets size distribution at 20 percent water content

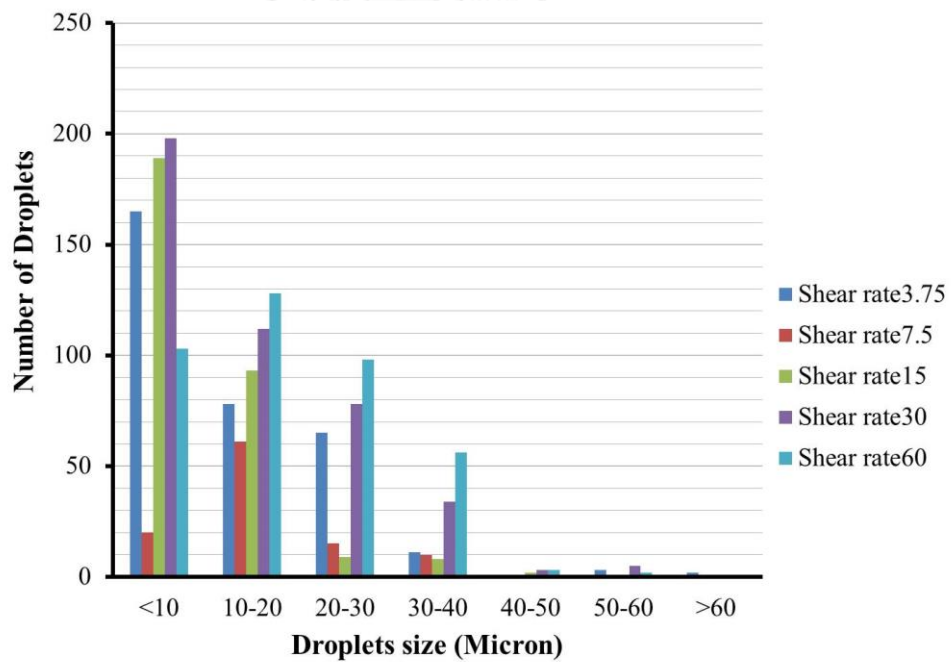


Microscopic observation of temperature 60°C in (a) shear rate 3.75 s⁻¹ (b) shear rate 7.5 s⁻¹ (c) shear rate 15 s⁻¹ (d) shear rate 30 s⁻¹ and (e) shear rate 60 s⁻¹ at 40 percent water content.

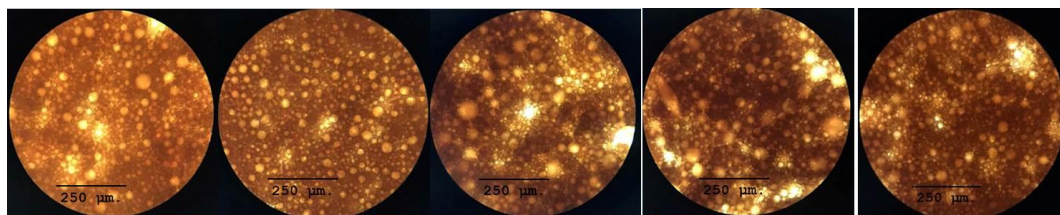


(a) (b) (c) (d) (e)

Droplets size distribution at 40 percent water content

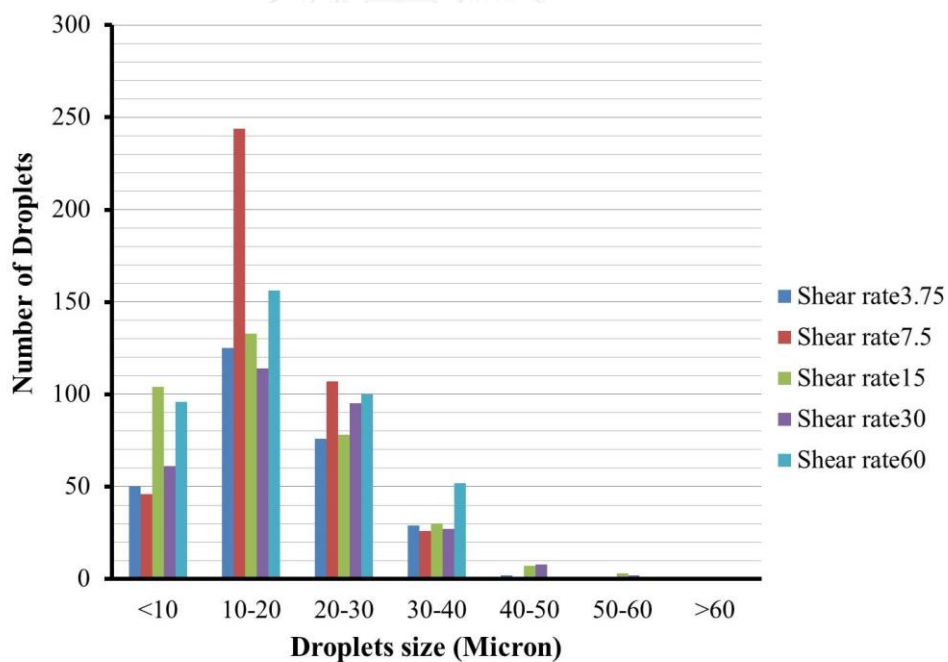


Microscopic observation of temperature 60°C in (a) shear rate 3.75 s⁻¹ (b) shear rate 7.5 s⁻¹ (c) shear rate 15 s⁻¹ (d) shear rate 30 s⁻¹ and (e) shear rate 60 s⁻¹ at 60percent water content.

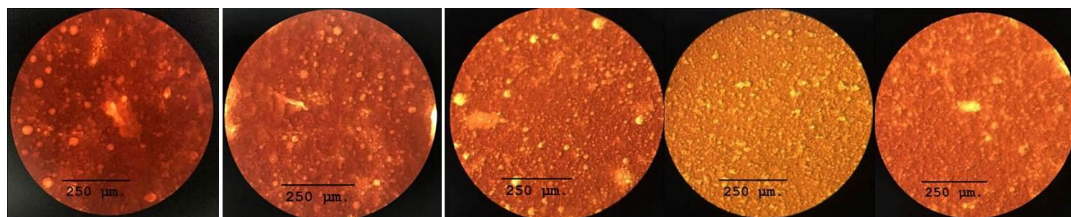


(a) (b) (c) (d) (e)

Droplets size distribution at 60percent water content

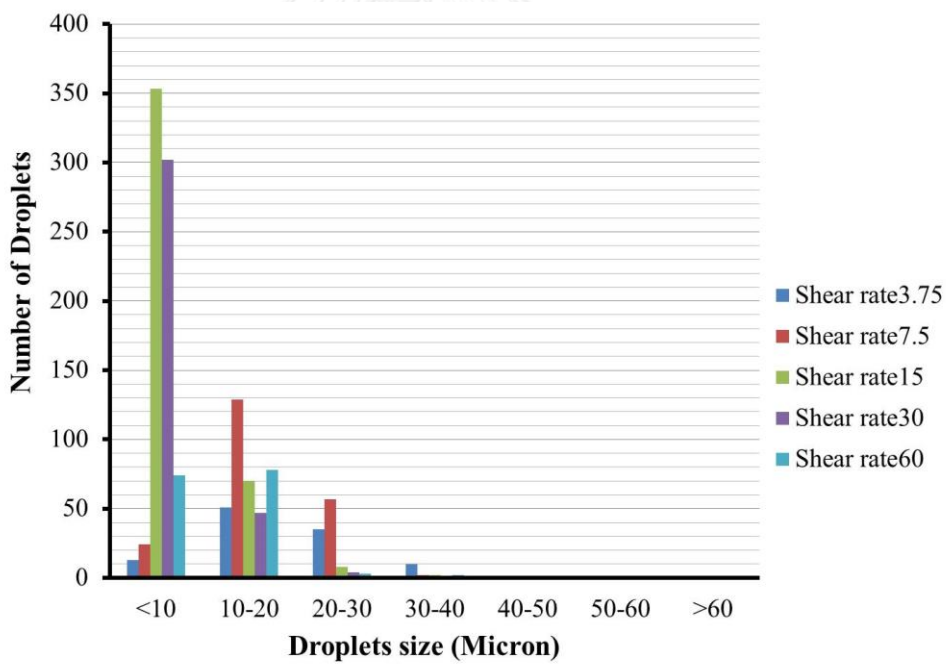


Microscopic observation of temperature 70°C in (a) shear rate 3.75 s⁻¹ (b) shear rate 7.5 s⁻¹ (c) shear rate 15 s⁻¹ (d) shear rate 30 s⁻¹ and (e) shear rate 60 s⁻¹ at 0 percent water content.

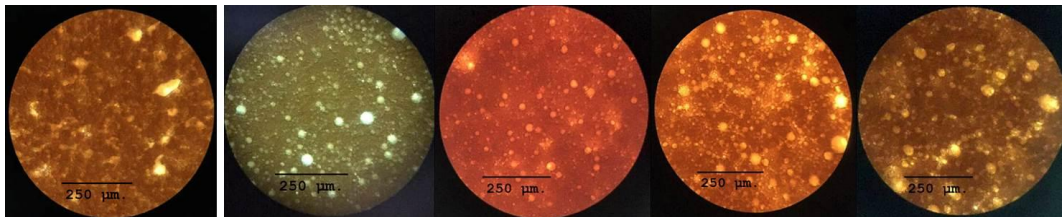


(a) (b) (c) (d) (e)

Droplets size distribution at 0 percent water content

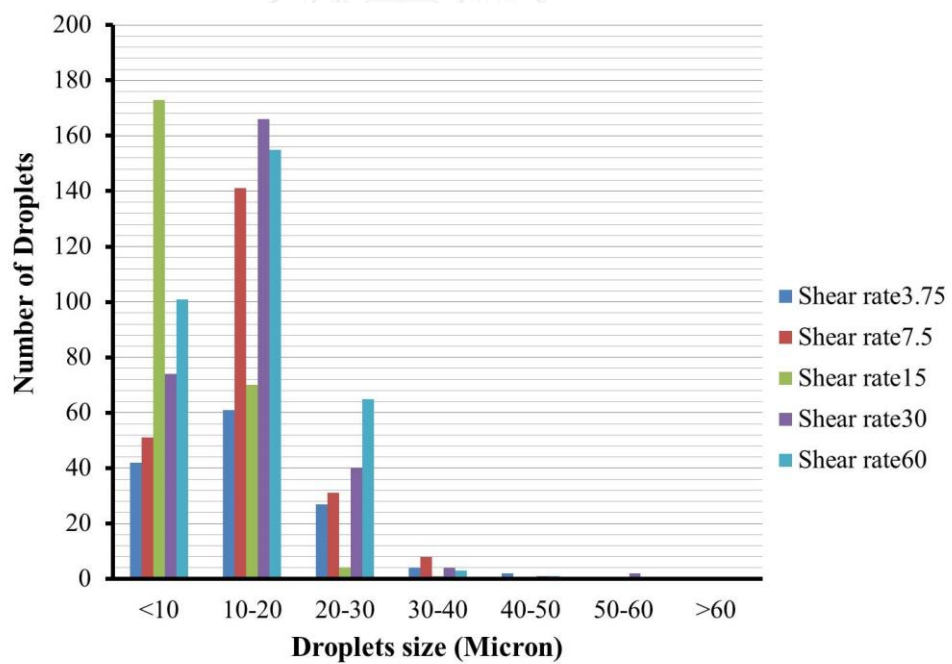


Microscopic observation of temperature 70°C in (a) shear rate 3.75 s⁻¹ (b) shear rate 7.5 s⁻¹ (c) shear rate 15 s⁻¹ (d) shear rate 30 s⁻¹ and (e) shear rate 60 s⁻¹ at 20 percent water content.

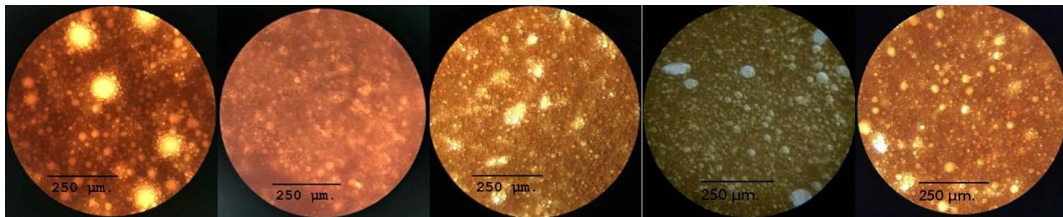


(a) (b) (c) (d) (e)

Droplets size distribution at 0 percent water content

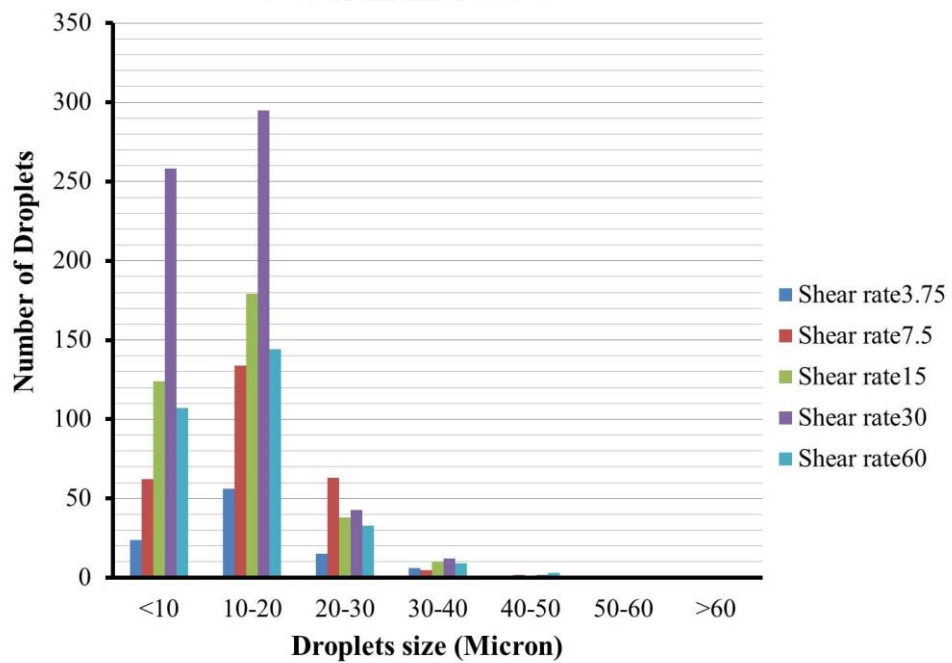


Microscopic observation of temperature 70°C in (a) shear rate 3.75 s^{-1} (b) shear rate 7.5 s^{-1} (c) shear rate 15 s^{-1} (d) shear rate 30 s^{-1} and (e) shear rate 60 s^{-1} at 20 percent water content.

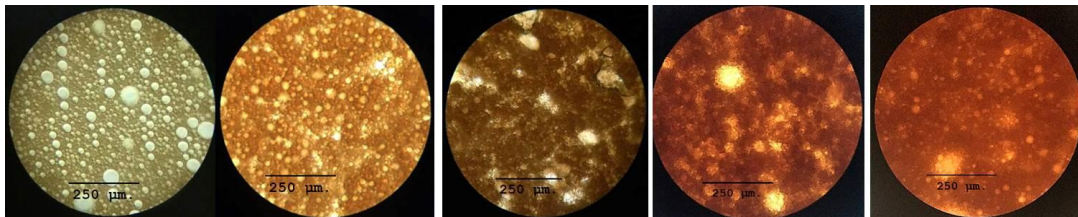


(a) (b) (c) (d) (e)

Droplets size distribution at 20 percent water content

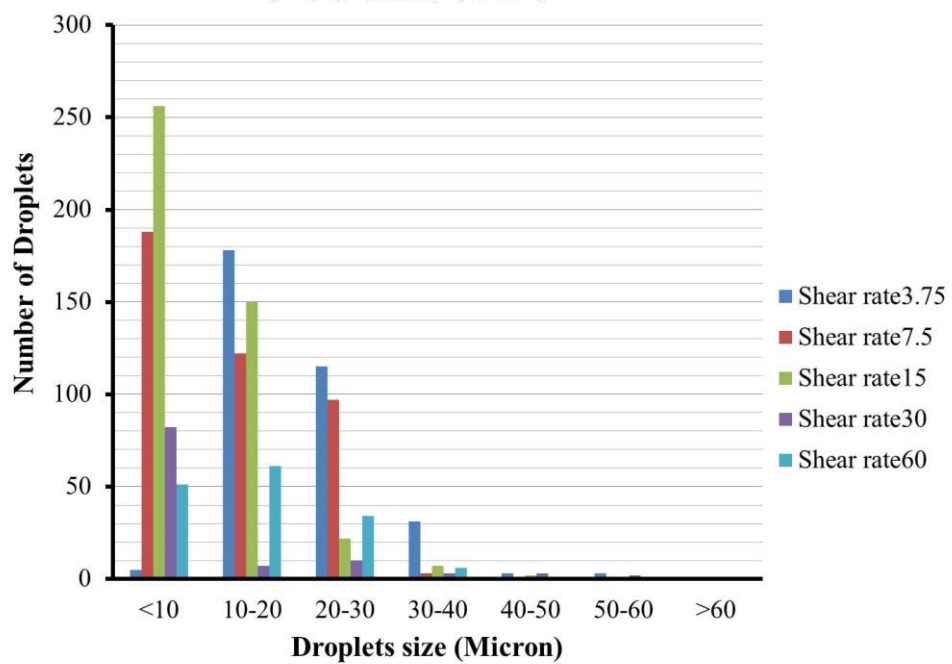


Microscopic observation of temperature 70°C in (a) shear rate 3.75 s⁻¹ (b) shear rate 7.5 s⁻¹ (c) shear rate 15 s⁻¹ (d) shear rate 30 s⁻¹ and (e) shear rate 60 s⁻¹ at 40 percent water content.

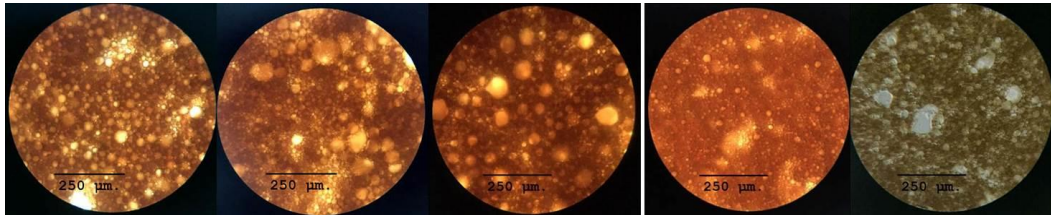


(a) (b) (c) (d) (e)

Droplets size distribution at 40 percent water content

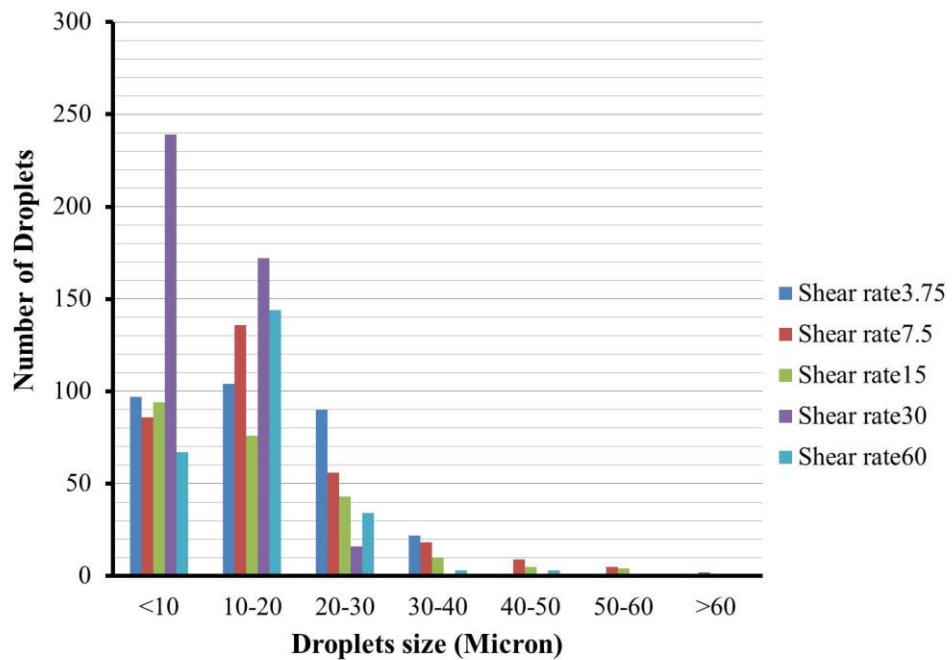


Microscopic observation of temperature 70°C in (a) shear rate 3.75 s⁻¹ (b) shear rate 7.5 s⁻¹ (c) shear rate 15 s⁻¹ (d) shear rate 30 s⁻¹ and (e) shear rate 60 s⁻¹ at 60 percent water content.

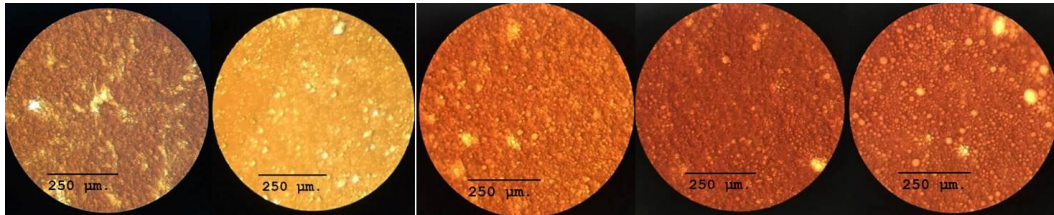


(a) (b) (c) (d) (e)

Droplets size distribution at 60 percent water content

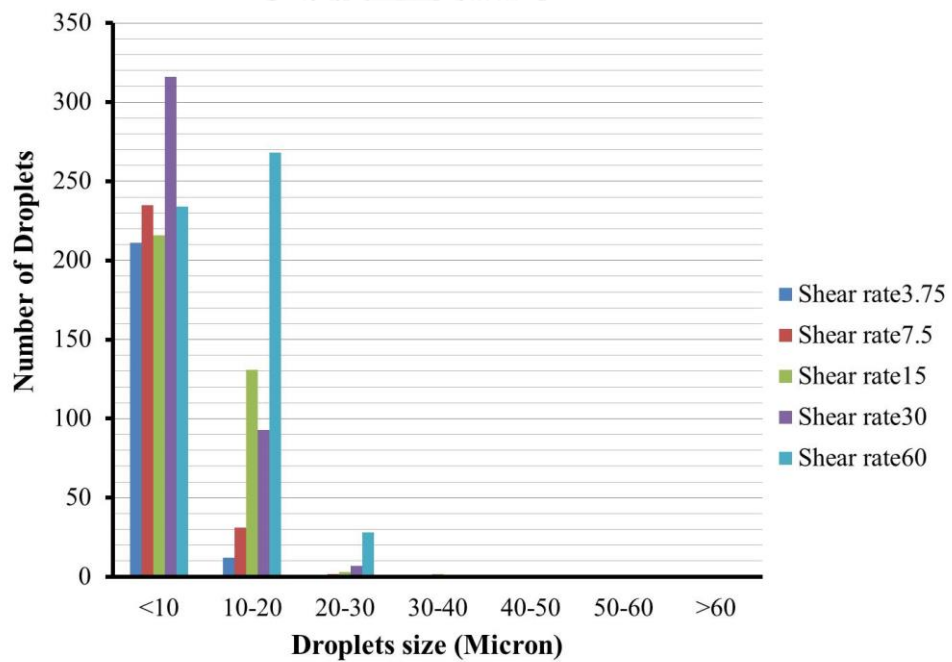


Microscopic observation of temperature 80°C in (a) shear rate 3.75 s⁻¹ (b) shear rate 7.5 s⁻¹ (c) shear rate 15 s⁻¹ (d) shear rate 30 s⁻¹ and (e) shear rate 60 s⁻¹ at 0 percent water content.

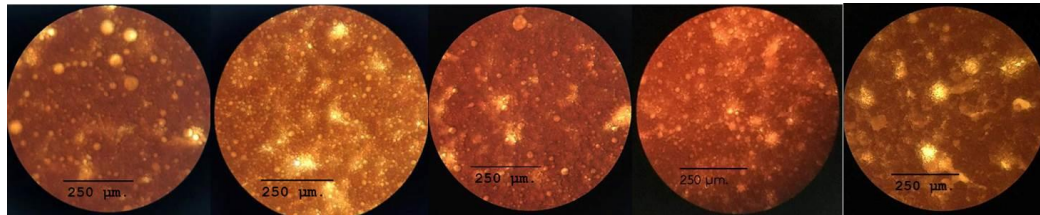


(a) (b) (c) (d) (e)

Droplets size distribution at 0 percent water content

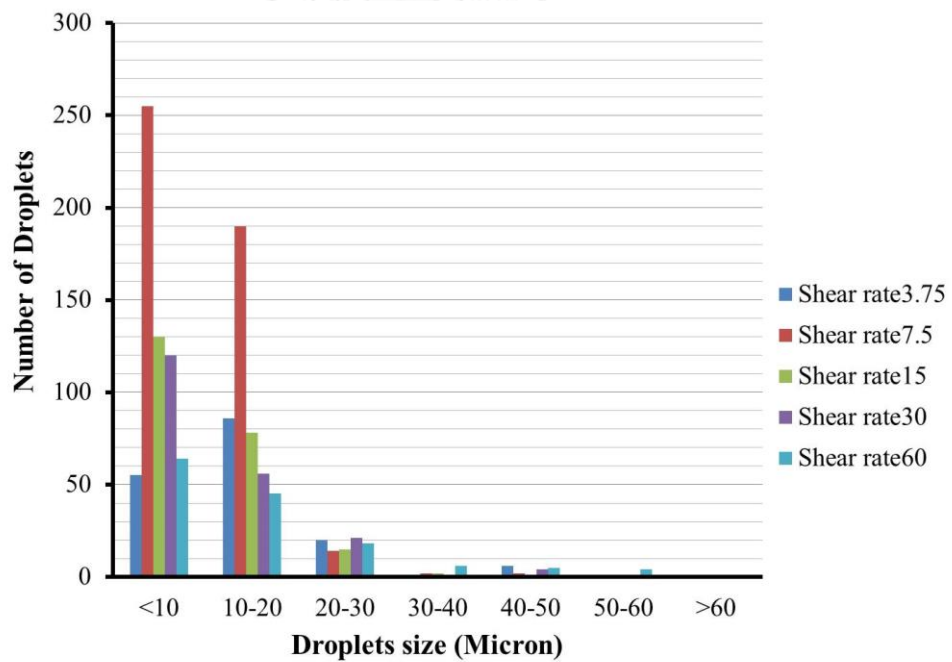


Microscopic observation of temperature 80°C in (a) shear rate 3.75 s⁻¹ (b) shear rate 7.5 s⁻¹ (c) shear rate 15 s⁻¹ (d) shear rate 30 s⁻¹ and (e) shear rate 60 s⁻¹ at 20 percent water content.

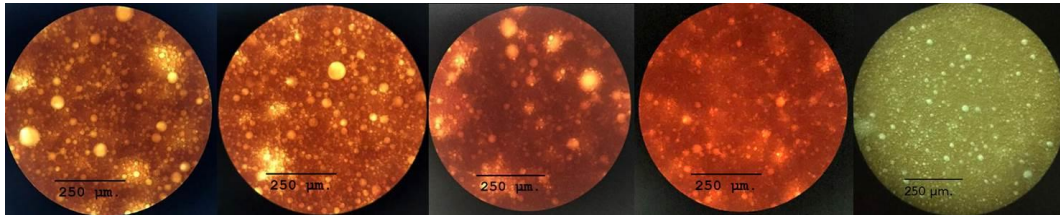


(a) (b) (c) (d) (e)

Droplets size distribution at 20 percent water content

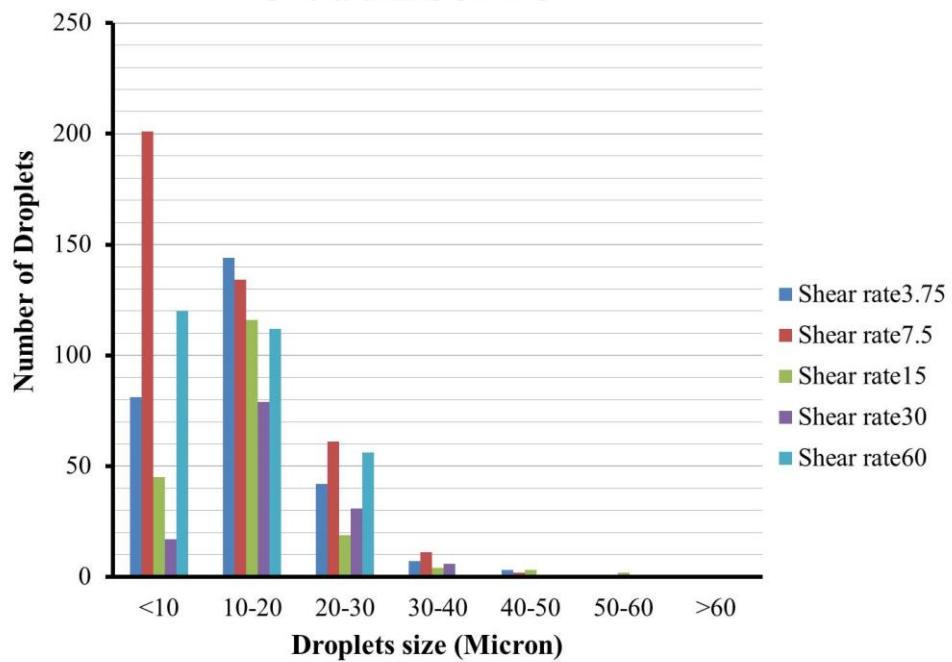


Microscopic observation of temperature 80°C in (a) shear rate 3.75 s⁻¹ (b) shear rate 7.5 s⁻¹ (c) shear rate 15 s⁻¹ (d) shear rate 30 s⁻¹ and (e) shear rate 60 s⁻¹ at 40 percent water content.

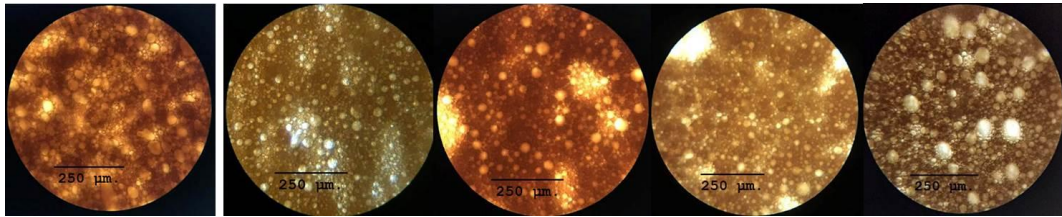


(a) (b) (c) (d) (e)

Droplets size distribution at 40 percent water content

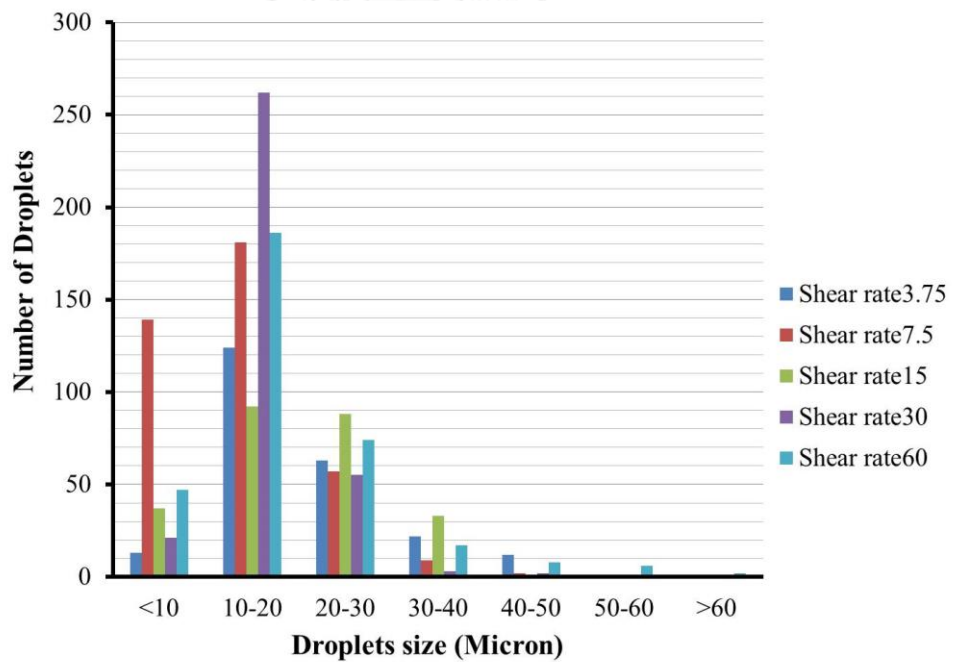


Microscopic observation of temperature 80°C in (a) shear rate 3.75 s⁻¹ (b) shear rate 7.5 s⁻¹ (c) shear rate 15 s⁻¹ (d) shear rate 30 s⁻¹ and (e) shear rate 60 s⁻¹ at 60 percent water content.



(a) (b) (c) (d) (e)

Droplets size distribution at 60 percent water content



VITA

Miss Onchanok Juntarasakul was born on July 2, 1990 in Yala, The south of Thailand. She received her Bachelor degree in Sciences from Department of Earthsciences, Faculty of Sciences, Kasetsart University in 2013. After graduation, she has been a student in the Master' Degree program in georesource Engineering at Department of Mining and Petroleum Engineering, Faculty of Engineering, Chulalongkorn University.

